COMPARISON OF FOUR SIMPLE

WAVE RESISTANCE FORMULAS

by

PIERRE FRANCOIS KOCH

Ingenieur ENSAM (1978)
DEA de Metallurgie (1978)
Université de PARIS VI

SUBMITTED IN PARTIAL FULFILLMENT
OF THE REQUIREMENTS FOR THE
DEGREE OF

OCEAN ENGINEER

at the

MASSACHUSETTS INSTITUTE OF TECHNOLOGY

June 1980

© Massachusetts Institute of Technology 1980

Signature of Author_____
Department of Ocean Engineering
May 9, 1980

Certified by_____
Francis Noblesse
Thesis Supervisor

Accepted by_____
Douglas Carmichael
Chairman, Department Committee

COMPARISON OF FOUR SIMPLE
WAVE RESISTANCE FORMULAS

by

PIERRE FRANCOIS KOCH

Submitted to the Department of Ocean Engineering
on May 9, 1980 in partial fulfillment of the requirements
for the Degree of Ocean Engineer

ABSTRACT

A simple slender-ship wave resistance formula and
the related approximations of Michell, Hogner and Yim
are compared to one another. Differences between these
four wave resistance approximations reside in that the
waterline integral is included and the thin-ship approxi-
mation is used in some of the approximations and not in
the others. Calculations are performed for several
hull forms, namely a family of Wigley hulls, the Inui
hull, the parabolic strut used by Sharma, the high speed
hull Athena and a mathematical hull with a fine bow and
a blunt stern. The results are compared to available
experimental measurements and to other numerical results.

Thesis Supervisor: Professor Francis Noblesse

Title: Assistant Professor of Ocean
Engineering
Henry L. Doherty Professor in
Ocean Utilization

ACKNOWLEDGEMENTS

I would like to express my sincere appreciation to Professor Francis Noblesse who has provided me with continuous guidance on the subject and gave me helpful encouragement.

The numerical calculations reported in this thesis were performed as part of the M.I.T. Sea Grant College Program with support from the Office of Sea Grant in the National Oceanic and Atmospheric Administration, U.S. Department of Commerce.

TABLE OF CONTENTS

LIST OF FIGURES

LIST OF TABLES

INTRODUCTION

The main object of this thesis is to present results of wave-resistance calculations based on three simple wave-resistance formulas. These are the "zeroth-order slender-ship wave-resistance approximation given in [1], the Hogner approximation, and the classical Michell thin-ship approximation.

The zeroth-order slender-body approximation corresponds to simply taking the velocity potential of the disturbance flow caused by the ship as zero. This wave-resistance formula involves a surface integral over the ship hull surface and a line integral along the ship waterline. The Hogner approximation is the particular case of the zeroth-order approximation obtained by neglecting the waterline integral. Finally, the Michell approximation may be obtained as the thin-ship limit of the Hogner approximation.

Numerical results are presented for a variety of hull forms. Some of these are idealized mathematical hull forms with fine ends, while others are more real ship-like hull forms. The theoretical predictions given by the three above-mentioned wave-resistance formulas are compared to experimental measurements.

CHAPTER I

BASIC FORMULAS

A nondimensional wave resistance, R say, is defined as $R \equiv R*/\rho V^2 L^2$, where $R*$ is the dimensional resistance, g is the acceleration of gravity, ρ is the density of water, V is the speed of the ship and L is a reference length which will be taken as half the length of the ship in this study. R can be evaluated by means of the well known "Havelock wave-resistance formula"

$$R = (4F^4/\pi) \int_0^\infty |K(t)|^2 \ (1+t^2)^{-3/2} \ dt. \tag{1-1}$$

where F is the Froude number based on the ship half length, i.e. $F = V/(gL)^{1/2}$.

The function K(t) in formula (1-1) is the "Kochin free-wave spectrum function." It is related to the free wave pattern trailing behind the ship. In the zeroth-order slender-ship approximation where ϕ is taken equal to zero [1], K(t) is given by

$$2K_0(t) = \int_h E(x,y,z;t) \nu(\vec{x}) da(\vec{x})$$

$$+F^2 \int_c E(x,y,0;t) \nu^2(\vec{x}) \mu(s) ds \tag{1-2}$$

where

$$E(x,y,z;t) = (1+t^2) F^{-4} \exp[zF^{-2}(1+t^2)$$

$$-i(xF^{-2}+yF^{-2}t)(1+t^2)^{1/2}] \tag{1-3}$$

The significance of the various symbols will now
be explained. The z-axis is vertical, positive upwards,
with the undisturbed free surface taken as the plane
z=0, and the x-axis is parallel to the direction of
motion of the ship and pointing toward the ship stern.
The plane y=0 corresponds to the ship center plane. The
coordinates x, y, z and indeed all the variables which
appear in this study are made nondimensional with
respect to the above defined characteristic length L.
The nondimensional coordinates $\vec{x}$ (x, y, z) are thus
defined as $\vec{x} = \vec{X}/L$ where $\vec{X}$ is dimensional. In the
surface integral in formula (1-2), (h) represents the
wetted-hull surface of the ship in position of rest,
da is the differential element of area of (h) and $\nu(\vec{x})$
is defined as $\nu(\vec{x}) \equiv \vec{n}(\vec{x}) \cdot \vec{i}$, where $\vec{n}(\vec{x})$ represents the
unit inward (that is, $\vec{n}$ is pointing towards the interior
of the ship) normal vector to (h) at point $\vec{x}$ of (h), and
$\vec{i}$ is the unit positive vector along the x axis. In
the line integral around the waterline (c), ds represents
the differential element of arc length of (c), $\nu(s)$ is
defined as $\nu(s) \equiv \vec{n}(s) \cdot \vec{i}$, where $\vec{n}(s)$ is the normal to (h)
at point s of (c), and $\mu(s)$ is defined as $\mu(s) \equiv \vec{n}'(s) \cdot \vec{i}$,
where $\vec{n}'$ is the unit inward normal vector to (c) in
the plane z=0 (see Figure 1-1).
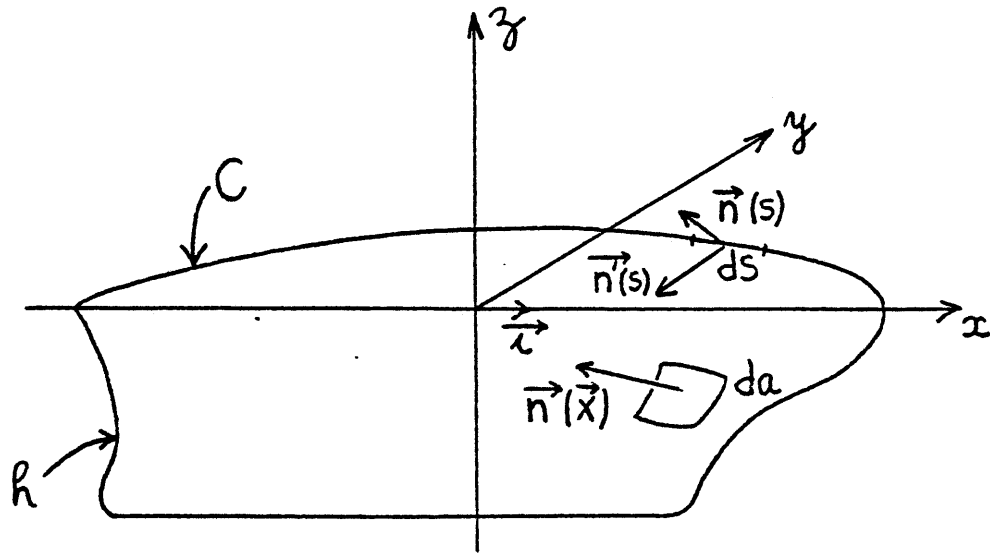
Figure 1-1

In the common case where the ship has port and starboard symmetry, the above formula for the Kochin free-wave spectrum function becomes

$$K_0(t) = \int_{h+} (1+t^2) F^{-4} \exp[(1+t^2)^{1/2} F^{-2}(-ix+(1+t^2)^{1/2}z]$$

$$\cos(ytF^{-2}(1+t^2)^{1/2} \nu(\vec{x}) da(\vec{x})$$

$$- \int_{c+} (1+t^2) F^{-2} \exp[-F^{-2}(1+t^2)^{1/2}ix]$$

$$\cos(ytF^{-2}(1+t^2)^{1/2}) \nu^2(s) \mu(s) ds \qquad (1-4)$$

In the hull surface integral in formula (1-4), (h^+) represents the starboard half of the wetted surface (h), that is the portion of the hull corresponding to y positive. In the line integral, (c^+) is the intersection of (h^+) with the plane z=0.

The waterline integral in (1-4) is especially important for blunt hull forms (for which ν and μ are not small at the bow and/or stern) for ship forms with small draft, and in the low speed limit ([2],[3]).

If the ship is sufficiently "fine," that is if the angle between the waterline (c) and the x-axis is sufficiently small, we have $\nu^2|\mu| << |\nu| << 1$. If the line integral in formula (1-4) is neglected in comparison with the surface integral, the Kochin free-wave spectrum function K_H say, becomes

$$K_H(t) = \int_{h^+} (1+t^2) F^{-4} \exp[F^{-2}(1+t^2)^{1/2}(-ix+(1+t^2)^{1/2}z)]$$

$$\cos(ytF^{-2}(1+t^2)^{1/2}\nu(\vec{x})da(\vec{x}) \qquad (1-5)$$

$K_H(t)$ corresponds to the Hogner approximation. If the ship is "thin," that is if y(x,z) is sufficiently small that the term $\cos(ytF^{-2}(1+t^2)^{1/2})$ may be approximated by 1, the Hogner "fine-ship approximation" $K_H(t)$ given in equation (1-5) becomes the well known Michell "thin-ship approximation" $K_M(t)$ say, which is given by

$$K_M(t) = \int_{h^+} (1+t^2) F^{-4} \exp[F^{-2}(1+t^2)^{1/2}$$

$$(-ix + (1+t^2)^{1/2} z)] \, v(\vec{x}) \, da(\vec{x}) \qquad (1\text{-}6)$$

The "thin-ship approximation" $y \ll 1$ used in deriving (1-6) for $K_M(t)$ from the Hogner approximation (1-5) not only implies geometrical thinness, characterized by $\varepsilon = B/L \ll 1$ (where B is the dimensional half beam and L the dimensional half length) but also "Froude thinness," $\varepsilon/F^2 \ll 1$: the differences between R_H and R_M (the wave resistance obtained by using K_H and K_M respectively in (1-1)) may be expected to be larger the bigger the beam and the smaller the Froude number.

Another formula of interest is obtained by keeping the waterline integral in (1-4), but approximating the term $\cos(ytF^{-2}(1+t^2)^{1/2})$ by 1. (The ship is "thin," but we allow for the influence of "large" angle between (c) and the x-axis at the bow and/or stern.) The expression for the Kochin free-wave spectrum function becomes

$$K_y(t) = \int_{h^+} (1+t^2) F^{-4} \exp\left[F^{-2}(1+t^2)^{1/2}\left(-ix + (1+t^2)^{1/2} z\right)\right] v(\vec{x}) \, da(\vec{x})$$

$$- \int_{C^+} F^{-2}(1+t^2) \exp\left[-F^{-2}(1+t^2)^{1/2} i x\right] v^2(\lambda) \mu(\lambda) \, d\lambda \qquad (1\text{-}7)$$

This expression was actually used by Yim [4].

In the case where, in addition to port and starboard symmetry, the ship hull has fore and aft symmetry, the expressions for K_0, K_H and K_y may be shown to become

$$K_0(t) = 2F^{-4}(1+t^2)\int_{h^-_+} i\cos\left(F^{-2}t(1+t^2)^{1/2}y\right)\sin\left(F^{-2}x(1+t^2)^{1/2}\right)\exp\left[F^{-2}(1+t^2)z\right]\nu(\vec{x})da(\vec{x})$$

$$+ 2F^{-2}(1+t^2)\int_{C^-_+} i\cos\left(F^{-2}t(1+t^2)^{1/2}y\right)\sin\left(F^{-2}x(1+t^2)^{1/2}\right)\nu^2(\Delta)\mu(\Delta)d\Delta \quad (1-8)$$

$$K_H(t) = 2F^{-4}(1+t^2)\int_{h^-_+} i\cos\left(F^{-2}t(1+t^2)^{1/2}y\right)\sin\left(F^{-2}x(1+t^2)^{1/2}\right)\exp\left[F^{-2}(1+t^2)z\right]\nu(\vec{x})da(\vec{x})$$

$$(1-9)$$

$$K_M(t) = 2F^{-4}(1+t^2)\int_{h^-_+} i\sin\left(F^{-2}(1+t^2)^{1/2}x\right)\exp\left[F^{-2}(1+t^2)z\right]\nu(\vec{x})da(\vec{x})$$

$$(1-10)$$

$$K_y(t) = 2F^{-4}(1+t^2)\int_{h^-_+} i\sin\left(F^{-2}(1+t^2)^{1/2}x\right)\exp\left[F^{-2}(1+t^2)z\right]\nu(\vec{x})da(\vec{x})$$

$$+ 2F^{-2}(1+t^2)\int_{C^-_+} i\sin\left(F^{-2}(1+t^2)^{1/2}x\right)\nu^2(\Delta)\mu(\Delta)d\Delta \quad (1-11)$$

In the surface integrals in formulas (1-8) through (1-11), (h_+^-) represents the quarter of the hull for which y is positive and x is negative. $(c_\pm^-)$ in the waterline integrals is the intersection of (h_+^-) with the plane z=0.

CHAPTER II

NUMERICAL RESULTS FOR A SERIES OF THREE HULL FORMS:

WIGLEY, INUI, ATHENA

The calculations presented in this Chapter were
performed so as to make possible our participation to a
workshop on wave resistance organized by the DTNSROC in
Washington, D.C. in November 1979. It was requested
that we compute the wave resistance of several hull
forms, some of which were defined analytically (like
the Wigley hull) and some were not (Inui, high speed
hull Athena). A general numerical technique was thus
selected, which we briefly describe below.

As far as the definition of the hull is concerned,
all dimensions of the ship are made nondimensional with
respect to the half length L of the ship, that is
$\vec{x}=\vec{X}/L$ where $\vec{X}$ is dimensional. As a consequence, x varies
from -1 to +1, y from -b to +b and z from -d to zero
(where b and d are the nondimensional half beam and
the draft respectively). (See Figure 2-1).

The hull surface is defined either analytically
by a relation in the form $y=\pm y(x,z;b,d)$, or numerically
by a series of cross-sections.
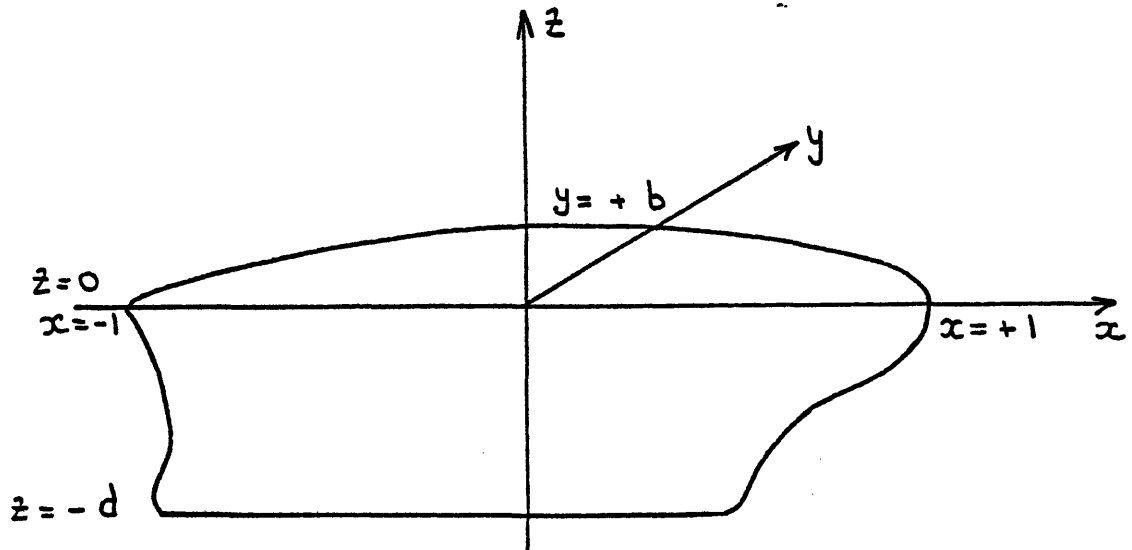
Figure 2-1

The wave resistance is given by formula (1-1) and
the Kochin free-wave spectrum function K(t) by (1-8)
in the case where the hull has fore and aft symmetry
(Wigley and Inui hull forms) and by (1-4) when the
hull has only port and starboard symmetry (high speed
hull Athena).

The determination of K(t) requires the evaluation
of a surface integral on the hull of the ship and of a line
integral along the waterline.

In order to evaluate the surface integral, the
surface of the hull is divided into small planar triangles.
On each of these triangles, ν is constant and the integral
can be evaluated analytically (see Appendix I). The

surface integral over the entire hull is then taken as the sum of the integrals over all the planar triangles.

The choice of the triangles is made as follows. The centerplane is divided in small triangles as shown on Figure 2-2. The horizontal lines must cross the fore (respectively aft) border line of the centerplane at points where vertical lines end, in order for the centerplane to be partitioned in triangles only.
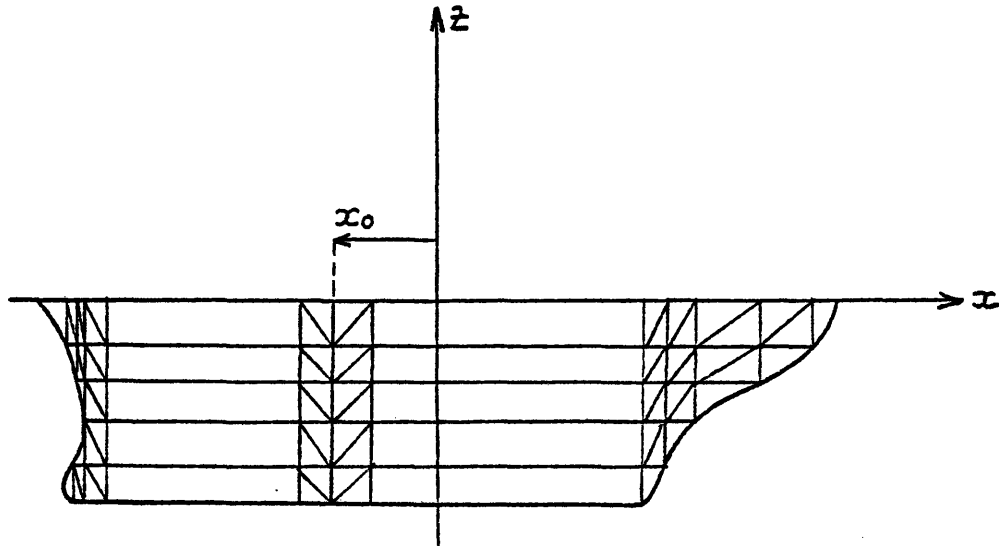
Figure 2-2

It is also obrious that the fore (and aft) part of the centerplane are generated by triangles of a different orientation. As a consequence, we change the orientation of the triangles at a value, x_0 say, of x which may (but need not) be chosen equal to zero (cf Figure 2-2).

In the case of fore and aft symmetry however (Wigley, Inui), this problem does not arise since we only consider the first half of the centerplane.

Having done this partition of the centerplane, we generate a "partition of the hull" by associating to each triangle of the centerplane, a triangle on the hull. This new triangle has vertices with the same x and y coordinates as the vertices of the corresponding triangle on the centerplane and y-coordinates so chosen that the vertices are on the hull.

The evaluation of the line integral follows a similar approach. The waterline is divided in linear segments over which ν and μ are constant. Analytical integration is performed on each interval (see Appendix II) and the line integral over the waterline is taken equal to the sum of the integrals over all the linear segments.

It is important to know how many horizontal and vertical lines to choose, that is how small the planar triangles on the hull and the linear segments on the waterline should be in order for the surface and line integrals to be determined with satisfactory accuracy. At low values of the Froude number, the wave length of the radiated waves is small. Since we expect the influence of the waterline integral to be larger, the smaller the Froude number, we must choose our linear

segments small enough compared to the wavelength so that the precision on the line integral is sufficient.

Numerical evaluation of the line integral for the Wigley hull and for a rhombus-like hull form have shown that the number N_L of segments necessary for the line integral to converge increases when F decreases. For F=0.1, the value of N_L was found to be 60. However the surface integral did converge for a number of horizontal lines M=10 and a number of vertical lines N_S=20.

Numerical investigations were made with N_S=20, M=10 and N_L=80 (for nonanalytical hull (Inui, Athena) there is a practical limitation on M and N).

The use of the triangles made possible a calculation of the surface area of the hull which can be valuable to compute the wave resistance coefficient for a nonanalytical hull or for a series of hull forms like, say, a set of Wigley hull forms with different draft or entrance angle.

II-1 Wigley Hull

The Wigley hull has parabolic framelines and parabolic waterline. It is analytically defined by the equation

$$y = \pm b(1-x^2)(1-z^2/d^2)$$

where x, y, z, b and d are made nondimensional with respect to the half length L of the ship, b is the non-dimensional half beam and d the nondimensional draft.

The evaluation of the wave resistance coefficient was made for b=0.1 and d=0.125.

In order to determine the wave resistance, one has to integrate the Kochin free-wave spectrum function K(t) from t=0 to t=∞, as indicated in equation (1-1). The upper limit +∞ was replaced by t_F=6, corresponding to an angle θ=80°, where θ is the angle between the x axis and the direction of propagation of the radiated wave, as shown on Figure (2-3). It was assumed that such diverging waves would have only little effect on the overall wave resistance. This assumption is again considered in Chapter III-2 where it is justified.
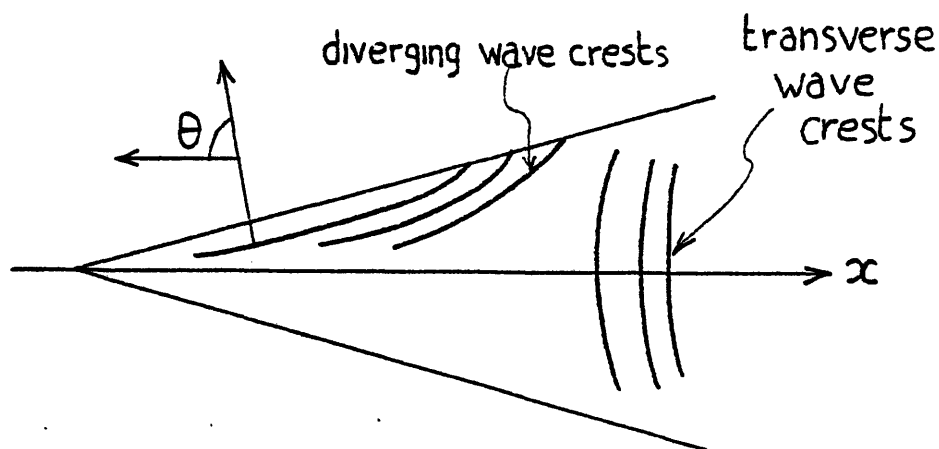
Figure 2.3

Results obtained by Michell's and Hogner's wave
resistance formulas are given in Table I and results
are given by the zeroth approximation in Table II. All
results are shown on Figure 2-4, where calculations
based on Hogner's formula, Michell's formula and the
zeroth approximation are identified by the symbols H,
M and O respectively.

The experimental results provided by the DTNSROC
were obtained for a model free to trim and sink whereas
the effect of sinkage and trim is not taken into account
in the present study. Direct comparison of our results
with the experimental results is thus not relevant.
However we know that the wave resistance coefficient is
appreciably decreased when the model is constrained (see
[6] and [7] for example). Thus the effect of the line
integral can be seen to be in the "right direction," where-
as   Hogner's and Michell's approximations will over
predict the resistance.

On Figure (2-4) are also shown the results obtained
numerically by C. W. Dawson [8]. These can be seen to
be in surprisingly good agreement with the results given
by the zeroth approximation1

Results obtained by K. J. Bai [9] are also shown
in the case of a large and deep towing tank (W/L=D/L=1.25)

which is the closest the author comes to the assumption

of unbouded fluid. Here again, agreement with the results

given by the zeroth approximation is fairly good for

relatively high values of the Froude number, say $Fn \geq 0.40$.

(where Fn is the Froude number based on the length of

the ship $Fn=V/(g \cdot 2L)^{1/2}=V/2^{1/2}$.

Note that the results obtained by Dawson and

Bai are for fixed models like in our case, which makes

these comparisons meaningful.

II-2 The Inui Hull

The Inui hull, as the Wigley hull, is still a thin

ship with fine ends and fore and aft symmetry. But,

unlike the Wigley hull, it is not defined analytically.

It is defined as the hull form obtained by Inui, by

tracing streamlines for infinite flow past a linear

source strength distributed on the centerplane. The

nondimensional half beam b and draft d are given by

b = 0.2458

d = 0.3916.

The first quarter of the hull ($y>0$, $x<0$) is defined

by a series of 14 cross-sections. These are given in

Table III. Like for the Wigley hull, the integral in

equation (1-1) was evaluated with an upper limit of

integration $t_F= 6$. (It was verified that increasing t_F

up to 18 did not lead to any significant change).

Results obtained by Hogner's wave resistance formula are given in Table IV together with the results given by the zeroth approximation.

These results are also shown on Figure (2-5) where the curves corresponding to the Hogner formula and the zeroth approximation are identified by H and O respectively. The same remark as before applies here to the previously drawn conclusions [5]. On Figure (2-5) are the results given by Dawson [8], Bai [9] and Chang [10]. The results by Bai fit almost exactly with the results obtained by Hogner's formula.

Values given by Dawson are lower, i.e. closer to the results obtained by the zeroth approximation, except at Froude numbers less than say 0.35, where they seem to be out of phase with our results, and much more oscillatory. On the other hand, results given by Chang are very close to the experimental results. This may appear surprising in view of the fact that these results were evaluated for a model fixed (see [10]).

It is interesting to note that the numerical results obtained with the simple Hogner formula are similar to the results obtained with much more sophisticated numerical procedures. In addition, the zeroth

approximation appears to give results closer to experimental measurements than the results given by Hogner's formula or Dawson, for relatively small Froude numbers, say Fn<0.32. At relatively high Froude numbers, say Fn>0.35, the zeroth approximation consistently predicts wave resistance coefficients lower than the ones obtained for a model free to sink and trim, like Dawson but unlike Chang.

II-3 The high speed hull "Athena"

This hull differs in many ways from the hulls studied previously. Specifically it is defined numerically, does not have fore and aft symmetry, and is not vertical sided at the waterline. In addition, it has a transom stern, is broader at midship and less deep than the two previous hull forms. The nondimensional half beam b and draft d are given by

b = 0.1470

d = 0.0642.

The hull is defined by a series of 25 cross-sections, given in Table V.

Figure (2-6) shows a top view of the hull.
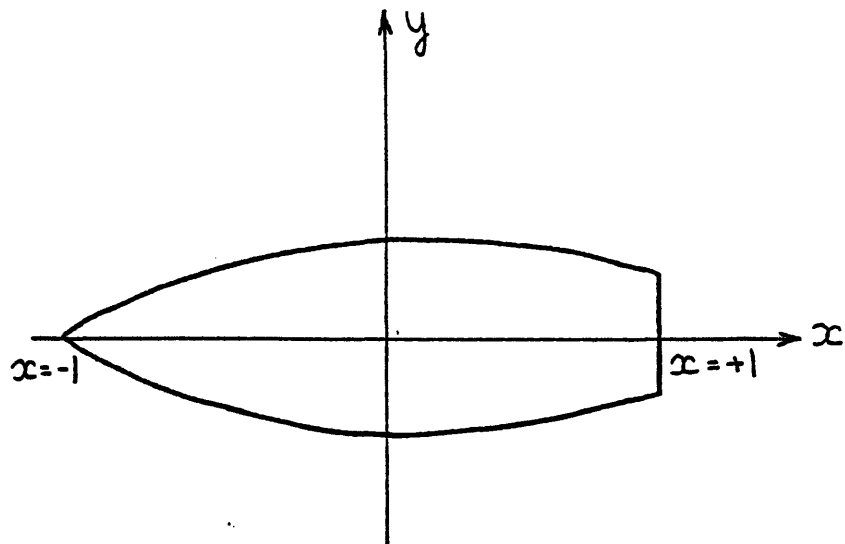
Figure 2-6

The transom stern will obviously cause some difficult problem. Potential flow theory assumes that there is no separation, i.e. the streamlines remain close to the actual ship hull.

Thus one should consider the wave resistance as given by a source distribution over the whole surface of the hull. The simplified theory presently used predicts that the wave resistance will be the same, no matter the direction in which the ship moves. It is intuitively obvious however that the wave resistance of the Athena hull going backwards will be much larger than the resistance of the same hull going forwards.

It is commom practice to disregard the transom end
of the hull.   The underlying reasoning is that, due to
separation, the stern does not participate to the wave
making.

Figure (2-7) presents the results obtained by the
Hogner approximation and by the zeroth approximation.
The wave resistance curve is seen to oscillate much less
than previously.   The influence of the waterline increases
with increasing Froude numbers.   This figure also shows
the calculated values of the wave resistance obtained
by Dawson [8] and Chang [10].

The results presented by Chang were referred to as the
resistance coefficient in [10].   They were explained to
be the sum of the wave resistance and of the "hydrostatic
pressure resistance."   We thus show the values given in
the reference and the difference between these and
the hydrostatic resistance.   The same remark holds for
the experimental results which are shown, one curve
corresponding to the residual resistance and the other
being deduced from the former by subtracting the hydro-
static resistance.

If we compare results obtained by Hogner's formula
and the zeroth approximation with the "experimental"
results obtained by subtracting the hydrostatic resistance
from the residual resistance, we note the following: at

low Froude number 0.27<Fn<0.35 say, both the Hogner

and the zeroth approximation give results very close

to the experimental results. For moderately high

Froude numbers, 0.35<Fn<0.65 say, both the Hogner and

the zeroth approximation overpredict the wave resistance,

whereas the results presented by Chang are close to

the experimental values. For high values of the Froude

number, Fn>0.65 say, the Hogner and the zeroth approxi-

mations underpredict the wave resistance. The zeroth

approximation curve is closer to the values obtained by

Chang and the Hogner curve is closer to the experimental

results.

The results obtained by Dawson are very close to

the residual resistance curve, and much higher than the

experimental wave resistance coefficients given by

Chang. It must be noted that Dawson computed both the

residual resistance coefficient and the wave resistance

coefficient and they were very close to one another.

This seems to imply that the influence of the hydrostatic

presume resistance is weak, which is at variance with

the conclusion arrived at by Chang.

In summary, comparison between our results and

the experimental measurements shows that, they are out

of phase with, and very far from them. Furthermore, our

results are in relatively good agreement (at least at

moderately low Froude numbers) with the experimental

curve obtained by subtracting from the residual

resistance the hydrostatic pressure resistance computed

by Chang.

CHAPTER III

WAVE RESISTANCE OF MATHEMATICAL HULL FORMS

In this section, calculations are performed for several mathematical hull forms and the results are compared with experimental measurements. The hulls that are considered are i) a family of Wigley hulls, ii) the parabolic strut used by Sharma and iii) a hull with a fine bow and a blunt stern, which we shall refer to as the parabolic elliptic hull.

Instead of partitioning the hull in small planar triangles as in Chapter II, it was decided to use the equation defining the surface of the hull to perform numerical evaluations of $K(t)$ and R.

All the integrals which were performed were single integrals (over one variable). It was thus possible to study the behavior of the function ($f(\xi)$ say) which was to be integrated, in order to be sure to have sufficient accuracy.

The formulas for R and $K(t)$ used in this Chapter are slightly different from the ones used in Chapter II but are of course equivalent to them (see Appendix III and IV).

In the case where the hull has port and starboard symmetry, the wave resistance is given by

$$R = R^*/\rho V^2 L^2 = 4\pi^{-1} F^{-4} \int_0^\infty |K(t)|^2 (1+t^2)^{1/2} dt \tag{3-1}$$

$$K(t) = \int_{R^+} E\, n_x\, da - F^2 \int_{C^+} E\, n_x^2\, \sigma_y\, d\ell \tag{3-2}$$

$$E(x,y,z) = \exp\left[F^{-2}(1+t^2)z - iF^{-2}(1+t^2)^{1/2}x\right]\cos\left(F^{-2}t(1+t^2)^{1/2}y\right) \tag{3-3}$$

where all the symbols have the same meaning as before (see Chapter I).

In the case where the hull also has fore and aft symmetry, the above formulas become:

$$R = R^*/\rho V^2 L^2 = 16\pi^{-1} F^{-4} \int_0^\infty |K(t)|^2 (1+t^2)^{1/2} dt \tag{3-4}$$

$$K(t) = \int_{R^+_+} E\, n_x\, da - F^2 \int_{C^+_+} E\, n_x^2\, \sigma_y\, d\ell \tag{3-5}$$

$$E(x,y,z) = \exp\left[F^{-2}(1+t^2)z\right]\cos\left(F^{-2}t(1+t^2)^{1/2}y\right)\sin\left(F^{-2}(1+t^2)^{1/2}x\right) \tag{3-6}$$

For the Wigley models and the parabolic elliptic hull, some plots of the Kochin free-wave spectrum function K(t) are presented for some values of the Froude number F. The wave resistance curves predicted by the zeroth approximation and Hogner's and Michell's formulas are also shown.

III-1 A family of Wigley hull forms

In his studies of the Michell wave resistance formula, Wigley [6,11] selected a family of hull forms defined by the equation

$$y = b\left(1 - z^2/d^2\right)\left(1 - (1+\gamma)x^2 + \gamma x^4\right) \; ; \; -1 \leqslant x \leqslant +1 \; ; \; -d \leqslant z \leqslant 0 \; . \qquad (3\text{-}7)$$

where x, y, z, b and d are made dimensionless with respect to the half length L of the ship; b and d are the half beam and the draft respectively. γ is a coefficient which will be given the values -0.2, 0., 0.6 and 1.0. This will enable us to compare our results with the experimental results obtained by Shearer [7].

The parameter γ characterizes the angle of entrance. It is easily verified that for values of γ less than 0.2, the hull is convex and for γ greater than 0.2, the hull is concave (see Figure 3-1).

$$\gamma < 0.2 \qquad\qquad \gamma > 0.2$$
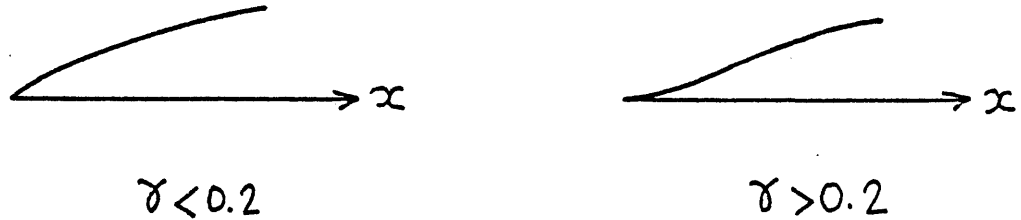
Figure 3-1

By using equation (3-7) in equations (3-4), (3-5) and (3-6), we may obtain

$$R = R^* / \rho V^2 L^2 = 64 \, b^2 \, \pi^{-1} \int_0^\infty |K(t)|^2 \left(1+t^2\right)^{1/2} dt \qquad (3\text{-}8)$$

$$K(t) = \int_0^1 x \left(1 + \gamma - 2\gamma x^2\right) \sin\left(F^{-2}\left(1+t^2\right)^{1/2} x\right) I \, dx \qquad (3\text{-}9)$$

$$I = d F^{-2} \int_0^1 \exp\left[-F^{-2}\left(1+t^2\right) d\zeta\right] \cos\left[F^{-2} t \left(1+t^2\right)^{1/2} b \left(1 - (1+\gamma) x^2 + \gamma x^4\right)\left(1-\zeta^2\right)\right]\left(1-\zeta^2\right) d\zeta$$
$$- \frac{4 \, b^2 x^2 \left(1 + \gamma - 2\gamma x^2\right)^2}{1 + 4 b^2 x^2 \left(1 + \gamma - 2\gamma x^2\right)^2} \cos\left[F^{-2} t \left(1+t^2\right)^{1/2} b \left(1 - (1+\gamma) x^2 + \gamma x^4\right)\right] \qquad (3\text{-}10)$$

(see Appendix V for the derivation of (3-8), (3-9) and (3-10)).

In order to simplify the numerical evaluation of K(t)
(and of R), the integral over ζ in I (equation 3-10) is
approximately evaluted. One can first simplify the
expression of I by introducing two new variables β and δ:

$$\delta = F^{-2}(1+t^2)d \tag{3-11}$$

$$\beta = t(1+t^2)^{-1/2}bd^{-1}\left[1-(1+\gamma)x^2+\gamma x^4\right] \tag{3-12}$$

$$I = dF^{-2}I(\beta,\delta) - \frac{4b^2x^2(1+\gamma-2\gamma x^2)^2}{1+4b^2x^2(1+\gamma-2\gamma x^2)^2}\cos\left[F^{-2}t(1+t^2)^{1/2}b(1-(1+\gamma)x^2+\gamma x^4)\right] \tag{3-13}$$

where

$$I(\beta,\delta) = \int_0^1 \exp(-\delta\zeta)\cos(\beta\delta(1-\zeta^2))(1-\zeta^2)\,d\zeta \tag{3-14}$$

Replace the range [0,1] of integration over ζ by three
intervals: $[0,\alpha]$, $[\alpha,1-\alpha]$ and $[1-\alpha,1]$; over each of these
intervals, the function $(1-\zeta^2)$ in the argument of the
cosine function in (3-14) is replaced by a linear
function, as shown in Figure 3-2.

$$f(\zeta) = 1-\zeta^2$$
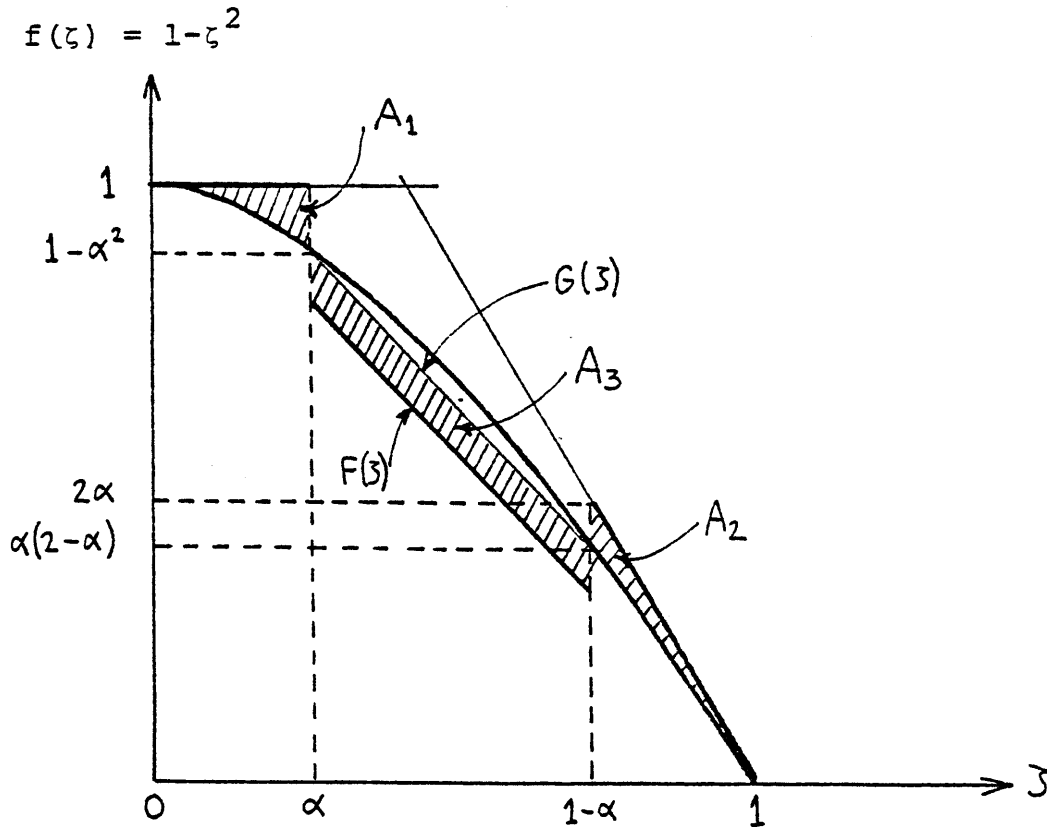
Figure 3-2

- $0 \leq \zeta < \alpha$ $f(\zeta)$ is replaced by $f_1 = 1$
- $\alpha \leq \zeta \leq 1-\alpha$ $f(\zeta)$ is replaced by $f_2 = F(\zeta)$
- $1-\alpha \leq \zeta \leq 1$ $f(\zeta)$ is replaced by $f_3 = 2(1-\zeta)$.

The functions f_1 and f_2 are so chosen as to conserve the slope of $f(\zeta)$ at $\zeta = 0$ and $\zeta = 1$;

α is a priori arbitrary (it will be taken equal to $1/\zeta$ in the actual calculations);

$G(\zeta)$ is the function describing the linear segment joining the points $(\alpha, 1-\alpha^2)$ and $(1-\alpha, \alpha(2-\alpha))$;

$F(\zeta)$ is the function describing a linear segment, parallel to the one described by $G(\zeta)$ and chosen so that we have $A_3=A_1+A_2$, where A_1, A_2 and A_3 are the surface areas between the curve $f(\zeta)$ and the three linear segments used to approximate it (see Figure 3-2).

It is easy to see that $F(\zeta)$ is of the form

$$F(\mathfrak{Z}) = -\mathfrak{Z} + c \qquad \qquad (3\text{-}15)$$

The requirement that $A_1+A_2=A_3$ leads to

$$c = (1-2\alpha)^{-1} \left(7/6 - 2\alpha - \alpha^2 \right) \qquad \qquad (3\text{-}16)$$

If we choose $\alpha=1/3$, we obtain $c=7/6$.

It may be noted that in the Michell approximation, $f(\zeta)=1-\zeta^2$ is replaced by $g(\zeta)=0$.

In order to check that the replacement of $f(\zeta)$, by the three linear functions previously described permits a precise evaluation of $I(\beta,\delta)$, we evaluated numerically the difference between the exact value of $I(\beta,\delta)$ and the value of $I(\beta,\delta)$ obtained with the simplification of $f(\zeta)$, and which we call I^a. The method was as follows:

$$I = \int_0^\alpha g(\zeta) d\zeta + \int_\alpha^{1-\alpha} g(\zeta) d\zeta + \int_{1-\alpha}^1 g(\zeta) d\zeta \qquad (3-17)$$

where $g(\zeta) = \exp[-\delta\zeta]\cos[\beta\delta(1-\zeta^2)](1-\zeta^2)$

We can rewrite (3-17) as

$$I = \left(I_o^a - I_o^n\right) + \left(I_m^a - I_m^n\right) + \left(I_1^a - I_1^n\right) \qquad (3-18)$$

or $\quad I = \left(I_o^a + I_m^a + I_1^a\right) - \left(I_o^n + I_m^n + I_1^n\right)$

or $\quad I = I^a - I^n$

where

$$I_o^a = \int_o^\alpha \exp(-\delta\zeta)\cos(\beta\delta)(1-\zeta^2) d\zeta \qquad (3-19)$$

$$I_o^n = \int_o^\alpha \exp(-\delta\zeta)\left[\cos(\beta\delta) - \cos(\beta\delta(1-\zeta^2))\right](1-\zeta^2) d\zeta \qquad (3-20)$$

$$I_m^a = \int_\alpha^{1-\alpha} \exp(-\delta\zeta)\cos(\beta\delta(c-\zeta))(1-\zeta^2) d\zeta \qquad (3-21)$$

$$I_m^n = \int_\alpha^{1-\alpha} \exp(-\delta\zeta)\left[\cos(\beta\delta(c-\zeta)) - \cos(\beta\delta(1-\zeta^2))\right](1-\zeta^2) d\zeta \qquad (3-22)$$

$$I_1^a = \int_{1-\alpha}^1 \exp(-\delta\zeta)\cos(2\beta\delta(1-\zeta))(1-\zeta^2) d\zeta \qquad (3-23)$$

$$I_1^n = \int_{1-\alpha}^{1} \exp(-\delta \zeta) \left[\cos(2\beta \delta(1-\zeta)) - \cos(\beta \delta(1-\zeta^2)) \right] (1-\zeta^2) d\zeta \quad (3\text{-}24)$$

$$I^a = I_o^a + I_m^a + I_1^a \quad (3\text{-}25)$$

$$I^n = I_o^n + I_m^n + I_1^n \quad (3\text{-}26)$$

I^a can be evaluted in closed form (see Appendix VI)

I^n was computed numerically.

Comparison of I^a and I^n was made for several values of

F, $\gamma=0$, $\alpha=1/3$ and $c=7/6$.

The difference was of a few percents. The expression

$I(\beta,\delta)$ is thus well approximated by I^a.

The Kochin free-wave spectrum function can now be

obtained from the simple integral

$$K(t) = \int_0^1 g(x) dx$$

where g(x) is given by

$$g(x) = x(1+\gamma - 2\gamma x^2) \sin\left(F^{-2}(1+t^2)^{1/2} x\right) I \quad (3\text{-}27)$$

and I is now given by

$$I = I^a - \frac{4b^2x^2(1+\gamma-2\gamma x^2)^2}{1+4b^2x^2(1+\gamma-2\gamma x^2)^2} \cos\left[F^{-2}t(1+t^2)^{1/2} b\left(1-(1+\gamma)x^2+\gamma x^4\right)\right] \qquad (3\text{-}28)$$

If I were not an oscillatory function of x, equation (3-27) would indicate that the function g(x) would oscillate with a pseudo period T stemming from the term $\sin(xF^{-2}(1+t^2)^{1/2})$ and having the value

$$T = 2\pi F^2 (1+t^2)^{-1/2} \qquad (3\text{-}29)$$

The range of integration over x is 1. Imposing to take 24 points over each period when integrating g(x), would make it necessary to take a number C_i of points to integrate g(x) over the whole interval [0,1]. C_i would be given by

$$C_i = 24\, \Delta x/T = 24/T \simeq 3.8\, F^{-2}(1+t^2)^{1/2}$$

$$C_i = 3.8\, F^{-2}(1+t^2)^{1/2} \qquad (3\text{-}30)$$

Since I also oscillates when x varies, it is not obvious that the pseudo period of g(x) will be the one

given by equation (3-29).

Plots of g(x) are shown in Figures (3-3) through (3-5) for F=0.3 and t=0, t=1 and t=2; γ was always taken equal to 0. It can be seen that the number of points necessary to carry out the integration of g(x) with sufficient accuracy is fairly well predicted by equation (3-30). It was decided to use C_i as given by

$$C_i = 2 \text{ INT} \left(2 F^{-2} \left(1 + t^2 \right)^{1/2} \right) + 1 \tag{3-31}$$

where we are careful to take C_i as an odd integer. (This will enable us to use Simpson's rule, for example.)

The next step is to integrate K(t) in order to obtain the wave resistance as given by equation (3-8) which we can rewrite as

$$R = 64 \, b^2 \, \pi^{-1} \int_0^{t_F} g(t) dt \tag{3-32}$$

where $\quad g(t) = \left| K(t) \right|^2 \left(1 + t^2 \right)^{1/2} \tag{3-33}$

and where t_F, strictly speaking, is infinite.

When t tends to infinity, the amplitude of the corresponding waves decreases very much. The value of g(t) is expected to become negligible for t greater than a value t_F. Plots of g(t) are thus presented for several values of F, in order to determine how t_F and the pseudo period of g(t) (and so the number of points necessary to compute the integral of equation (3-32)) depend on F. These curves are presented on Figures (3-6) through (3-15) for values of γ equal to 0, 1 and -0.2, and values of F equal to 0.2, 0.3, 0.4, 0.5 and 1. Several interesting features can be observed.

The amplitude of g(t) decreases very rapidly when t increases. The function g(t) also oscillates when t increases, with a frequency which decreases when F increases. The value t_F of t, after which the amplitude of g(t) becomes negligible is also dependent on F and increases where F increases.

Also when γ increases from $\gamma=0$ to $\gamma=1$ (i.e. when the bow becomes thinner) t_F decreases, for a given value of F. When considering a slightly thicker hull, by taking $\gamma=-0.2$, it cannot be seen any major difference with the case $\gamma=0$. Also, when F is large (F=1 say) there is no difference between the values of t_F obtained for $\gamma=0$, $\gamma=1$ or $\gamma=-0.2$.

For the case $\gamma=0$, the following empirical formulas for t_F and C_j (which is the number of points required for integrating (t) with sufficient accuracy) were used:

$$t_F = 5 \; F^{0.4} \tag{3-34}$$

$$C_j = 2 \; \text{INT}\left(t_F \cdot F^{-2}\right) + 1 \tag{3-35}$$

For determining C_j, it was chosen to impose 16 points for each "period," instead of 24 as before. Equations (3-34) and (3-35) were also used for other values of γ. The only consequence was to overpredict t_F.

To compute the wave resistance in the Hogner approximation, the line integral term in equation (3-28) was deleted and (I) was thus made equal to (I^a) in (3-27).

$$I_H = I^a \tag{3-36}$$

where the subscript H stands for Hogner.

To compute the wave resistance in the Michell approximation, we replace equation (3-10) by

$$I = d \; F^{-2} \int_0^1 \exp\left[F^{-2}(1+t^2)d\zeta \right] (1-\zeta^2)d\zeta \tag{3-37}$$

This integral can be easily evaluted and I is then given by

$$I_M = dF^{-2}\left[\delta^{-1} + 2(\delta+1)\,\delta^{-3}\exp(-\delta) - 2\,\delta^{-3}\right] \qquad (3\text{-}38)$$

where the subscript (M) stands for Michell.

The results for $\gamma=0$ are shown on Figure (3-16). The case $\gamma=0$ was already examined in Chapter II. These calculations were done nevertheless, in order to check our previous results and the new program.

In Figure (3-16), R/F_n^2 is presented for convenience, versus $1/F_n^2$. R is the nondimensional wave resistance and F_n the (real) Froude number based on the length of the ship, i.e. $F_n = U(2gL)^{-1/2} = F\sqrt{2}$.

Again it can be noted that the wave resistance predicted by Hogner's approximation is the highest. Michell's approximation yields a slightly smaller value of the wave resistance. The zeroth approximation yields much smaller values and results obtained by Yim's method are slightly smaller than the latter.

It is interesting to note that the differences between Hogner and Michell on the one hand, and the zeroth approximation and Yim on the other hand, are comparable, and both much less than the difference between sa: "ogner

and the zeroth approximation. The results given by the
four methods are all in phase. The envelope of the maxima
is first increasing for values of F_n^{-2} comprised between
0 and 18, and then slowly decreasing.

The line integral can thus be seen to decrease the
value of the wave resistance. The small difference
between the results obtained by the zeroth approximation
and Yim's method indicate that the latter can be used to
obtain results close to the ones obtained by the zeroth
approximation but with much greater simplicity.

Figure (3-17) presents the results obtained for
$\gamma=0.6$ and the experimental results obtained by Shearer
[7]. At high values of the Froude number the results
given by the zeroth approximation are smaller than those
given by Hogner's approximation and closer to the
experimental results. But for $F_n^{-2}>9$, i.e. for $F_n<.33$,
the experimental results become larger than even results
obtained with Hogner's approximation, and much less
oscillatory.

Also, when F_n^{-2} increases, the difference between
the Hogner and the zeroth approximation decreases and
becomes negligible for $F_n^{-2}>16$ (which corresponds to $F_n=$
0.25). For a hull with very fine bow and stern, the
line integral does not change the wave resistance
appreciably.

Contrary to the case $\gamma=0$ where the envelope of the maximum was first increasing and then decreasing, for $\gamma=0.6$ this envelope decreases rapidly. We note that the experimental results decrease much less rapidly than the computed ones.

Figure (3-18) shows the results obtained for $\gamma=1$. The general configuration is the same as on Figure (3-17), for $\gamma=0.6$. There are negligible differences between the Hogner and the Michell approximations and only relatively small differences between the Hogner and the zeroth approximations. Again these differences decrease when F_n^{-2} increases. In this case, even at low values of F_n^{-2} (i.e. high values of F_n) the presence of the line integral does not bring a great improvement. The experimental results are less out of phase with the computed ones and, at high values of F_n^{-2}, much closer to the Hogner curve.

The results obtained for $\gamma=-0.2$ are shown on Figure (3-19). $\gamma=-0.2$ corresponds to a hull which is thicker than in the case $\gamma=0$. We see that the general shape of the wave resistance curves is different from the one we had with fine ends ($\gamma=0.6$ and $\gamma=1$).

It can be seen that the envelope of the maxima begins to increase. The difference between results obtained

with Hogner's formula and with the zeroth approximation
is much larger than before. The experimental results
are somewhere between the Hogner and the zeroth appro-
ximation curves for $0 < F_n^{-2} < 10$. For $F_n^{-2} > 10$ the experimental
results are much smaller than the computed ones, less
oscillatory and decreasing when F_n^{-2} increases.

In summary, it can be seen that for this family of
Wigley hulls, when the angle of entrance increases
i) the width of the spectrum $|K(t)|^2 (1+t^2)^{1/2}$ increases
for a given F and, ii) the influence of the line integral
increases.

III-2 Sharma's parabolic strut

We now consider a very thin body, defined by
the equation

$$y_0 = \pm b\left(1 - x^2\right) \tag{3-39}$$

where the nondimensional half beam b and draft d are
b = 0.05
d = 0.30
The wave resistance can be calculated by using equation
(3-18).

The Kochin free-wave spectrum function is now given by

$$K(t) = \int_0^1 x \cos\left(F^{-2} t (1+t^2)^{1/2} b (1-x^2)\right) \sin\left(F^{-2}(1+t^2)^{1/2} x\right) I \, dx \qquad (3-40)$$

where I is defined by

$$I = (1+t^2)^{-1} \left[1 - \exp\left(-F^{-2}(1+t^2)d\right) \right] - \frac{4b^2 x^2}{1+4b^2 x^2} \qquad (3-41)$$

(see Appendix VII for details).

Computations were performed by using the Michell and by the Yim approximations. In the Michell approximation, equation (3-40) and (3-41) become

$$K_M(t) = \int_0^1 x \sin\left(F^{-2}(1+t^2)^{1/2} x\right) I_M \, dx \qquad (3-42)$$

$$I_M = (1+t^2)^{-1} \left[1 - \exp\left(-F^{-2}(1+t^2)d\right) \right], \qquad (3-43)$$

While in the Yim approximation, we have

$$K_y(t) = \int_0^1 x \, \sin\left(F^{-2}(1+t^2)^{1/2} x\right) I_y \, dx \qquad (3\text{-}44)$$

$$I_y = (1+t^2)^{-1}\left[1 - \exp\left(-F^{-2}(1+t^2)d\right)\right] - \frac{4\,b^2\,x^2}{1+4\,b^2 x^2} \qquad (3\text{-}45)$$

Results are presented in Figure (3-20), together with the experimental data obtained by Sharma [13].

It can be seen that the effect of the line integral is very weak. The experimental results are in very good agreement with computed results for $0 < F_n^{-2} < 7$ and in good agreement for $7 < F_n^{-2} < 14$. The computed results are almost in phase with the experimental results. We also note that, for this fine hull, the envelope of the maxima decreases when F_n^{-2} increases. The half angle of entrance of this parabolic strut is of about 5.7°, compared to 4.5° for the Wigley hull with $\gamma = 0.6$. It is somewhat surprising to note that the computed wave resistance for both hulls decrease when F_n^{-2} increases (when oscillating of course) whereas the experimental wave resistance curve is seen to slightly increase for the Wigley hull and to decrease for the parabolic strut.

The results obtained for the parabolic strut are
consistent with those obtained previously for the Wigley
hulls. The influence of the line integral is seen to be
negligible for hulls which have extremely fine ends.

III-3 The Elliptic-parabolic hull

The mathematical hulls that were studied until now
suffered from unrealistic features. First, they all
had fore and aft symmetry. Secondly, they had fine ends,
whereas a real ship often had a blunt stern.

We expect the influence of the line integral to be
important for blunt bodies. To study in more detail
the influence of the waterline, a hull form was selected
which i) is analytically defined, ii) does not have fore
and aft symmetry, and iii) has a fine bow and a blunt
stern.

The hull which was chosen has elliptic cross-sections.
The waterline is parabolic in the fore part (for $0<x<a$,
see Figure (3-21)) and elliptic in the after part
$(a<x<1)$.
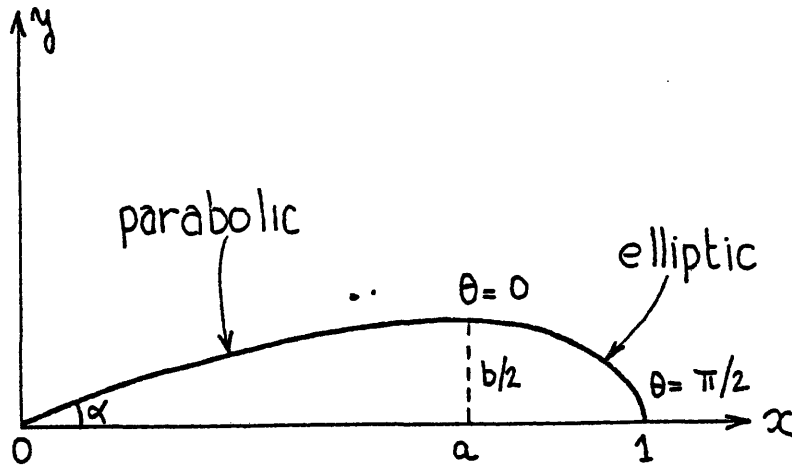
Figure 3-21

The hull surface is described by the following equations:

a.   In the fore part:

$$\mathcal{X} = x \tag{3-46}$$

$$y = b(x/a)(1 - x/2a)\sin\varphi \tag{3-47}$$

$$\gamma = -d\cos(\varphi) \tag{3-48}$$

for $0 \leq x \leq a$

and $0 \leq \phi \leq \pi/2$

b.   In the after part:

$$\mathcal{X} = a + (1-a)\sin\theta \tag{3-49}$$

$$y = b/2 \cos\theta \sin\phi \qquad (3\text{-}50)$$

$$z = -d \cos\phi \qquad (3\text{-}51)$$

for $0 \leq \theta \leq \pi/2$

and $0 \leq \phi \leq \pi/2$.

The curve $y(x)$ or $y(\theta)$ describing the waterline, is continuous and has a continuous slope at $x=a$, for any value of a. To insure that also the curvature be continuous at $x=a$, we must choose a so that

$$a = 1 \Big/ \left(1 + 1/\sqrt{2}\right) \simeq 0.586$$

The nondimensional beam b and draft d are respectively chosen as

b=0.15

d=0.05

The half angle of entrance is then $\alpha = 14°36''$

The nondimensional wave resistance R and the Kochin free-wave spectrum function are given by

$$R = 4\, b^2\, \pi^{-1}\, F^{-4} \int_0^\infty |K(t)|^2 (1+t^2)^{1/2}\, dt \qquad (3\text{-}52)$$

$$K(t) = a^{-1} \int_0^a \exp\left[-i F^{-2}(1+t^2)^{1/2} x\right](1 - x/a) I_1 \, dx$$

$$- 1/2 \, \exp\left(-i F^{-2}(1+t^2)^{1/2} a\right) \int_0^{\pi/2} \exp\left(-i F^{-2}(1+t^2)^{1/2}(1-a)\sin\theta\right) \sin\theta \, I_2 \, d\theta \qquad (3\text{-}53)$$

$$I_1 = d \int_0^{\pi/2} \exp\left(-\delta \cos\varphi\right) \cos\left(\beta_1 \, \delta \sin\varphi\right) \sin^2\varphi \, d\varphi - F^2 \cos\left(\beta_1 \delta\right) \frac{b^2(1 - x/a)^2}{a^2 + b^2(1 - x/a)^2} \qquad (3\text{-}54)$$

$$I_2 = d \int_0^{\pi/2} \exp\left(-\delta \cos\varphi\right) \cos\left(\beta_2 \, \delta \sin\varphi\right) \sin^2\varphi \, d\varphi - F^2 \cos\left(\beta_2 \delta\right) \frac{b^2 \sin^2\theta}{4(1-a)^2\cos^2\theta + b^2\sin^2\theta} \qquad (3\text{-}55)$$

$$\delta = d F^{-2}(1+t^2) \qquad (3\text{-}56)$$

$$\beta_1 = b a^{-1} d^{-1} t (1+t^2)^{-1/2} x(1 - x/2a) \qquad (3\text{-}57)$$

$$\beta_2 = b (2d)^{-1} t (1+t^2)^{-1/2} \cos\theta \qquad (3\text{-}58)$$

(see Appendix VIII).

The integral in equations (3-54) and (3-55) are evaluated by using a number of points C_1 and C_2 respectively, where

$$C_1 = 2 \, \text{INT}\left[2(b/a) F^{-2} t (1+t^2)^{1/2}\right] + 1 \qquad (3\text{-}59)$$

and
$$C_2 = 2 \text{ INT}\left[b F^{-2} t (1+t^2)^{1/2} \right] + 1 \qquad (3\text{-}60)$$

where INT stands for "integer part of." The expressions
for C_1 and C_2 were determined empirically by looking at
the shape of the function of ϕ which had to be integrated.

Similarly, it was found that the number of points C_x
and C_Θ say, necessary to evalute the integrals over x and
Θ respectively in equation (3-53) are given by

$$C_x = 2 \text{ INT}\left(1.5 \, F^{-2} (1+t^2)^{1/2} \right) + 1 \qquad (3\text{-}61)$$

$$C_\Theta = 2 \text{ INT}\left(2(1-a) F^{-2} (1+t^2)^{1/2} \right) + 1 \qquad (3\text{-}62)$$

To determine the number of points necessary to evaluate
the integral in equation (3-52) as well as the limit of
integration, t_F say, we plotted the function g(t) for
several values of the Froude number, where g(t) is
defined as

$$g(t) = |K(t)|^2 (1+t^2)^{1/2}.$$

These plots are presented on Figures (3-22) to (3-25) for
F=0.25, F=0.4, F=0.707 and F=1.

It can be readily seen that the behavior of g(t) is
different from what it was for the Wigley hulls.

While still oscillating, the function g(t) does
not vanish any more at the minima. This is due to the
fact that the hull does not have fore and aft symmetry.
The function g(t) is now less oscillating than for.·
the Wigley hulls. This is particulary striking at low
Froude numbers. Also, g(t) becomes negligible at
values of t_F which are much larger than those found for
the Wigley hull. (It is interesting to compare these
results with those obtained for the Wigley hull with
$\gamma=0$. This hull had the same entrance angle as the hull
now considered. It was somewhat thinner at the mid-
shipsection and much deeper.)

The limit of integration t_F and the number of points
N_t necessary to integrate g(t) was found to be accurately
predicted by the following empirical formulas:

$$t_F = 16\,F \tag{3-63}$$

$$N_t = 2\,\text{INT}\left(6/F\right) + 1 \tag{3-64}$$

The results for the wave resistance are presented in
Figure (3-26).

The Hogner approximation (H) and the corresponding
Michell thin ship approximation (M) may be seen to be
very close to eachother, as for the Wigley hull ($\gamma=0$)
(although the Michell curve is here very slightly above,
rather than below, the Hogner curve). The zeroth-order
approximation (0) and its corresponding Yim thin-ship
approximation (Y), on the other hand, are very far apart
(more precisely, the Yim curve is much higher than the
zeroth order curve), which is at variance with the
results obtained for the Wigley hull ($\gamma=0$). The fact
that the Yim curve (Y) is quite different (much higher)
than the zeroth-order curve (0) mainly stems from the
use of the thin-ship approximation in the waterline
integral, rather than the hull integral. Indeed
differences between the zeroth-order curve (0) and the
curve (MW), which corresponds to the use of the thin-
ship approximation in the hull integral alone (that is,
the thin-ship approximation y=0 is not used in the
waterline integral) remain moderate, although larger
than the differences between the Hogner and Michell curves
and increasing with decreasing Froude number. Furthermore,
differences between the curve (w), which corresponds to
the use of the waterline integral alone (that is, the
hull integral is neglected) in Formula (3-21), and its
corresponding thin-ship approximation (w_0) are very

large; more precisely, the curve (w_0) is much higher than the curve (W), and this may explain why the Yim curve (Y) is much higher than the curve (0). Comparison between the curves (W) and (M), and between the curves (w_0) and (M) also demonstrate the primordial importance of the waterline integral. It may finally be noted that (due to the waterline integral) the differences between the Michell approximation (M) and the zeroth-order approximation (0) are quite large. In particular, the Michell curve is lower than the zeroth-order curve for sufficiently high values of the Froude number (for $1/F_n^2 < 39$, i.e. for $F_n > .16$, approximately), while the opposite is true for sufficiently low speed (for $1/F_n^2 > 55$, i.e. for $F_n < .13$ approximately). An appreciable phase shift between the Michell and the zeroth-order curves may also be observed.

The fact that the line integral has a relatively small influence for the very fine-ended hull forms (Wigley, Sharma) and a very large influence for a blunt-ended form may be verified by a crude "order of magnitude analysis." For a fine-ended hull, if we denote by β and δ the beam/length ratio and the draft/length ratio, respectively , the terms n_x and τ_y in formula (3-2) may be shown to be of order β, and the hull

integral and the waterline integral can be seen to be
of order $\beta\delta$ and β^3, respectively, so that the waterline
integral is "an order of magnitude smaller" than the
hull integral.

For a blunt-ended form, the terms n_x and τ_y are
of order 1 at the ship stern or (and) bow (over a width
of order β), and the hull and waterline integrals in
formula (3-2) are of order $\beta\delta$ and β respectively, so
that the waterline integral now is "an order of magnitude
larger" than the hull integral.

This order of magnitude analysis regarding the
relative importance of the hull and the waterline inte-
grals (and thus the conclusion that the waterline
integral is an order of magnitude smaller or larger
than the hull integral for a slender hull with fine or
blunt ends, respectively) is based entirely upon "geo-
metrical arguments," which evidently ignore any possible
influence of the Froude number. One would, however,
espect the relative importance of the hull and .the
waterline integrals in formula (3-2) to depend on the
Froude number, as well as on the shape of the hull.
Indeed, in the limit $F\to0$, the hull and the waterline
integrals can be proved to be asymptotically equivalent

[3], which results in a drastic reduction in the
wave resistance. This reduction in wave resistance
at low Froude number may in fact be observed in
Figure (3-26), where the zeroth-order curve (0) is
significantly below both the Hogner "hull-integral-
alone" curve (H) and the "waterline-integral-alone"
curve (W) for $1/F^2 > 56$, i.e. for $F < 0.13$. One must
also expect the waterline integral to be primordial
in the high-Froude-number limit. Indeed, formula
(3-3) shows that we have $E \simeq 1$ as $F \to \infty$, so that formula
(3-2) yields

$$K(t) \simeq -F^2 \int_c n_x^2 \, z_y \, d\ell + \int_h n_x \, da \qquad as \quad F \to \infty \, ; \, t < \infty$$

The hull integral in the above formula can readily
be shown to be identically zero for any closed hull,
while the waterline integral vanishes for a waterline
with fore and aft symmetry. In summary, the waterline
integral may be seen to be important for blunt ship
forms, and in the low and high-Froude-number limits.

CONCLUSION

For fine-ended hull forms, differences between the
Michell, the Hogner, and the zeroth order slender-ship
approximations have been found to be relatively small,
although not negligible. More precisely, the Hogner
wave-resistance is slightly larger than the Michell
resistance while the zeroth-order resistance is somewhat
lower than Michell's.

However, quite different results have been obtained
for the blunt-ended hull form examined in the last
chapter. Specifically, the effect of the waterline
integral has been shown to be predominant, and differences
between the zeroth-order approximation and the Hogner
and the Michell approximations are considerable.

Comparison between theoretical predictions and
experimental measurements for the fine parabolic strut
of Sharma show reasonably good agreement, although there
are appreciable discrepancies. The corresponding com-
parison for the family of Wigley hull forms however appears
to be less conclusive. In particular, very large dis-
crepencies have been found for the two largest entrance
angles. It must however be noted that the experimental
results for the three Wigley hull forms do not appear

to be entirely consistent, so that the accuracy of
the measurements may be questionable.

BIBLIOGRAPHY

1. F. Noblesse., "Potential Theory of steady motion
    of ships Parts 1 and 2," Massachusetts Institute
    of Technology, Department of Ocean Engineering,
    Report No. 78-4, September 1978.

2. F. Noblesse, "Potential theory of steady motion
    of ships, Part 3: wave resistance," Massachusetts
    Institute of Technology, Department of Ocean
    Engineering, Report No. 78-5, November 1978.

3. F. Noblesse, "Theory of steady motion of ships,
    Part 4: Low Froude-number approximations,"
    Massachusetts Institute of Technology, Department
    of Ocean Engineering, Report No. 79-1, May 1979.

4. B. Yim, "Simple calculation of sheltering effect
    on wave resistance of low speed ships," Workshop
    on Wave Resistance Computations, David Taylor
    Naval Ship Research and Development Center,
    Bethesda, MD, November 1979.

5. P. Koch and F. Noblesse, "Wave resistance of the
    Wigley and Inui hull forms predicted by two simple
    slender-ship wave resistance formulas," Workshop
    on Wave Resistance Computations, David Taylor Naval
    Ship Research and Development Center, Bethesda, MD,
    November 1979.

6. W.C.S. Wigley, "Calculated and measured wave
    resistance of a series of forms defined algebraically,
    the prismatic coefficient and angle of entrance
    being varied independently," TRANS INA, 1967,
    pp52-74.

7. J.R. Shearer, "A preliminary investigation of the
    discrepancies between the calculated and measured
    wavemaking of hull forms," Trans. NECI, 1950-51,
    pp.43-68.

8. C.W. Dawson, "Calculations with the XYZ free surface program for five ship models," Workshop on Wave Resistance Computations, David Taylor Naval Ship Research and Development Center, Bethesda, MD, November 1979.

9. K.J. Bai, "Wave resistance in a restricted water by the localized finite element method," Workshop on Wave Resistance Computations, David Taylor Naval Ship Research and Development Center, Bethesda, MD, November 1979.

10. M.S. Chang, "Wave resistance predictions using a singularity method," Workshop on Wave Resistance Computations, David Taylor Naval Ship Research and Development Center, Bethesda, MD, November 1979.

11. C. Wigley, "The wave resistance of ships: a comparison between calculation and measurement for a series of forms," Congres International des Ingenieurs navals, Liege, 1939.

12. Table of Integrals, series and products. I.S. Gradshitcyn, F.M. Ryzhik.

13. S.D. Sharma, "Some results concerning the wavemaking of a thin ship," Journal of Ship Research, March 1969, Vol. 13, pp.72,81.
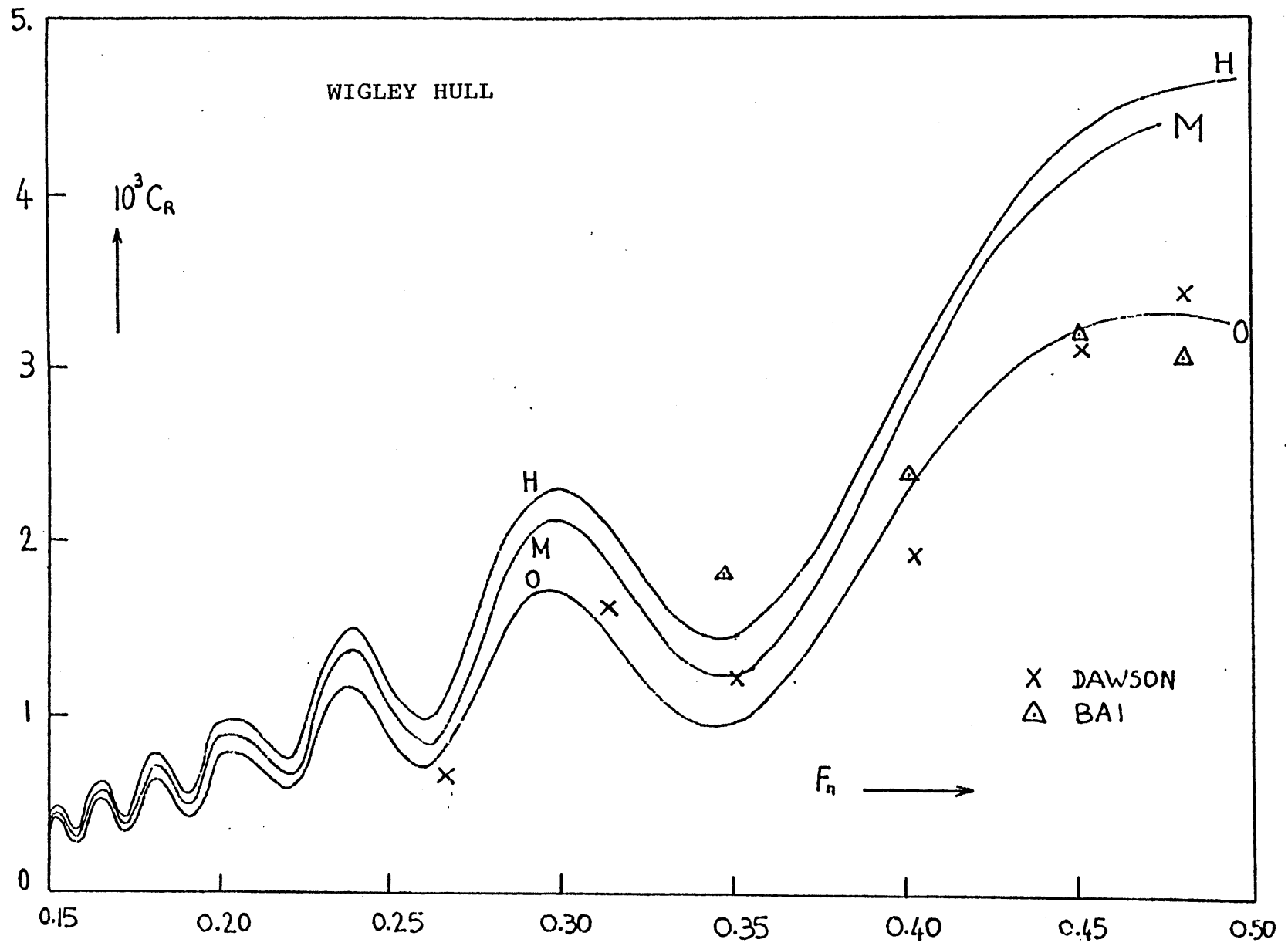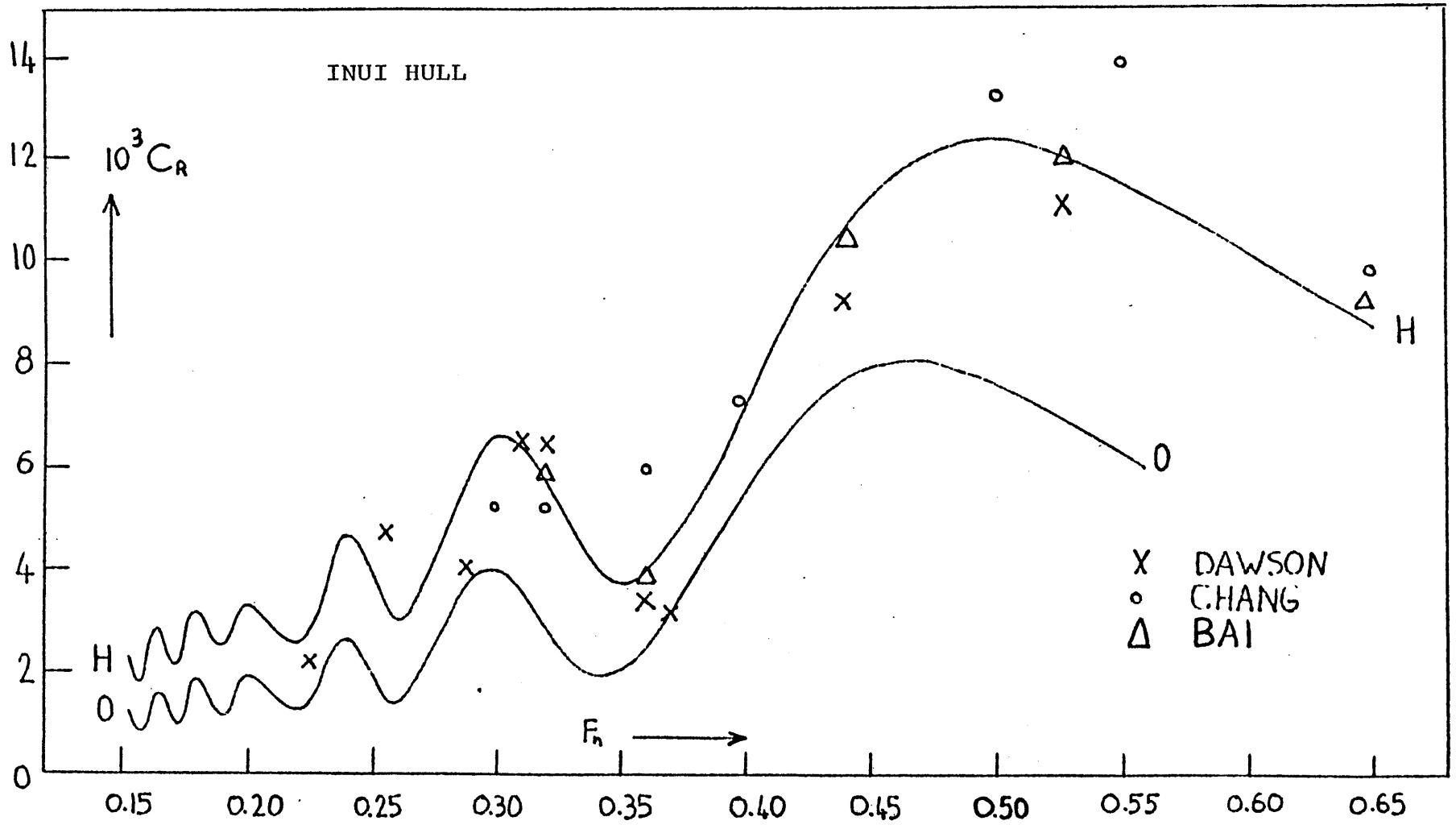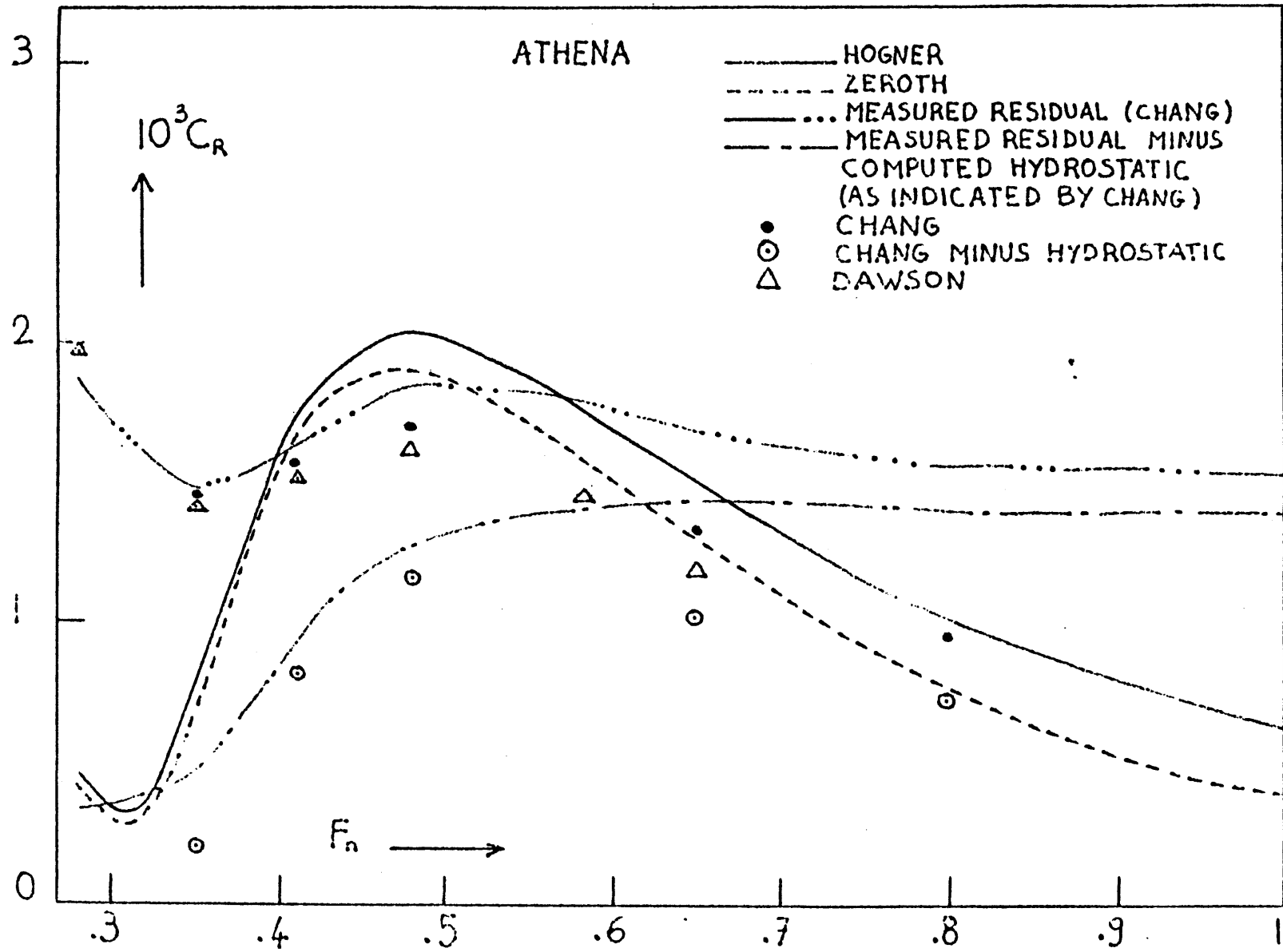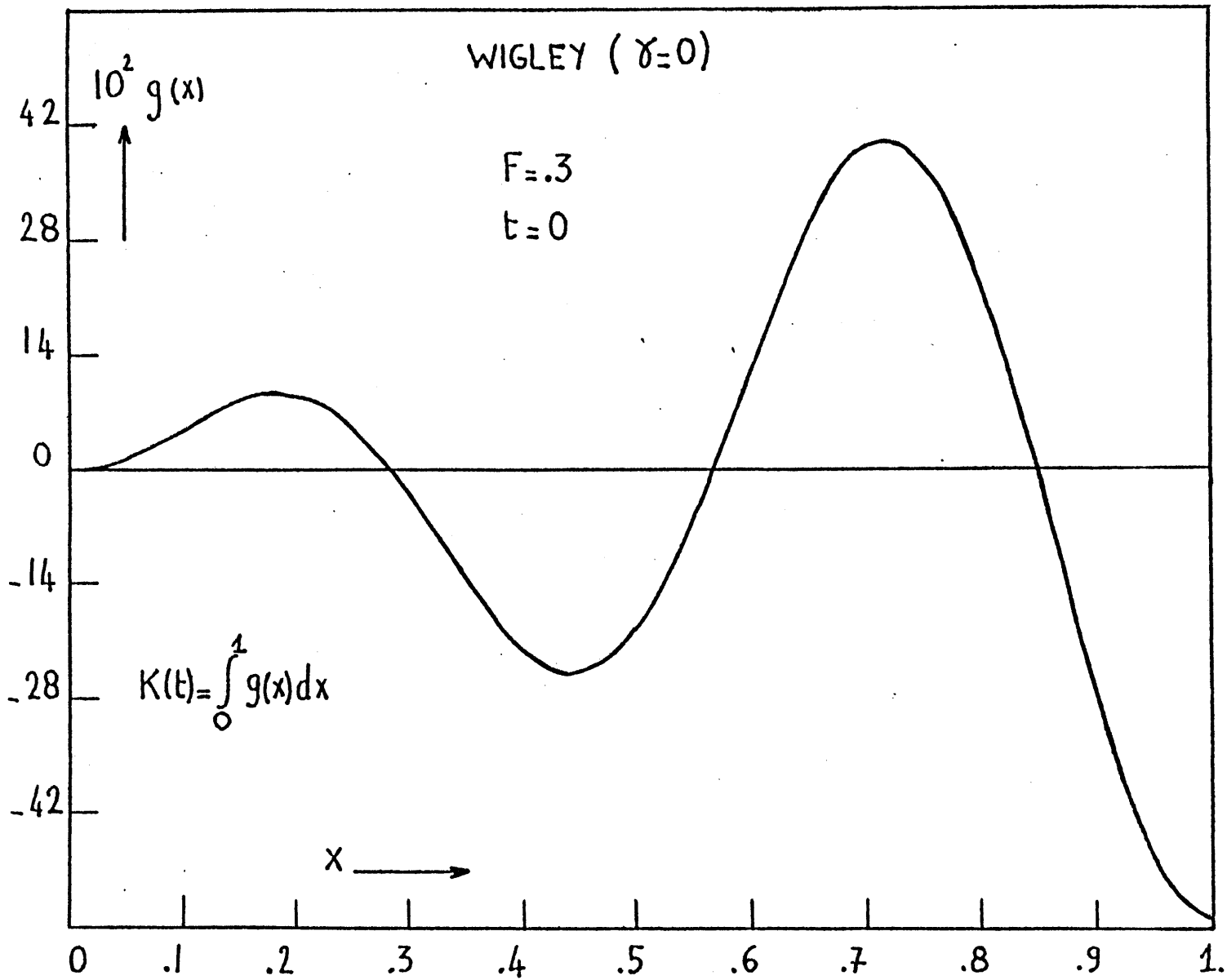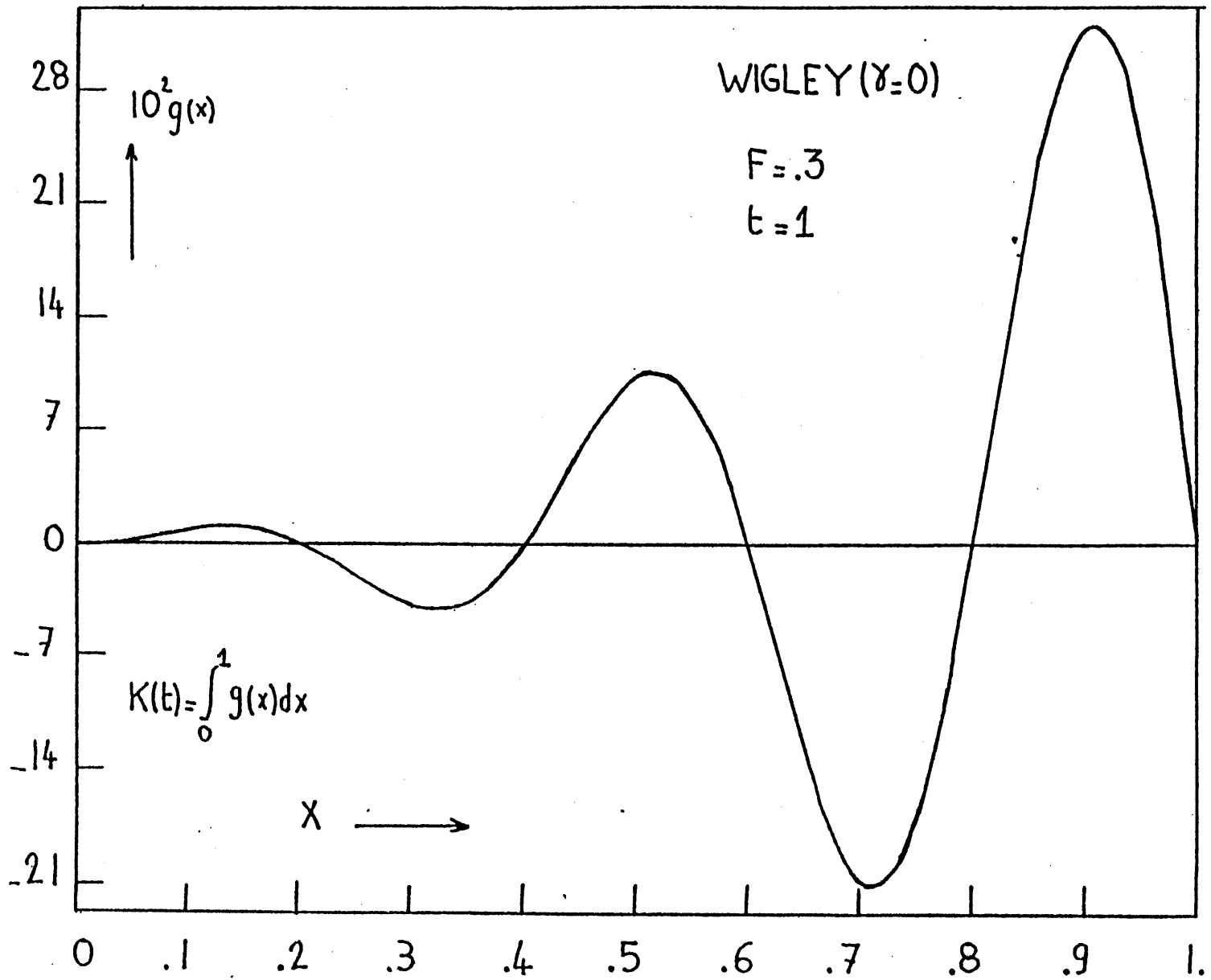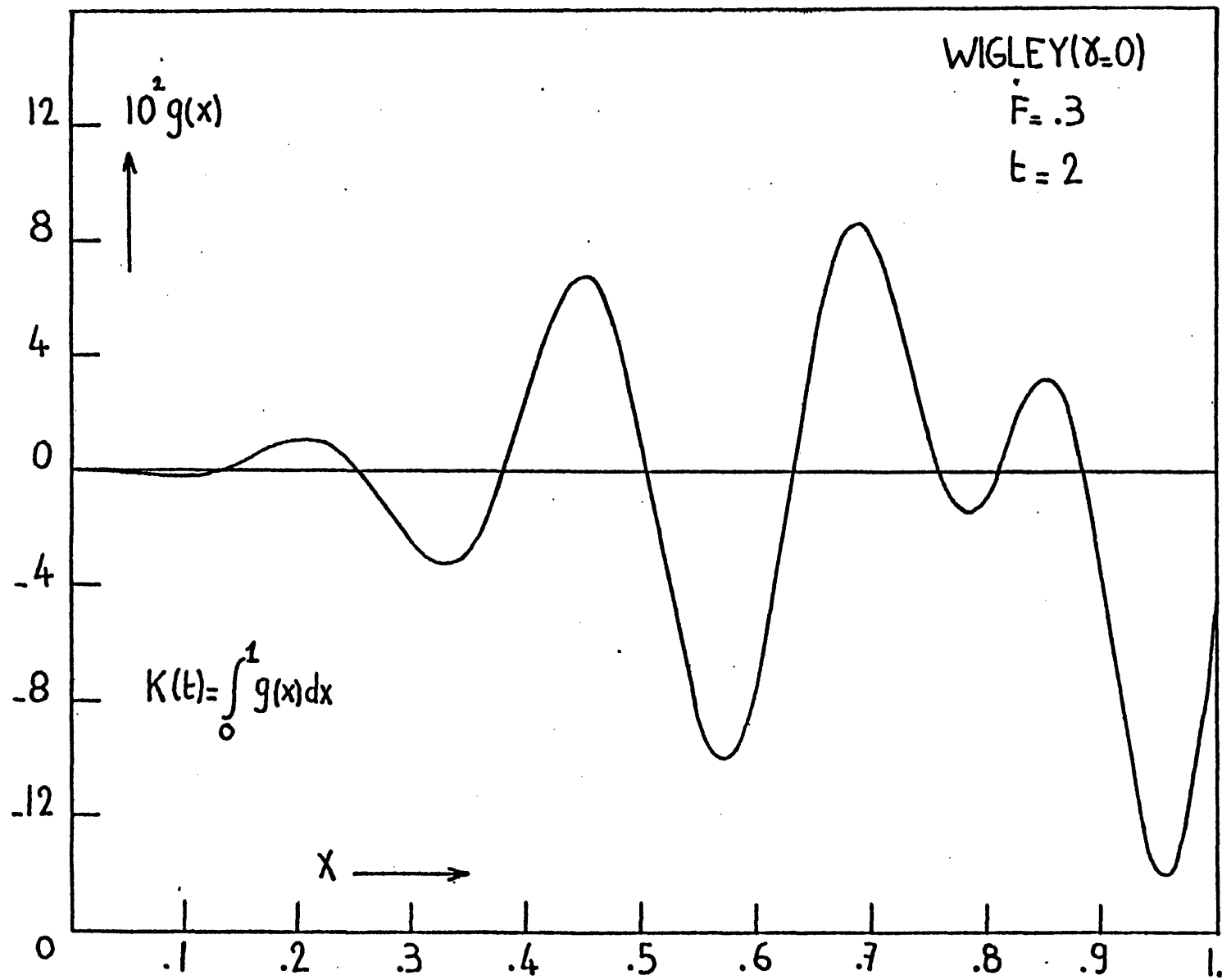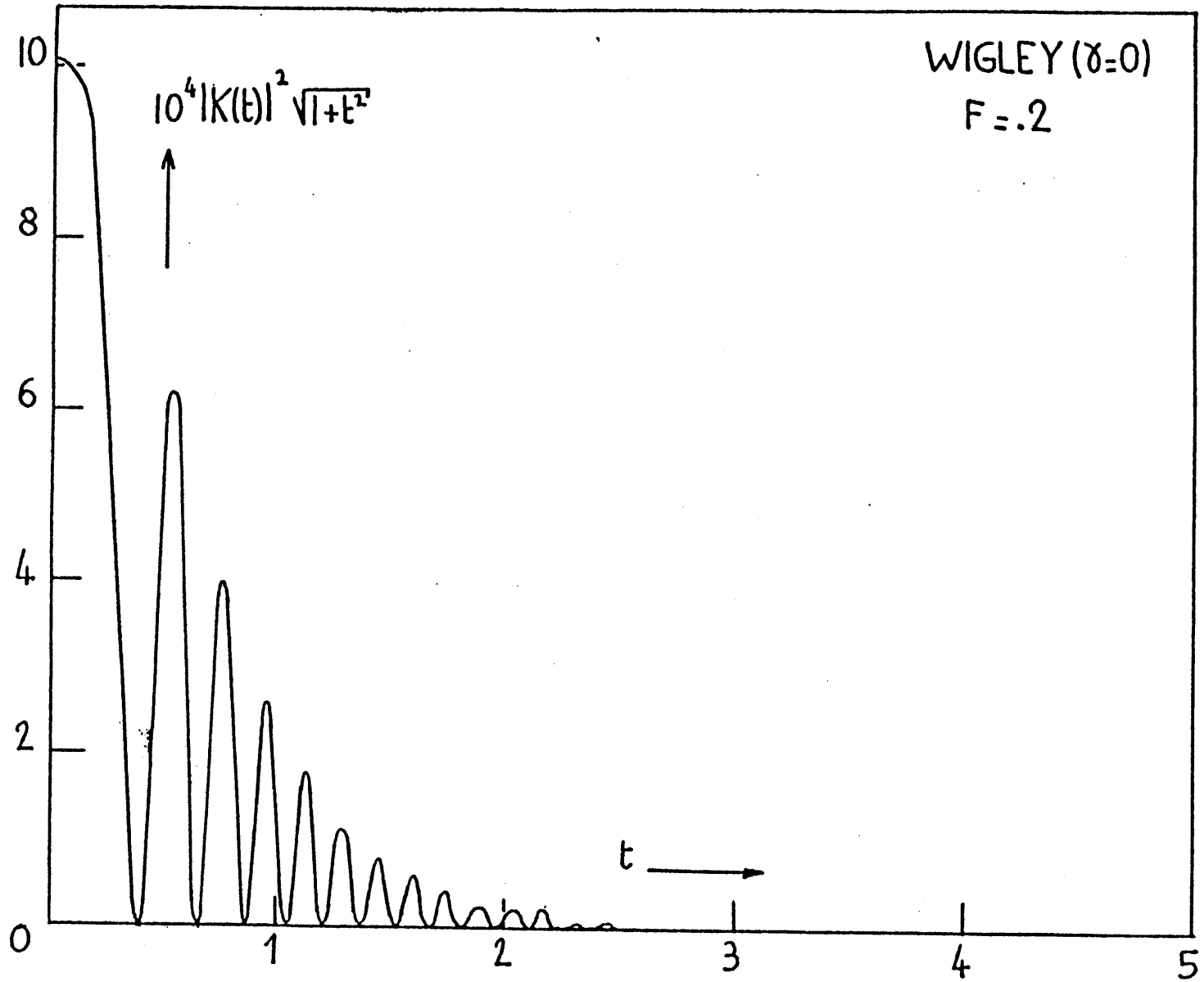
Figure 2-4

-62-

INUI HULL

$10^3 C_R$

F_n

X DAWSON
o C.HANG
△ BAI

H

0

Figure 2-7

-64-

WIGLEY ($\gamma=0$)

$10^2 g(x)$

F=.3

t=0

$K(t) = \int_0^1 g(x)dx$

X →

Figure 3-3

WIGLEY ($\gamma=0$)

F=.3

t=1

$10^2 g(x)$

$K(t) = \int_0^1 g(x)\,dx$

X $\longrightarrow$

WIGLEY($\gamma=0$)

$\dot{F}=.3$

$t=2$

$10^2 g(x)$

$K(t)=\int_0^1 g(x)dx$

$X \longrightarrow$

$10^4 |K(t)|^2 \sqrt{1+t^2}$

WIGLEY $(\gamma=0)$

$F = .2$

t

$$10^4 \ |K(t)|^2 \ \sqrt{1+t^2}$$

WIGLEY $(\gamma=0)$

F=.3

Figure 3-7

$10^4 |K(t)|^2 \sqrt{1+t^2}$

WIGLEY (γ_0)

$F_{=.4}$

$t \longrightarrow$

Figure 3-8

WIGLEY $(\gamma = 0)$

$F = .5$

$10^4 |K(t)|^2 \sqrt{1+t^2}$

Figure 3-9

$$10^5 |K(t)|^2 \sqrt{1+t^2}$$

WIGLEY $(\gamma=0)$
$F=1$

$t \longrightarrow$

Figure 3-10

WIGLEY $(\gamma = 1)$

$F = .3$

$10^4 |K(t)|^2 \sqrt{1+t^2}$

$t \longrightarrow$

Figure 3-11

WIGLEY ($\gamma=1$)
F=.5

$10^3|K(t)|^2 \sqrt{1+t^2}$

Figure 3-12

WIGLEY ($\gamma = 1$)
F = 1

$10^4 |K(t)|^2 \sqrt{1+t^2}$

Figure 3-13

WIGLEY $(\gamma = -.2)$
$F = .3$

$10^4 |K(t)|^2 \sqrt{1+t^2}$

$t \longrightarrow$

Figure 3-15

WIGLEY $(x=-.2)$

$F=1$

$10^4 \, |K(f)|^2 \, \sqrt{1+f^2}$

f

0 1 2 3 4 5 6 7 8 9 10

3.5 4 10.5

WIGLEY HULL

$10^3 r/F^2$

$1/F^2$

Hogner (H) —————
Michell (M) - - - - -
Zeroth (O) — — —
Yim (Y) ·····

Figure 3-16

-78-
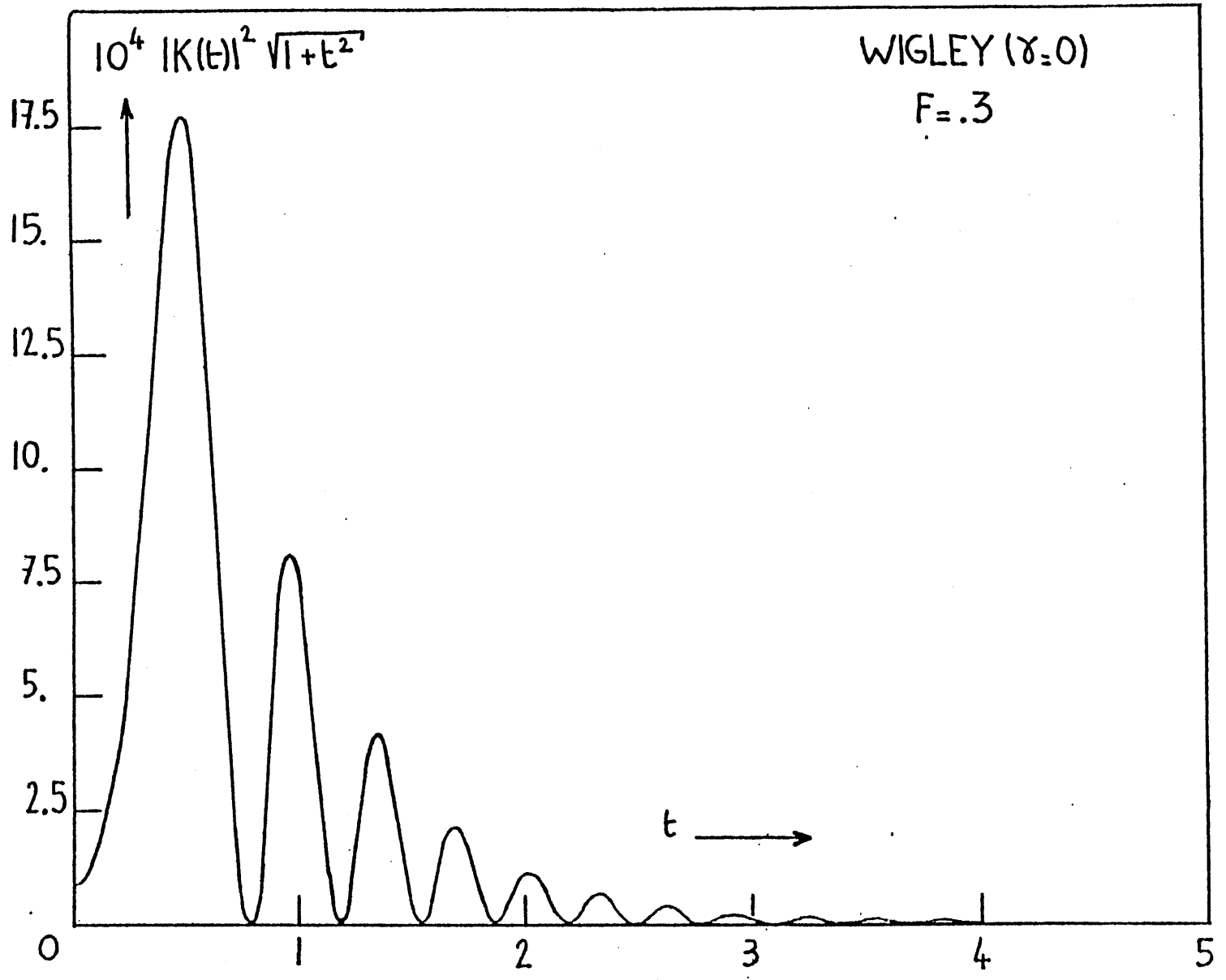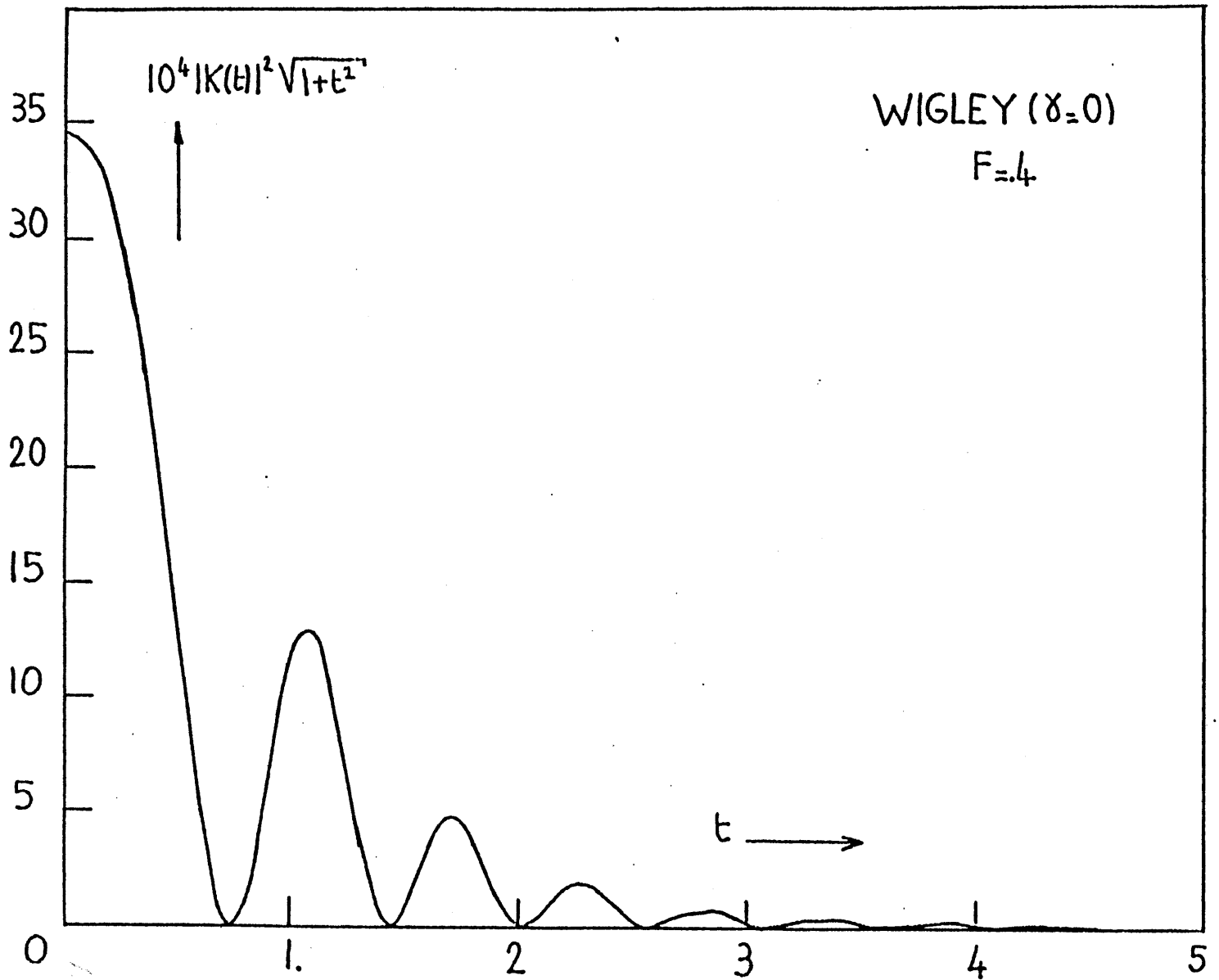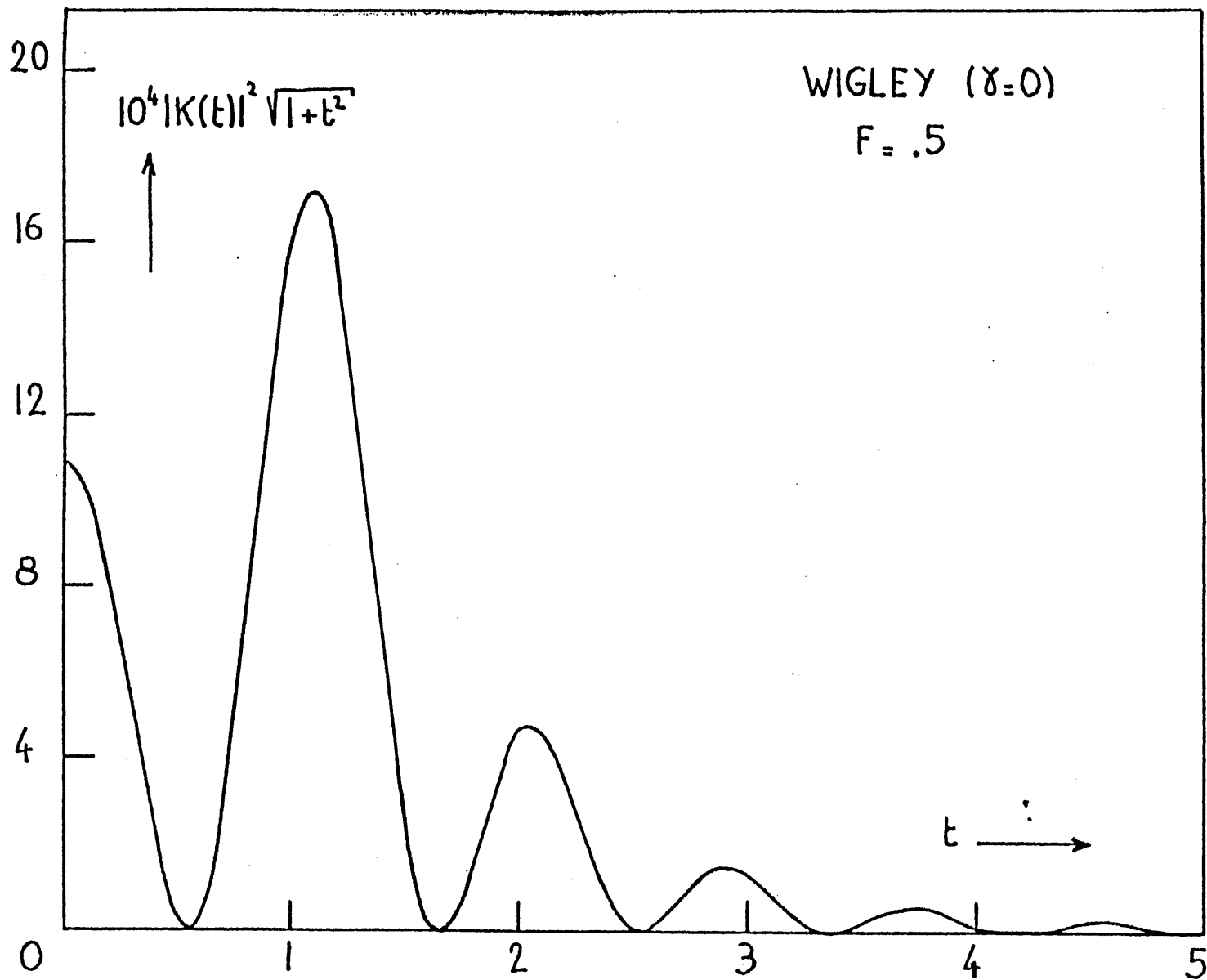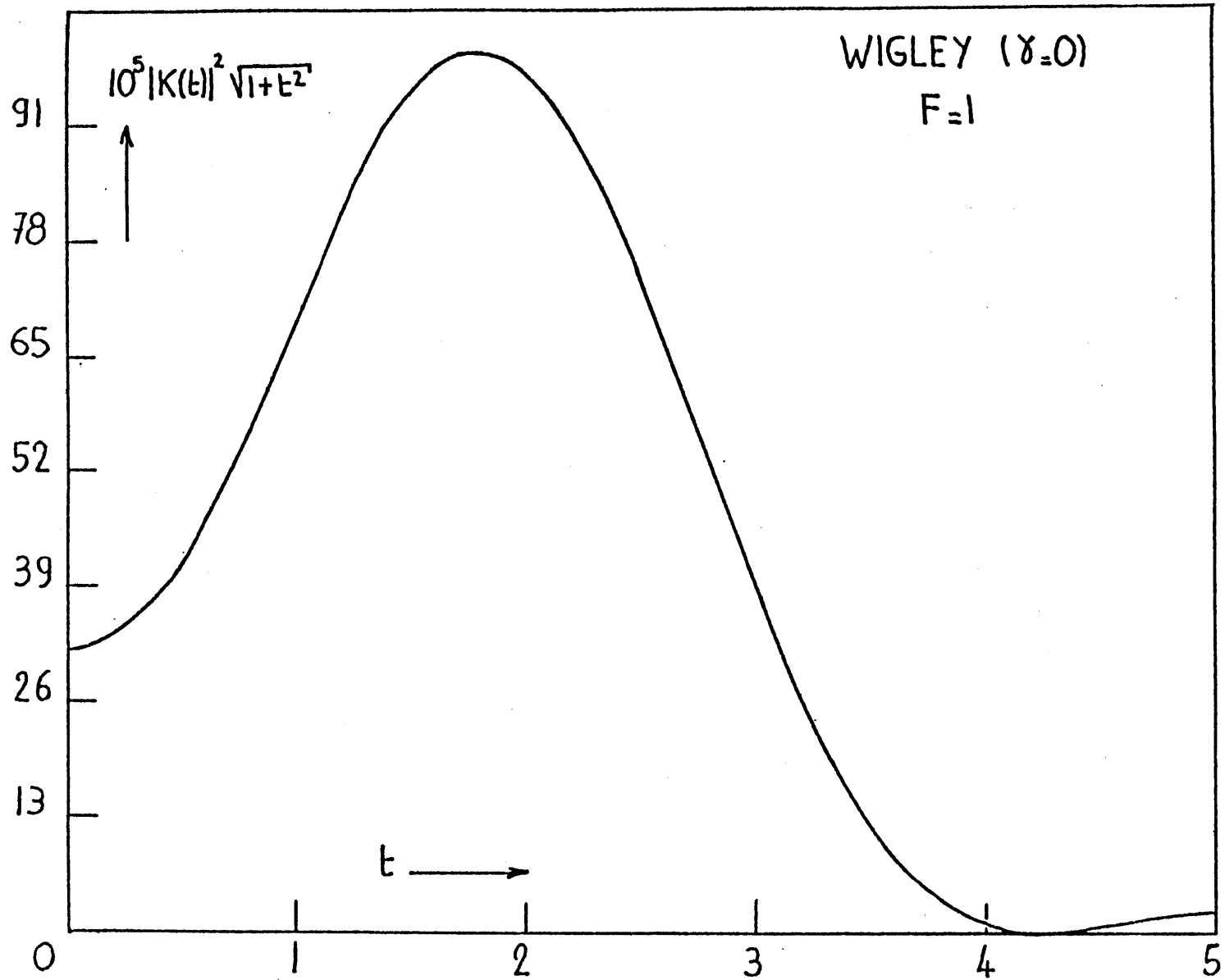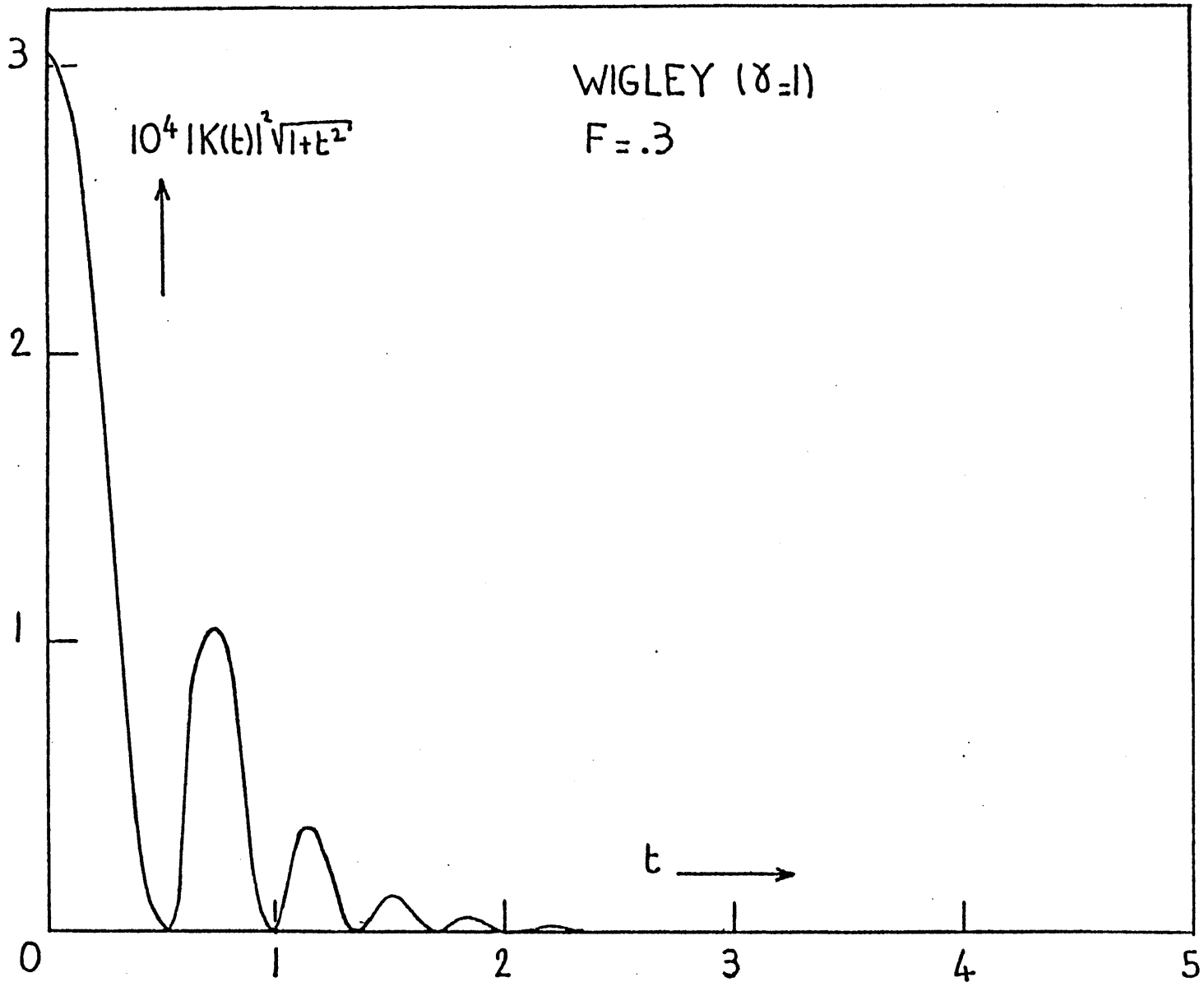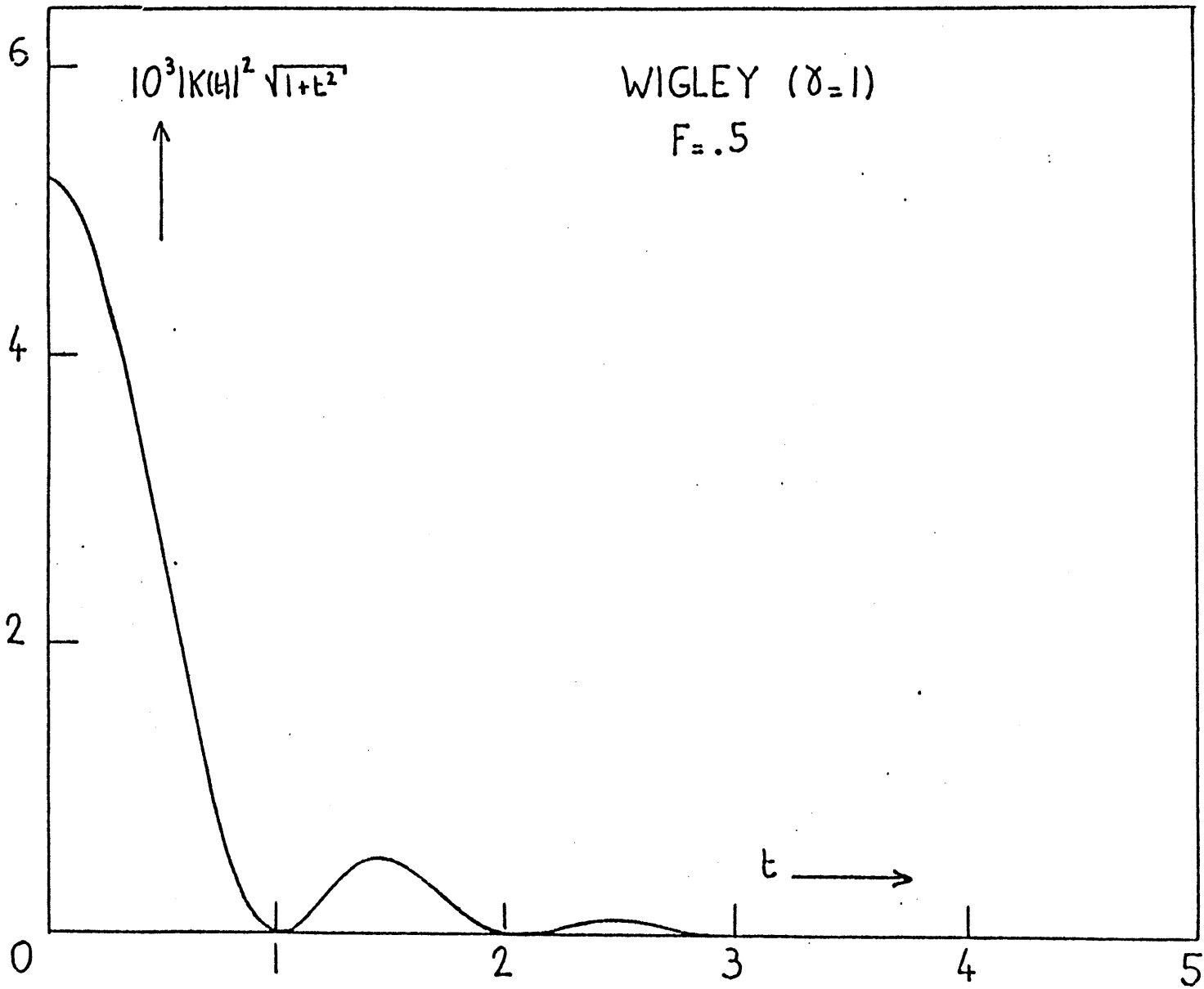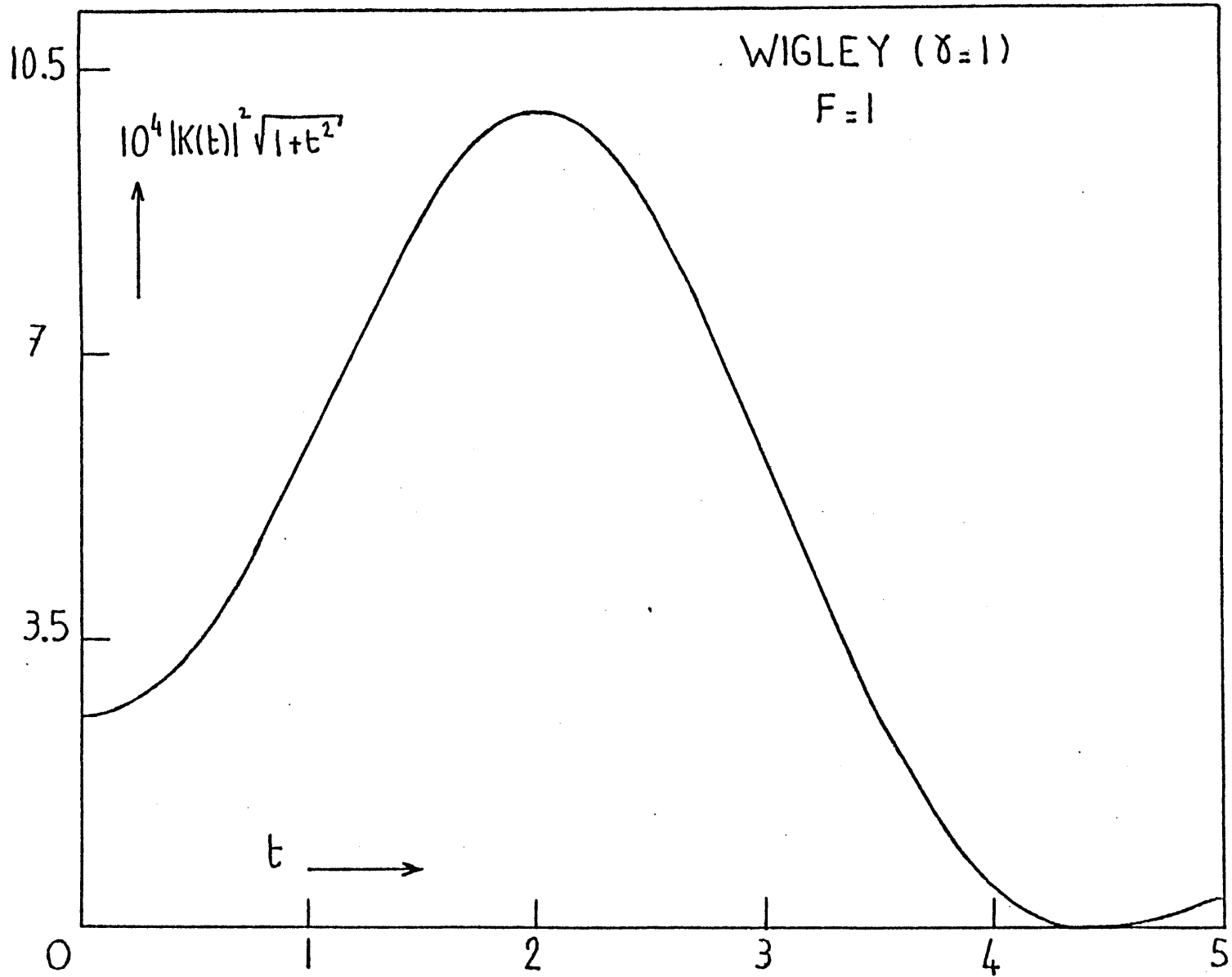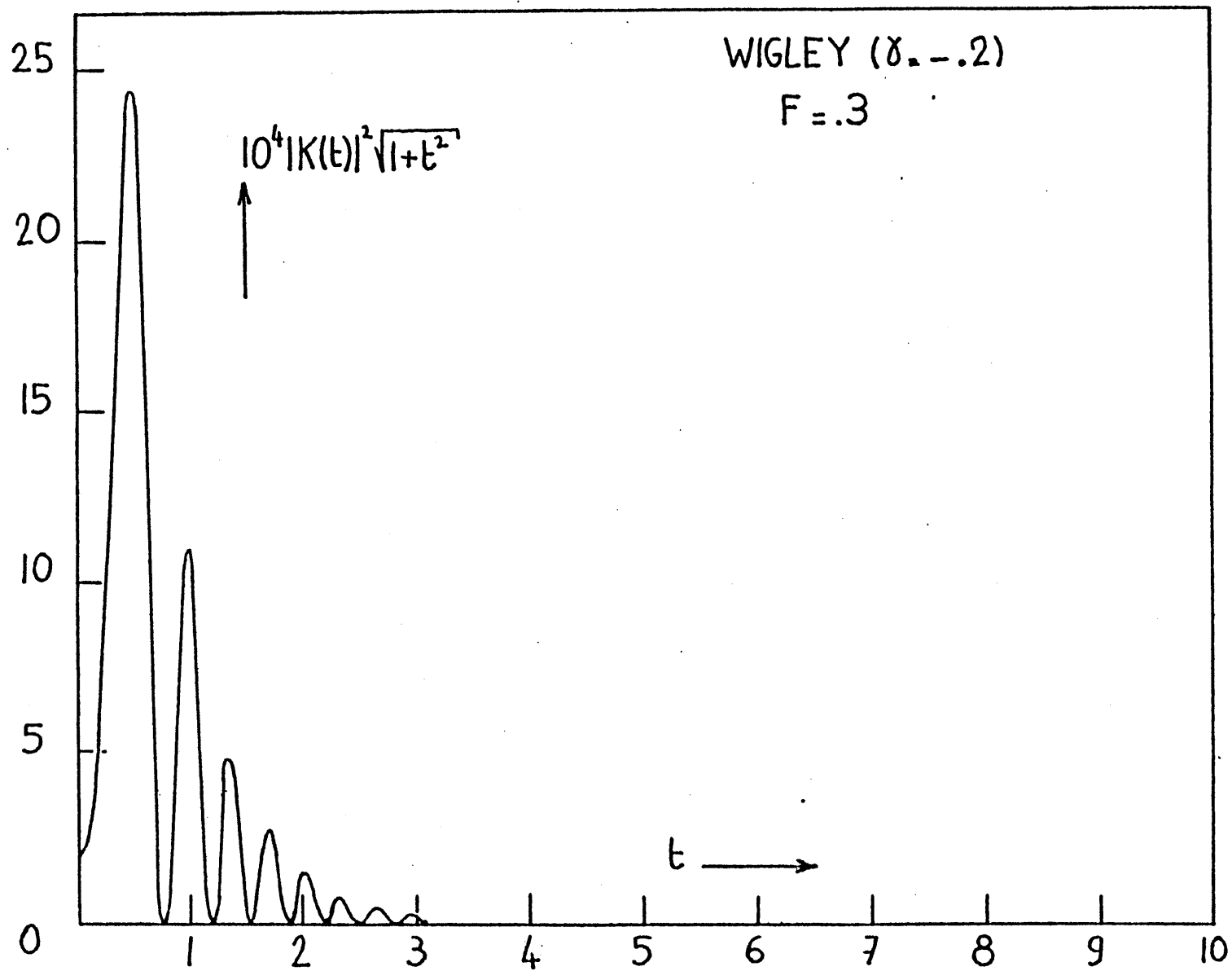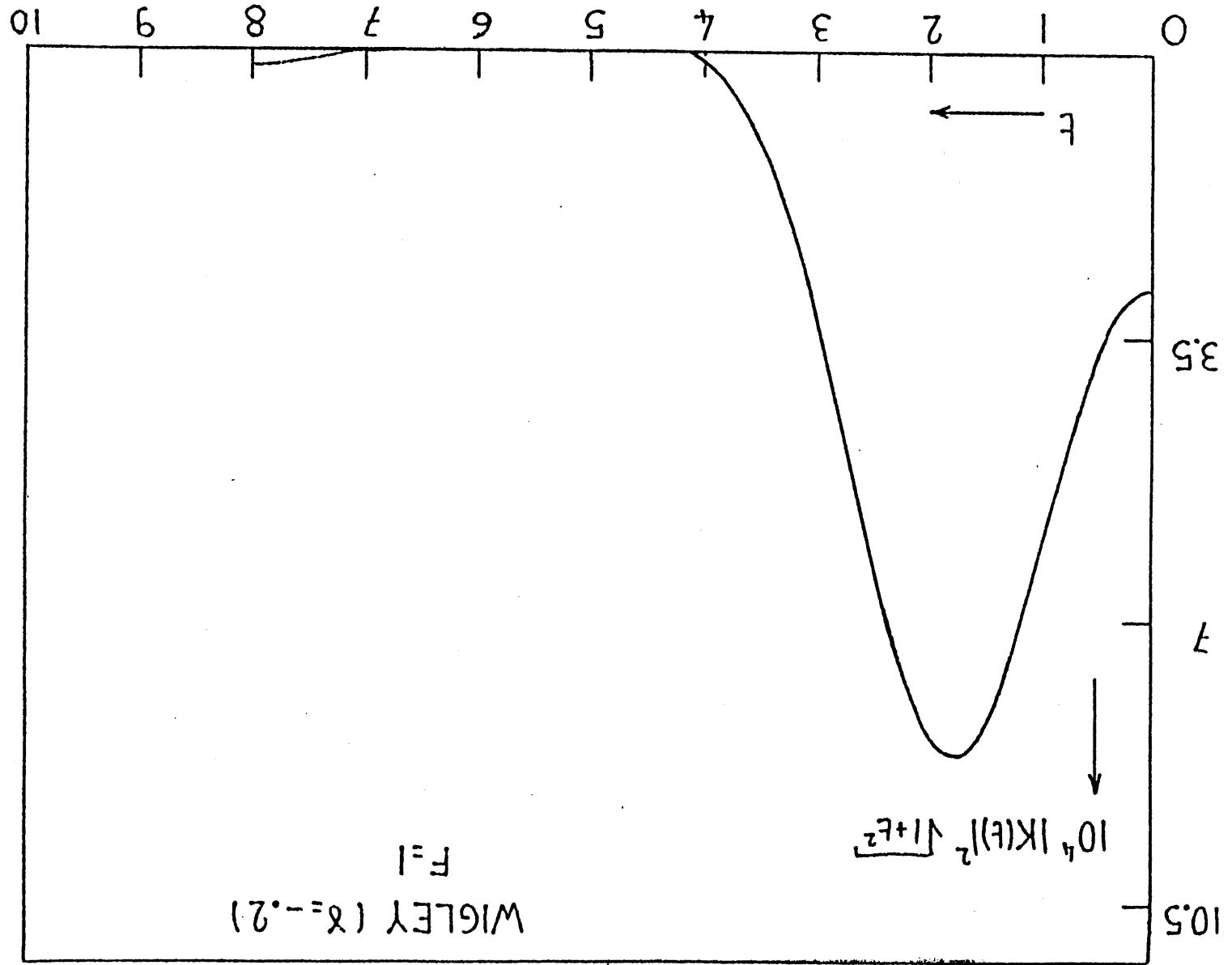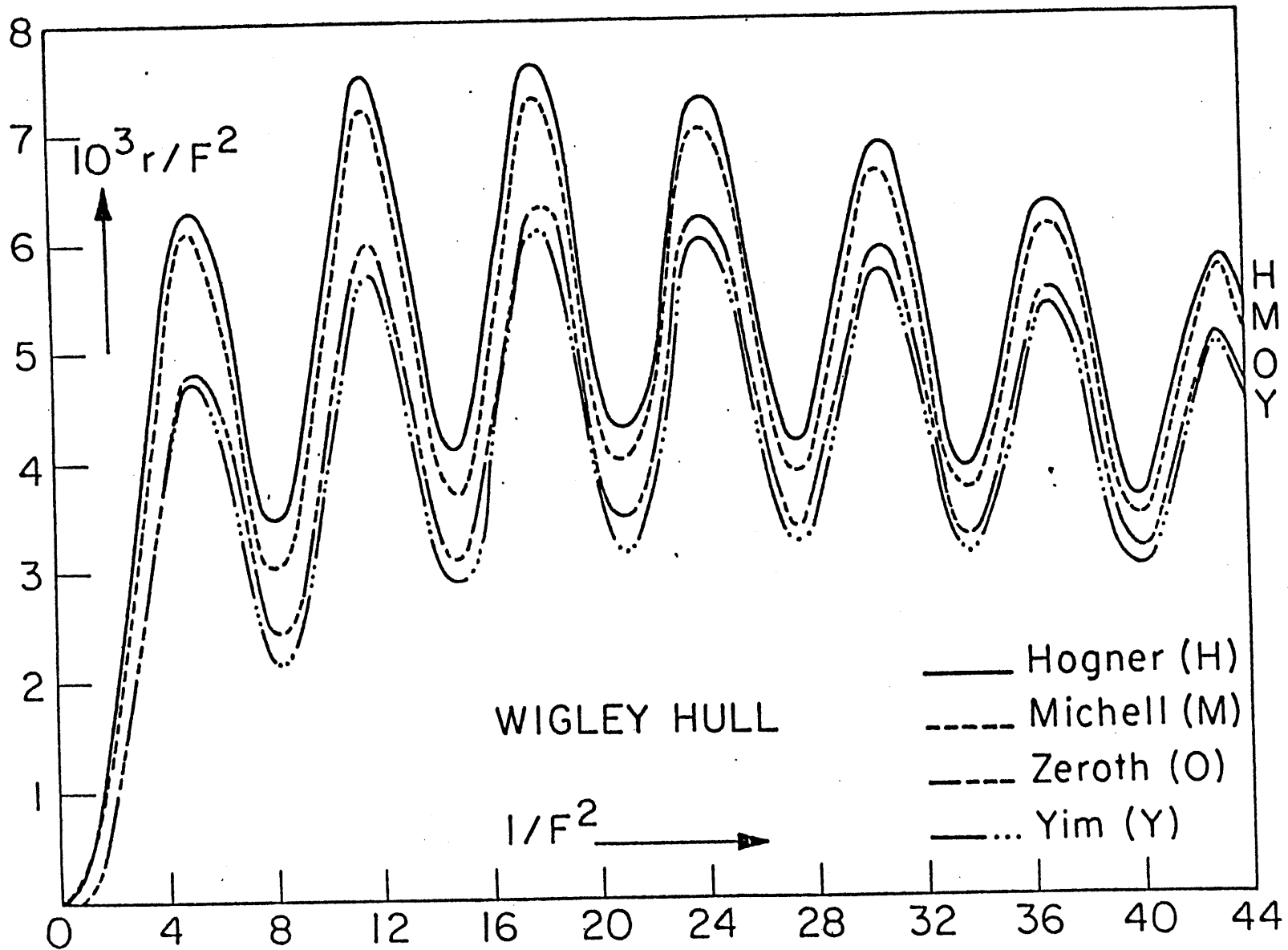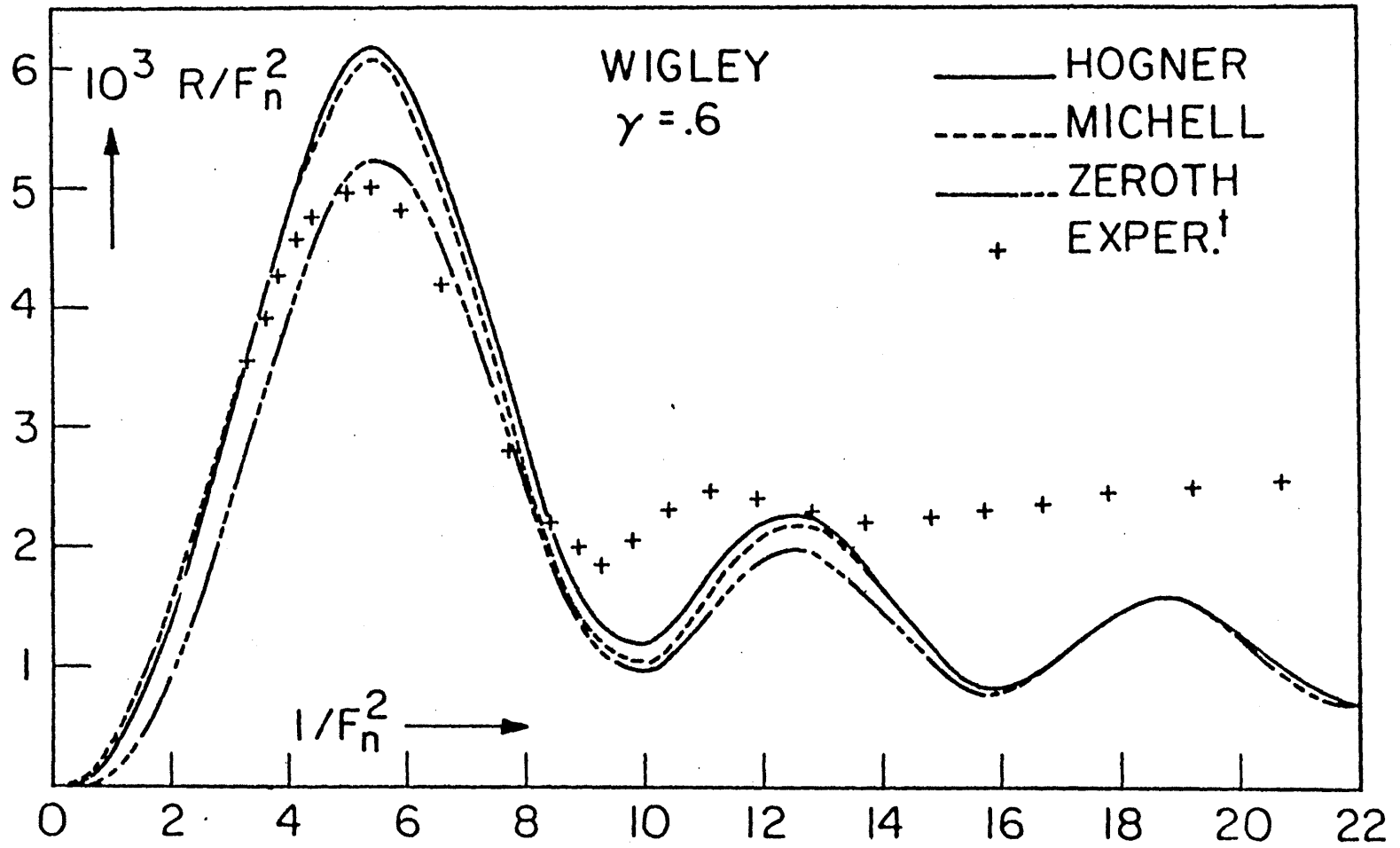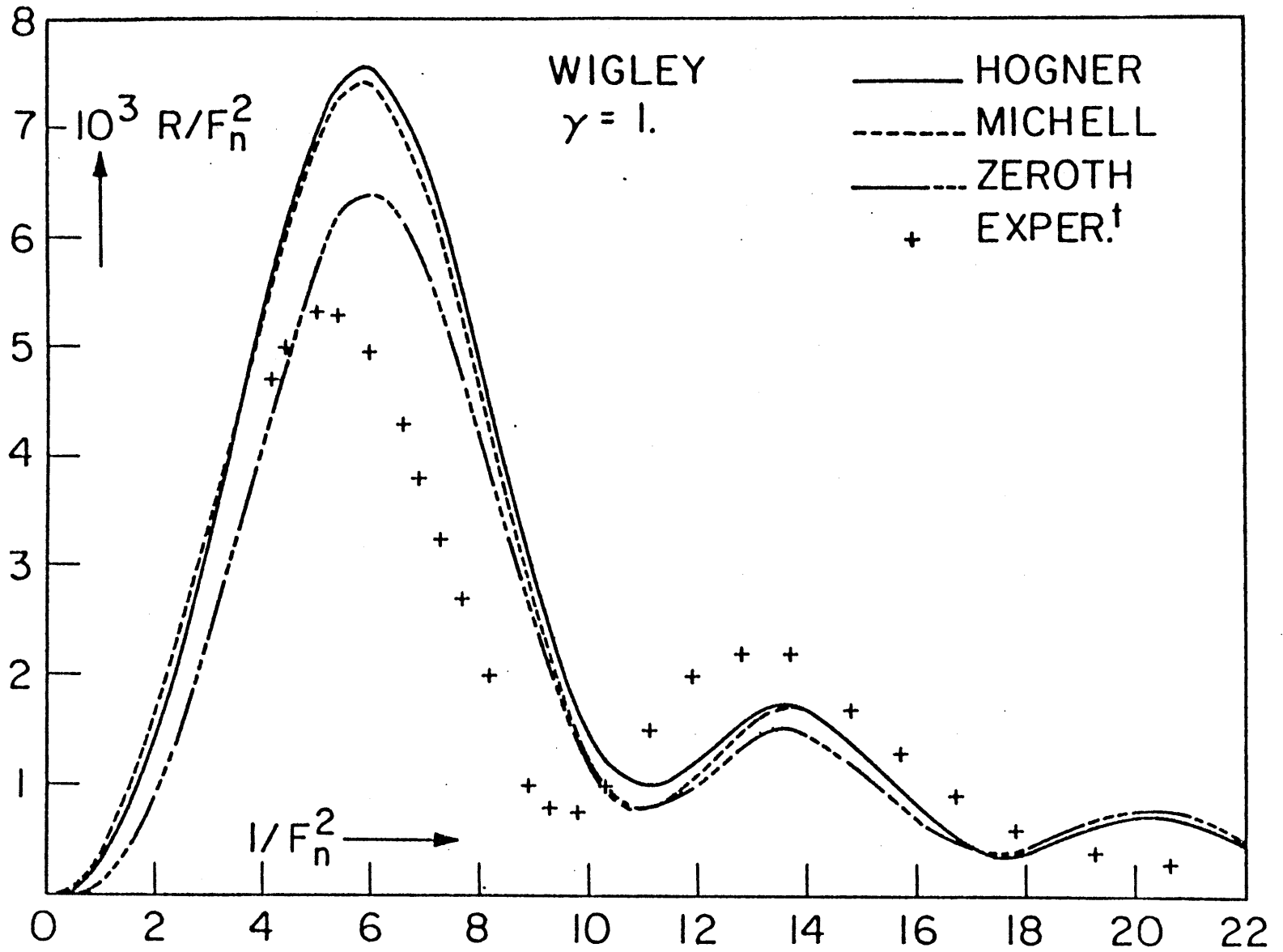
Figure 3-17

Figure 3-18

Figure 3-19

Figure 3-20

$10^6 |k(t)|^2 \sqrt{1+t^2}$

PARABOLIC ELLIPTIC

F = .25

Figure 3-22

PARABOLIC ELLIPTIC
$F = .4$

$10^4 |K(t)|^2 \sqrt{1+t^2}$

$t \longrightarrow$

PARABOLIC ELLIPTIC
F = .707

$10^3 |K(t)|^2 \sqrt{1+t^2}$

t ⟶

PARABOLIC ELLIPTIC

$F = 1$

$$10^2 |K(t)|^2 \sqrt{1+t^2}$$

$t \longrightarrow$

$10^2 r/2F^2(1+2F^2)$

$1/2F^2 \longrightarrow$
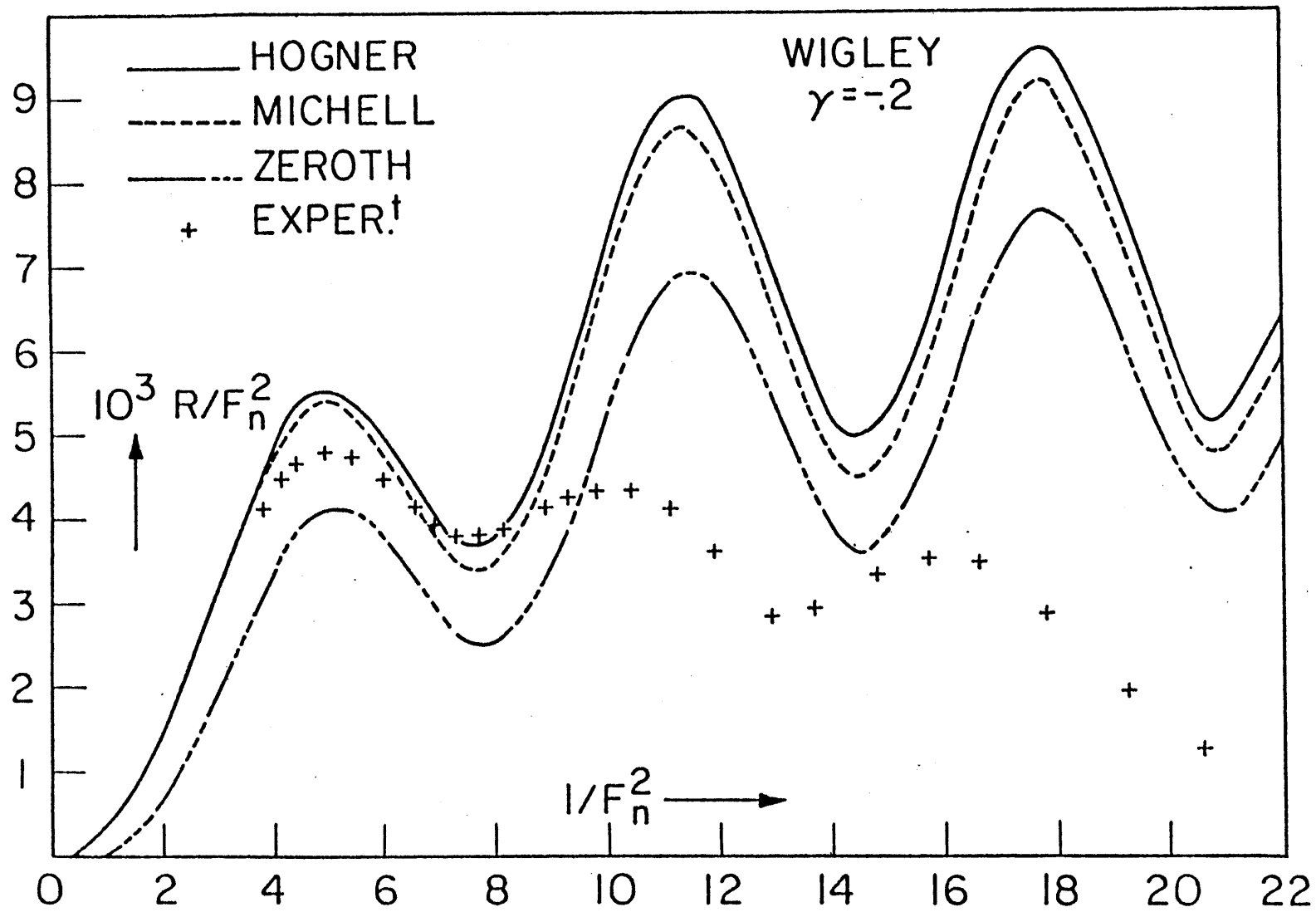
Hogner (H)
Michell (M)
Zeroth (O)
Yim (Y)
Michell+Waterline (MW)
Waterline (W)
Waterline with y=O (W₀)
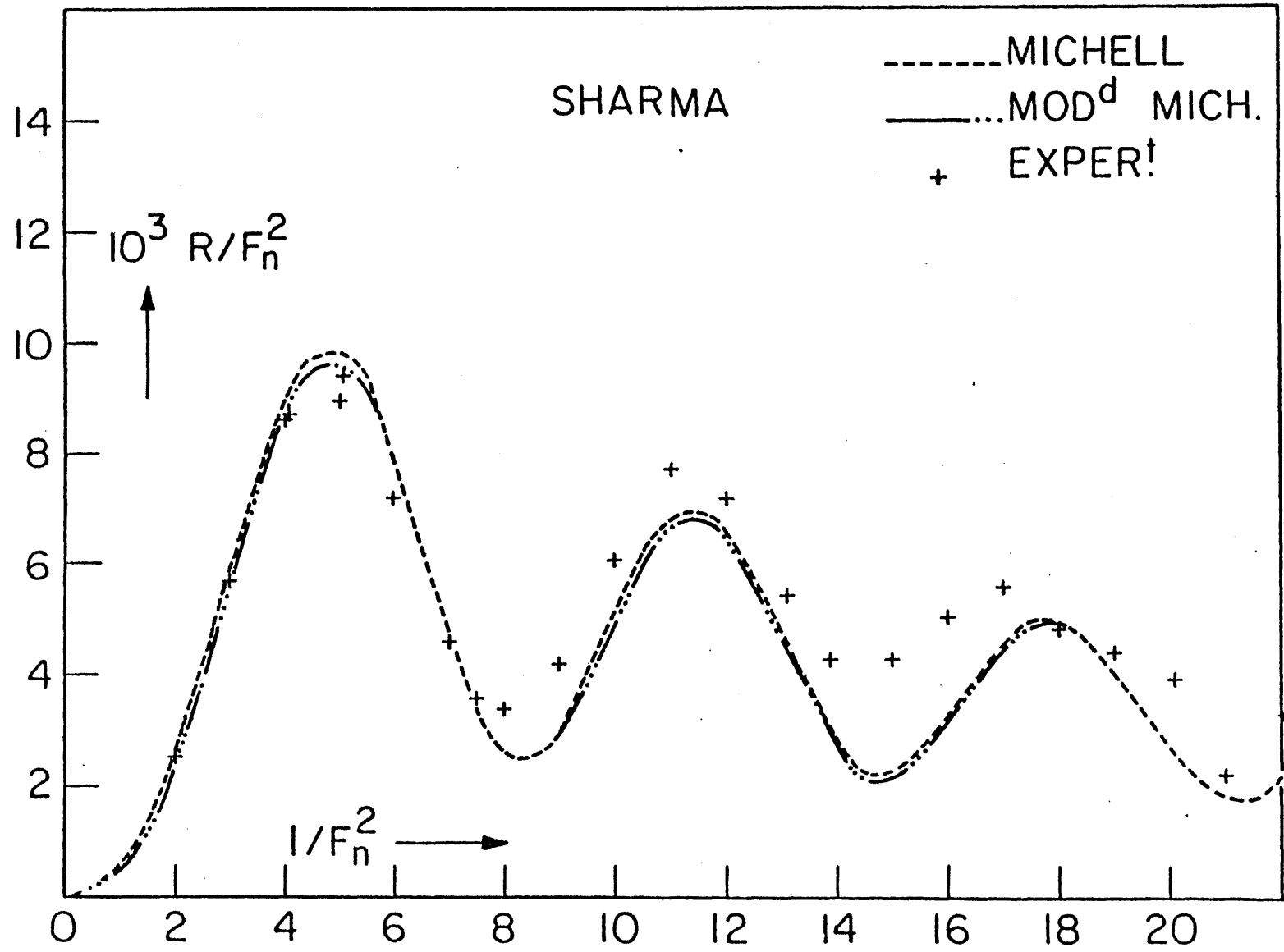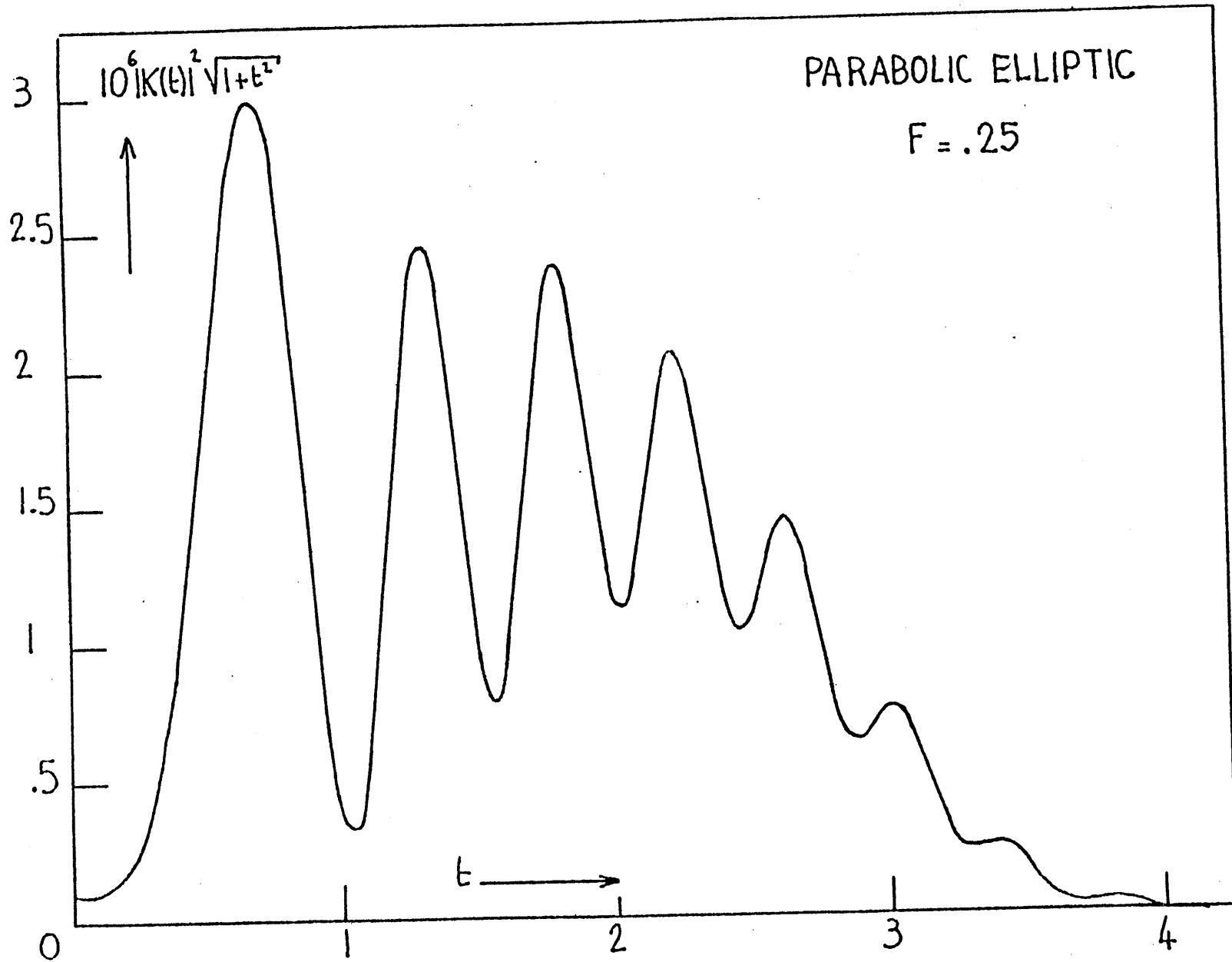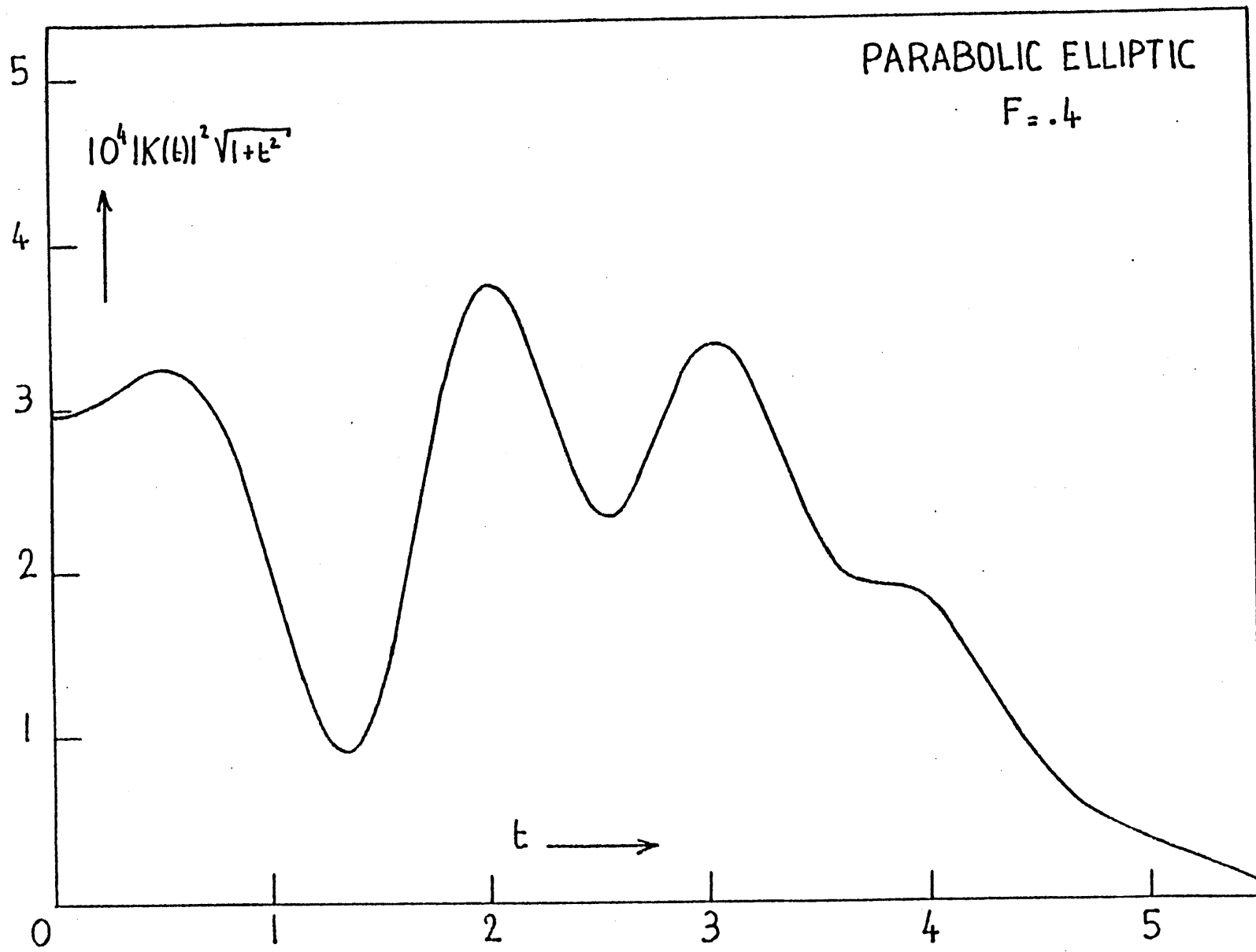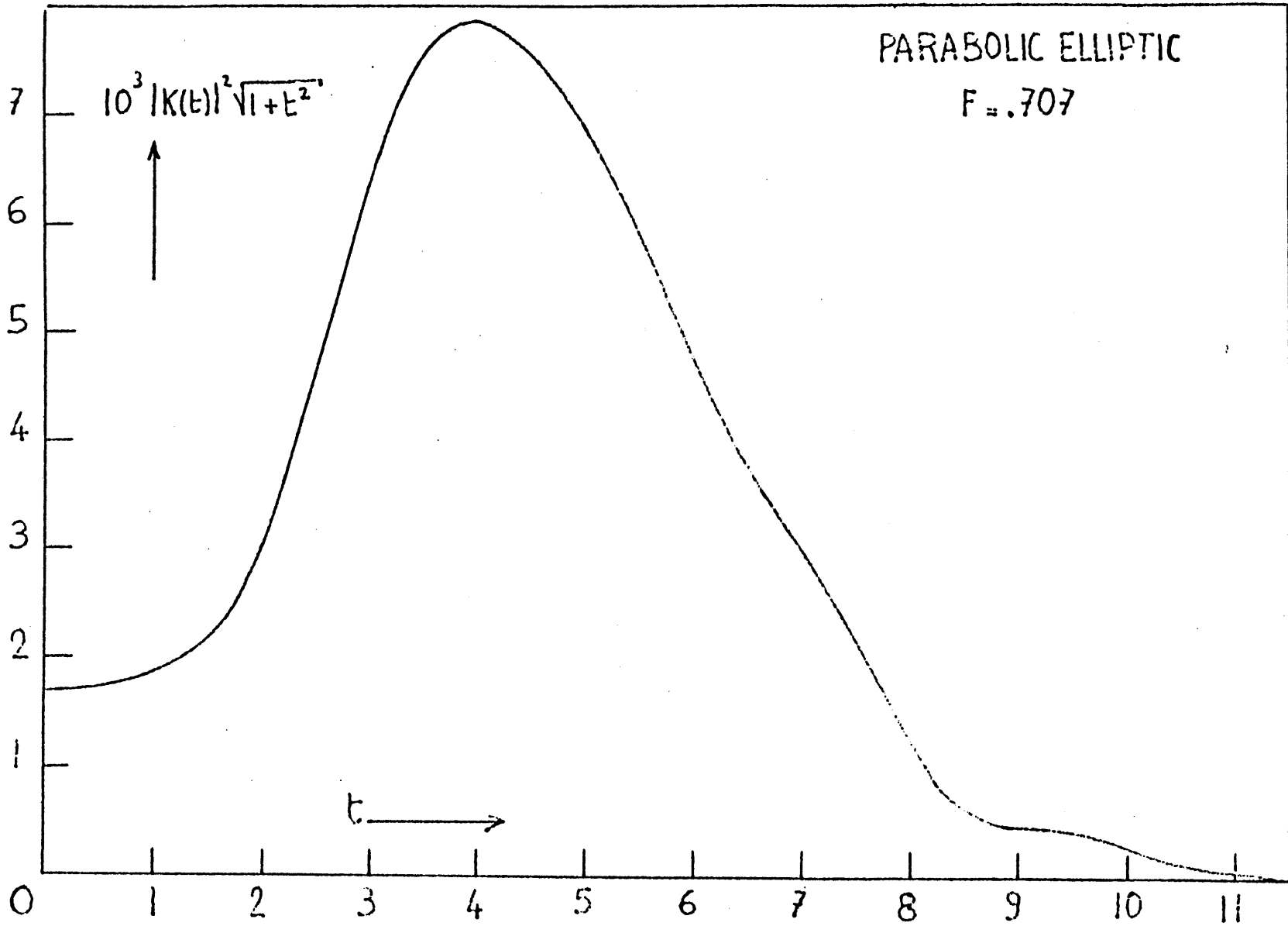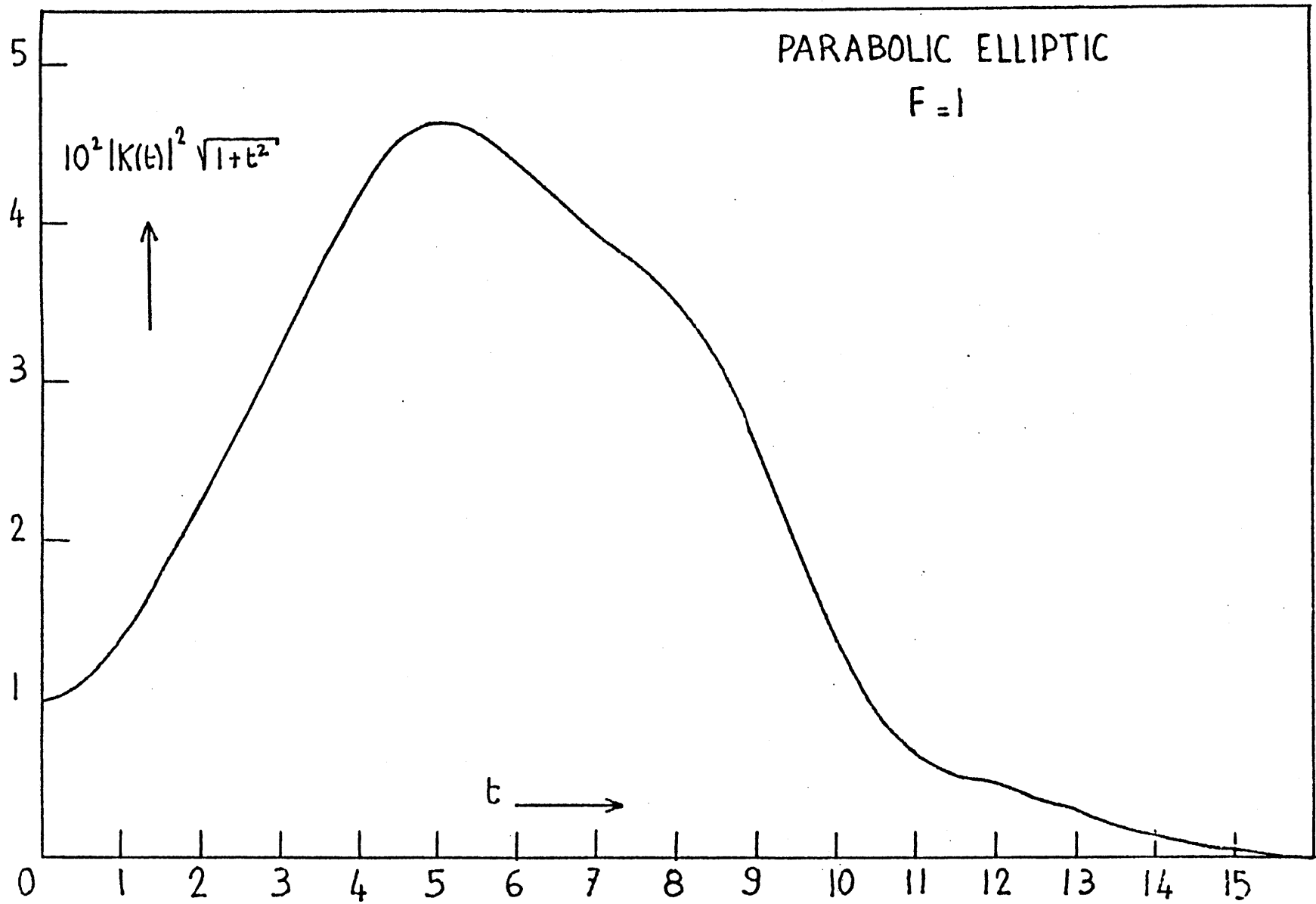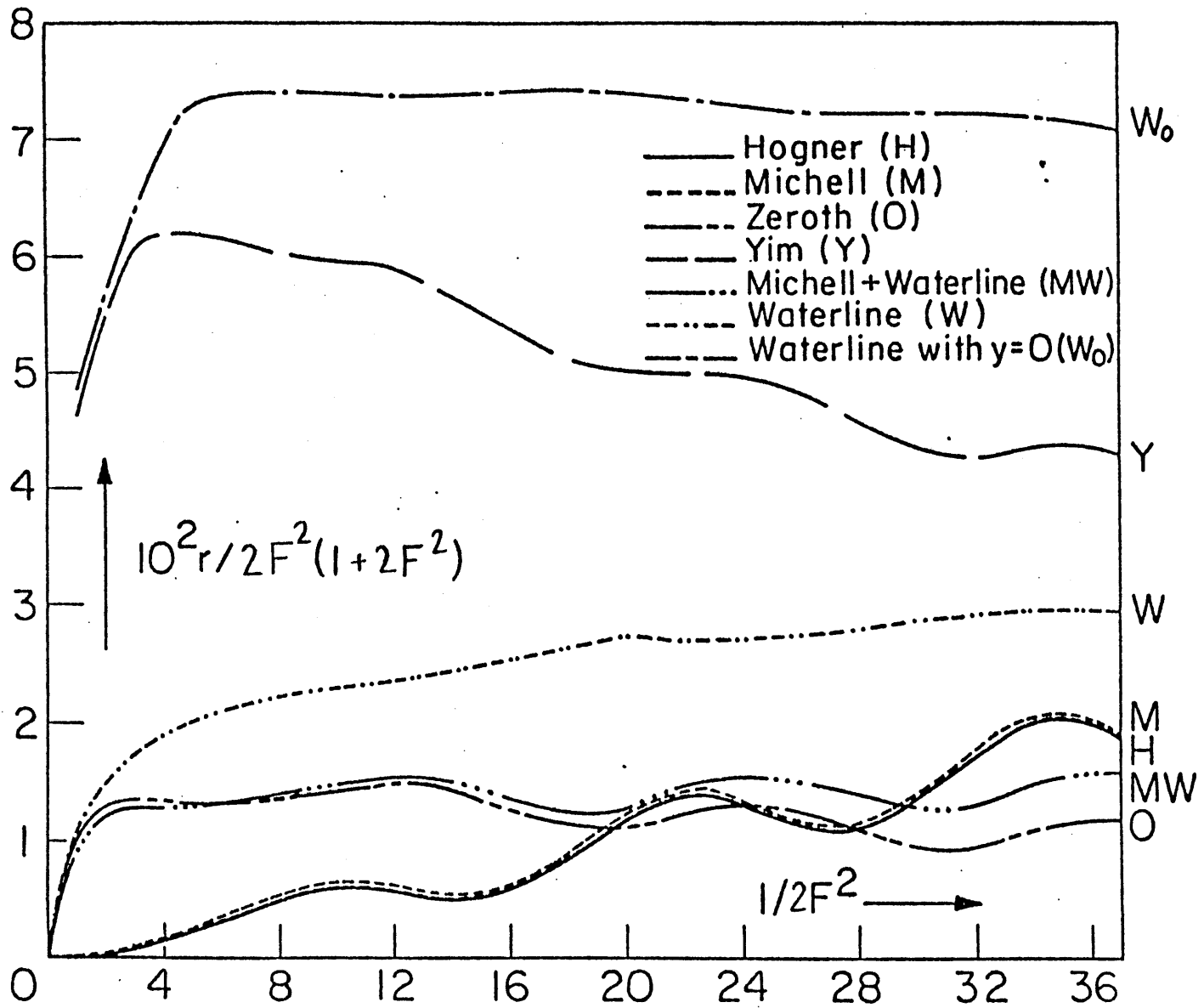
Figúre 3-26

TABLE I

Wave resistance coefficient of the Wigley model
given by Michell's and Hogner's wave resistance formulas

WIGLEY: MICHELL		WIGLEY: MICHELL		WIGLEY: HOGNER		WIGLEY: HOGNER	
F_N	$C_R \times 10^3$	F_N	$C_R \times 10^3$	F_N	$C_R \times 10^3$	F_N	$C_R \times 10^3$
0.150	0.361	0.250	1.065	0.150	0.390	0.300	2.311
0.152	0.442	0.260	0.847	0.155	0.422	0.313	2.098
0.155	0.380	0.270	1.092	0.157	0.345	0.330	1.638
0.157	0.307	0.280	1.603	0.160	0.380	0 340	1.477
0.160	0.348	0.290	2.016	0.166	0.598	C.350	1.472
0.163	0.512	0.300	2.142	0.170	0.464	0.360	1.602
0.166	0.558	0.310	1.995	0.175	0.488	0.402	3.036
0.168	0.491	0.320	1.711	0.180	0.774	0.430	3.907
0.170	0.407	0.330	1.432	0.185	0.695	0.452	4.360
0.172	0.369	0.340	1.263	0.190	0.536	0.470	4.550
0.175	0.454	0.350	1.245	0.200	0.962	0.482	4.618
0.177	0.570	0.360	1.378	0.210	0.908	0.500	4.661
0.180	0.715	0.370	1.634	0.220	0.741		
0.185	0.652	0.380	1.968	0.230	1.248		
0.190	0.475	0.390	2.344	0.240	1.494		
0.200	0.886	0.400	2.730	0.250	1.171		
0.210	0.832	0.410	3.095	0.260	0.978		
0.220	0.653	0.430	3.718	0.266	1.077		
0.230	1.166	0.440	3.957	0.290	2.169		
0.240	1.386	0.450	4.146				

TABLE II

Wave resistance coefficient of the Wigley model
given by the zeroth-order slender-ship approximation

WIGLEY: 0TH APPROX.		WIGLEY: 0TH APPROX.		WIGLEY: 0TH APPROX.			
F_N	$C_R \times 10^3$	F_N	$C_R \times 10^3$	F_N	$C_R \times 10^3$		
0.150	0.323	0.240	1.177	0.430	2.967		
0.153	0.401	0.250	0.874	0.440	3.117		
0.155	0.347	0.260	0.708	0.452	3.242		
0.157	0.275	0.266	0.792	0.460	3.294		
0.160	0.306	0.280	1.344	0.470	3.323		
0.163	0.474	0.290	1.657	0.482	3.319		
0.166	0.496	0.300	1.723	0.490	3.296		
0.168	0.427	0.313	1.486	0.500	3.249		
0.170	0.372	0.320	1.301	0.510	3.186		
0.172	0.330	0.330	1.077	0.520	3.110		
0.175	0.391	0.340	0.959				
0.177	0.498	0.350	0.973				
0.180	0.641	0.360	1.109				
0.185	0.563	0.370	1.339				
0.190	0.417	0.380	1.625				
0.200	0.787	0.390	1.955				
0.210	0.718	0.402	2.319				
0.220	0.566	0.410	2.533				
0.230	0.997	0.420	2.772				

TABLE III
OFF-SETS FOR MODEL S-201 (from Inui, 1957)

W.L. $x=X/L$	Half Breadth, Y							Height of Keel Line z
	L.W.L.	1	2	3	4	5	6	
	0	.286	.571	.857	1.143	1.429	1.714	
−1								1.000
−0.99	.057	.057	.057	.051				1.026
−0.95	.218	.210	.198	.175	.046			1.159
−0.90	.381	.371	.349	.309	.217			1.288
−0.85	.503	.495	.469	.419	.319			1.385
−.8	.606	.594	.571	.520	.415	.153		1.466
−.7	.762	.752	.730	.675	.570	.366		1.598
−.6	.893	.883	.858	.803	.705	.522		1.705
−.5	1.007	.994	.963	.906	.807	.635	.274	1.791
−.4	1.096	1.083	1.048	.984	.880	.710	.419	1.859
−.3	1.159	1.147	1.117	1.045	.937	.775	.504	1.908
−.2	1.198	1.189	1.153	1.087	.981	.822	.560	1.940
−.1	1.224	1.210	1.177	1.109	1.006	.846	.589	1.959
0	1.229	1.218	1.185	1.119	1.017	.857	.605	1.958

$y = Y/L = Y/5$

$z = Z/L = Z/5$

$b = B/L = 0.2458$
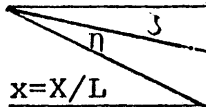
$d = D/L = 0.3916$

TABLE IV

Wave resistance coefficient of the Inui model

given by the Hogner and the zeroth approximations

INUI: HOGNER		INUI: HOGNER		INUI: 0TH APPROX.		INUI: 0TH APPROX.	
F_N	$C_R \times 10^3$	F_N	$C_R \times 10^3$	F_N	$C_R \times 10^3$	F_N	$C_R \times 10^3$
0.153	2.269	0.380	5.233	0.153	1.248	0.380	3.889
0.157	1.760	0.400	7.289	0.157	0.828	0.400	5.602
0.166	2.840	0.420	9.237	0.166	1.564	0.420	6.946
0.172	2.128	0.440	10.767	0.172	1.009	0.440	7.744
0.180	3.210	0.460	11.797	0.180	1.856	0.460	8.093
0.190	2.492	0.480	12.292	0.190	1.170	0.480	7.983
0.200	3.324	0.525	12.135	0.200	1.928	0.525	7.013
0.220	2.606	0.560	11.342	0.220	1.240	0.560	5.930
0.230	3.324	0.580	10.795	0.230	1.928	0.580	5.379
0.240	4.708	0.600	10.211	0.240	2.635	0.600	4.789
0.255	3.409	0.620	9.637	0.255	1.527	0.620	4.182
0.260	3.026	0.650	8.780	0.260	1.403	0.650	3.356
0.287	5.549	0.800	5.484	0.287	3.667	0.800	1.013
0.295	6.330	1.000	3.056	0.295	4.008	1.000	0.808
0.300	6.565	1.200	1.701	0.300	3.999	1.200	2.720
0.319	5.769	1.273	1.330	0.319	2.931	1.273	3.022
0.320	5.647	1.414	0.801	0.320	2.830		
0.340	4.110			0.340	1.935		
0.360	3.945			0.360	2.424		

TABLE V
OFFSETS FOR THE HIGH-SPEED HULL, ATHENA (from drawings for Model 4650-1)

$x = X/L$	η	0.125	.25	.50	.75	1.00
		0.0000	0.0000	0.0000	0.0000	0.0000	0.0048
.95	0.0000	0.0000	0.0246	0.0359	0.0451	0.0570
.90	0.0000	0.0000	0.0525	0.0818	0.0959	0.1110
.85	0.0000	0.0000	0.0838	0.1292	0.1462	0.1675
.80	0.0000	0.0000	0.1162	0.1766	0.2035	0.2257
.70	0.0000	0.0377	0.1955	0.2813	0.3104	0.3398
.60	0.0000	0.1029	0.2849	0.3891	0.4218	0.4478
.50	0.0000	0.1972	0.3989	0.4992	0.5280	0.5643
.40	0.0000	0.3036	0.4972	0.6009	0.6246	0.6462
.30	0.0000	0.4305	0.6190	0.6934	0.7070	0.7263
.20	0.0000	0.5918	0.7262	0.7783	0.7830	0.7967
.10	0.0000	0.7410	0.8346	0.8517	0.8448	0.8568
0	1.0000	0.8868	0.9240	0.9136	0.9002	0.9065
-.10	1.0000	1.0000	1.0000	0.9671	0.9420	0.9381
-.20	1.0000	0.8353	0.9519	1.0000	0.9762	0.9660
-.30	0.0000	0.4580	0.8424	1.0000	0.9942	0.9872
-.40	0.0000	0.0000	0.5765	0.9801	1.0000	1.0000
-.50	0.0000	0.0000	0.0581	0.9113	0.9865	0.9939
-.60	0.0000	0.0000	0.0000	0.7645	0.9575	0.9751
-.70	0.0000	0.0000	0.0000	0.4870	0.9227	0.9478
-.80	0.0000	0.0000	0.0000	0.0871	0.8731	0.9108
-.85	0.0000	0.0000	0.0000	0.0000	0.8545	0.8926
-.90	0.0000	0.0000	0.0000	0.0000	0.8345	0.8695
-.95	0.0000	0.0000	0.0000	0.0000	0.8068	0.8477
-1	0.0000	0.0000	0.0000	0.0000	0.8023	0.8289
b_N/b_1 = Max. half beam	0.0073	0.3538	0.5431	0.7937	0.9424	1.0000

$$\eta = Y/b\eta \qquad y = Y/L = 0.1470 * \eta * b_N/b_n \qquad z = Z/L = (i - \zeta) * 0.0642$$

APPENDIX I

EVALUATION OF THE SURFACE INTEGRAL OVER A PLANAR TRIANGLE

$$K_S(t) = \int_S 2^{-1} F^{-4}(1+t^2)\left(\exp(\vec{\alpha}_+ \cdot \vec{x}) + \exp(\vec{\alpha}_- \cdot \vec{x})\right) \nu \, da$$

where $\quad \vec{\alpha}_\pm = F^{-2}(1+t^2)^{1/2}\left\{-i, \pm it, (1+t^2)^{1/2}\right\}$

and $\quad \vec{x} = \left\{x, y, z\right\}$

S is the surface of the triangle.

The triangle is defined by three points $\vec{x}_i$, $\vec{x}_j$, $\vec{x}_k$ (see Figure 1-1). We will perform the integration over the two rectangle triangles 1 and 2 successively for α_+ and α_-, and then add all the partial results to obtain K_S.

$$K_S = K^+ + K^-$$

$$K^\pm = 2^{-1} F^{-4}(1+t^2) \nu \int_S \exp\left(\vec{\alpha}_\pm \cdot \vec{x}\right) da$$

$$K^\pm = 2^{-1} F^{-4}(1+t^2)\nu\left[K_1^\pm + K_2^\pm\right]$$

where the subscripts 1 and 2 stand for the triangles 1 and 2.

$$K_1^{\pm} = \int_{S_1} \exp\left[\vec{\alpha}_{\pm} \cdot \vec{x}\right] da$$

$$K_2^{\pm} = \int_{S_2} \exp\left[\vec{\alpha}_{\pm} \cdot \vec{x}\right] da$$

We shall make use of additional variables which are defined below

$$\vec{x}_{ij} = \vec{x}_j - \vec{x}_i$$

$$\vec{\alpha} \cdot \vec{x}_{ij} = \beta_{ij} = F^{-2}\left(1+t^2\right)^{1/2} \gamma_{ij}$$

$$\vec{\alpha} \cdot \vec{x}_i = \beta_i = F^{-2}\left(1+t^2\right)^{1/2} \gamma_i$$

It is obvious that $\quad \beta_{ij} = \beta_j - \beta_i$

and $\quad \gamma_{ij} = \gamma_j - \gamma_i$

To be consistent, we should use β_i^{+} and β_i^{-}. But, for the sake of clarity, we will only use the "β_i" notation, with the understanding that the β's involved in the calculation of $K_{1,2}^{+}$ are β^{+}'s and that the β's involved in the calculation of $K_{1,2}^{-}$ are β^{-}'s.
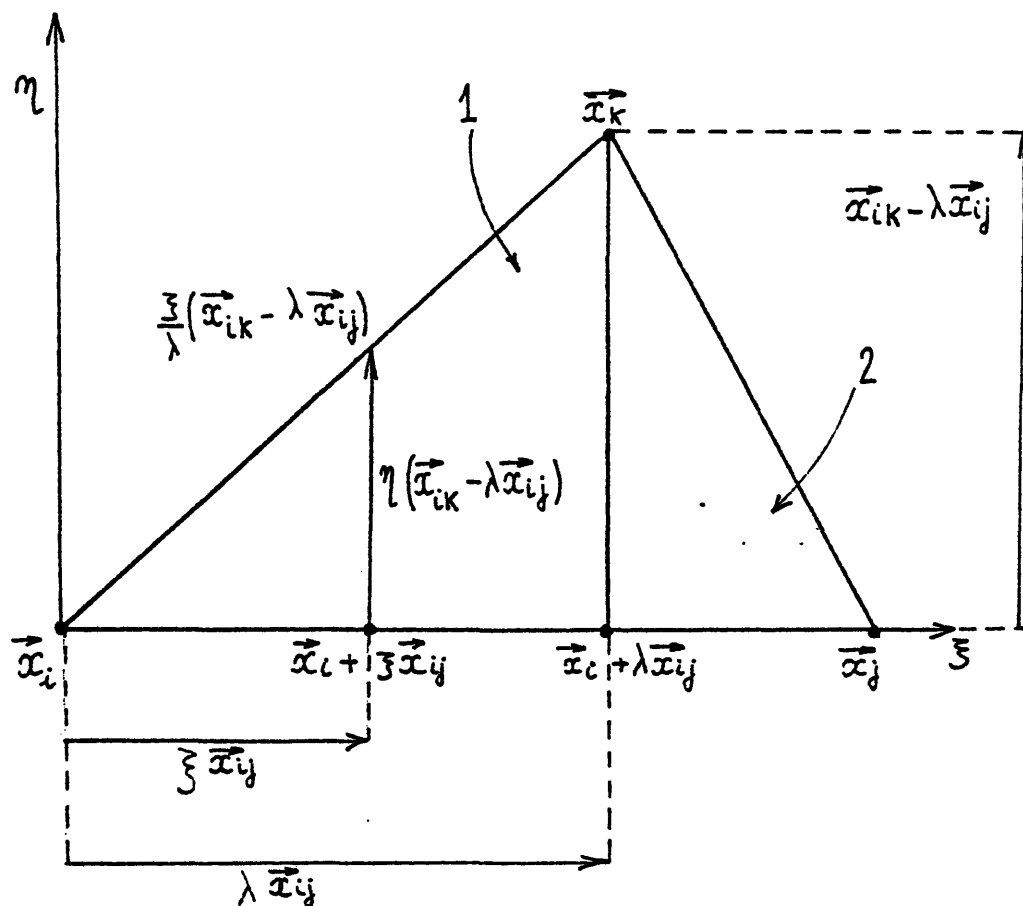
Figure 1-1

Figure 1-1 also shows the local frame of reference (ζ, η).
We express K^+ in the form

$$K^+ = K_1{}^+ + K_2{}^+$$

The term $K_1{}^+$ can be evaluated as follows

$$K_1^+ = \int_{S_1} \exp\left(\vec{\alpha}_+ \cdot \vec{x}\right) da$$

$$da = |\vec{x}_{ij}|\,|\vec{x}_{ik} - \lambda \vec{x}_{ij}|\, d\xi\, d\eta$$

$$\vec{x} = \vec{x_i} + \xi \vec{x_{ij}} + \eta \left(\vec{x_{ik}} - \lambda \vec{x_{ij}} \right)$$

$$\exp(\vec{\alpha_+} \cdot \vec{x}) = \exp(\beta_i) \exp(\xi \beta_{ij}) \exp\left((\beta_{ik} - \lambda \beta_{ij}) \eta \right)$$

$$\Rightarrow K_1^+ = |\vec{x_{ij}}| |\vec{x_{ik}} - \lambda \vec{x_{ij}}| \exp(\beta_i) \int_0^\lambda \exp(\beta_{ij} \xi) d\xi \int_0^{\xi/\lambda} \exp\left((\beta_{ik} - \lambda \beta_{ij}) \eta \right) d\eta$$

$$K_1^+ = \frac{|\vec{x_{ij}}| |\vec{x_{ik}} - \lambda \vec{x_{ij}}| \exp(\beta_i)}{\beta_{ik} - \lambda \beta_{ij}} \left[\frac{\lambda}{\beta_{ik}} \exp \beta_{ik} - \frac{\exp(\lambda \beta_{ij})}{\beta_{ij}} - \frac{\lambda}{\beta_{ik}} + \frac{1}{\beta_{ij}} \right]$$

$$(1-1)$$

The evaluation of the term K_2^+ is now considered.
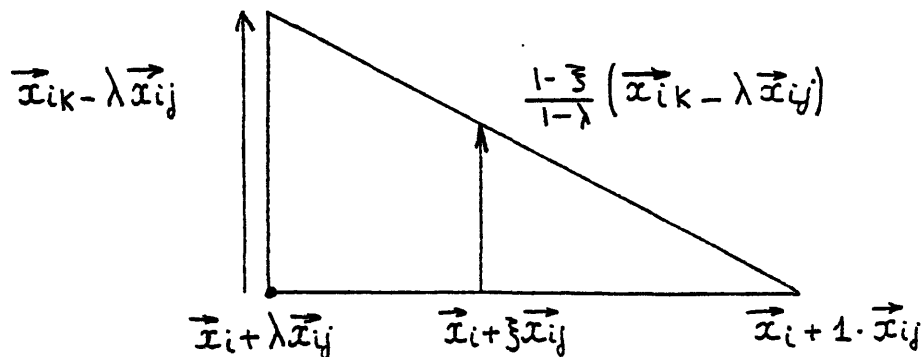
$$K_2^+ = \int_{S_2} \exp\left(\vec{\alpha_+} \cdot \vec{x}\right) da$$

$$K_2^+ = \left|\vec{x}_{ij}\right| \left|\vec{x}_{ik} - \lambda \vec{x}_{ij}\right| \exp(\beta_i) \int_\lambda^1 \exp\left(\beta_{ij}\, \xi\right) d\xi \int_0^{\frac{1-\xi}{1-\lambda}} \exp\left(\left(\beta_{ik} - \lambda\beta_{ij}\right)\eta\right) d\eta$$

$$K_2^+ = \frac{\left|\vec{x}_{ij}\right| \left|\vec{x}_{ik} - \lambda\vec{x}_{ij}\right|}{\beta_{ik} - \lambda\beta_{ij}} \left[\frac{(1-\lambda)\exp(\beta_{ij})}{\beta_{ij} - \beta_{ik}} - \frac{\exp(\beta_{ij})}{\beta_{ij}} - \frac{(1-\lambda)\exp(\beta_{ik})}{\beta_{ij} - \beta_{ik}} + \frac{\exp(\lambda\beta_{ij})}{\beta_{ij}} \right] \exp(\beta_i) \tag{1-2}$$

$$K_1^+ + K_2^+ =$$

$$\frac{\left|\vec{x}_{ij}\right| \left|\vec{x}_{ik} - \lambda\vec{x}_{ij}\right| \exp(\beta_i)}{\beta_{ik} - \lambda\beta_{ij}} \left[\frac{\beta_{ij}\exp(\beta_{ik}) - \beta_{ik}\exp(\beta_{ij})}{\beta_{ij} - \beta_{ik}} - 1 \right] \frac{\lambda\beta_{ij} - \beta_{ik}}{\beta_{ij}\,\beta_{ik}} \tag{1-3}$$

$$K^+ = \frac{1 + t^2}{2F^4}\, \nu \left[K_1^+ + K_2^+ \right]$$

$\nu = \vec{n} \cdot \vec{i}$ where $\vec{n}$ is the unit inward vector to the surface of the hull and i is the positive unit vector along the x-axis.

One convenient way of defining $\vec{n}$ is:

$$\vec{n} = \frac{\vec{x}_{ij} \wedge (\vec{x}_{ik} - \lambda \vec{x}_{ij})}{|\vec{x}_{ij}||\vec{x}_{ik} - \lambda \vec{x}_{ij}|}$$

$$y = \frac{(y_i - y_j)(z_k - z_i) + (y_k - y_i)(z_j - z_i)}{|\vec{x}_{ij}||\vec{x}_{ik} - \lambda \vec{x}_{ij}|} \tag{1-4}$$

Using (1-4) in (1-3) and making use of $\beta_{ij} - \beta_{ik} = \beta_{kj}$
yields

$$K^+ = \frac{1}{2} \frac{z_i(y_j - y_k) + z_j(y_k - y_i) + z_k(y_i - y_j)}{\gamma_{ij}\gamma_{jk}\gamma_{ki}} \left[\gamma_{ij} \exp(\beta_k^+) + \gamma_{jk} \exp(\beta_i^+) + \gamma_{ki} \exp(\beta_j^+) \right] \tag{1-5}$$

A similar computation would give

$$K^- = \frac{1}{2} \frac{z_i(y_j - y_k) + \gamma_j(y_k - y_i) + \gamma_k(y_i - y_j)}{\gamma_{ij}\gamma_{jk}\gamma_{ki}} \left[\gamma_{ij} \exp(\beta_k^-) + \gamma_{jk} \exp(\beta_i^-) + \gamma_{ki} \exp(\beta_j^-) \right] \tag{1-6}$$

APPENDIX II

EVALUATION OF THE LINE INTEGRAL OVER A LINEAR SEGMENT
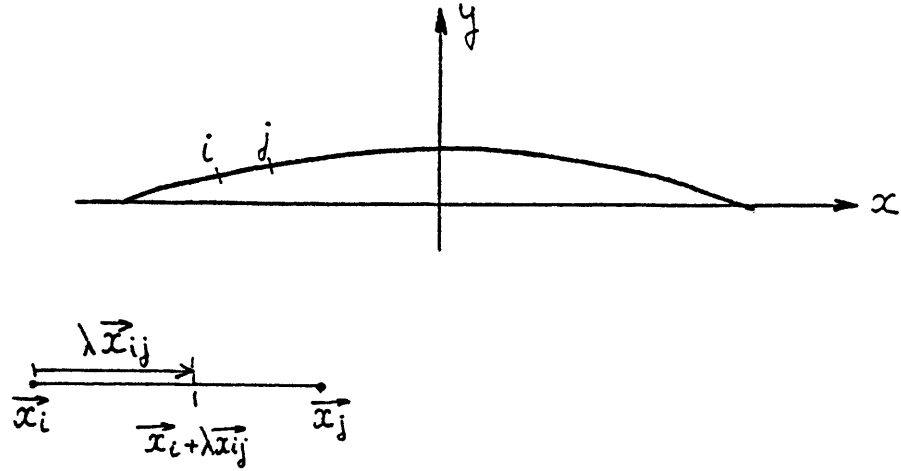
Figure 2-1

$$K_L = \frac{1+t^2}{2F^2} \int_i^j \left(\exp(\vec{\alpha_+} \cdot \vec{x}) + \exp(\vec{\alpha_-} \cdot \vec{x}) \right) \nu^2 \mu \, d\Delta = K_L^+ + K_L^-$$

$$K_L^{\pm} = \frac{1+t^2}{2F^2} \nu^2 \mu \int_i^j \exp\left(\vec{\alpha_\pm} \cdot \vec{x} \right) d\Delta$$

$$d\Delta = |\vec{x_{ij}}| \, d\lambda$$

$$\vec{x} = \vec{x_i} + \lambda \vec{x_{ij}}$$

$$\vec{\alpha} \cdot \vec{x} = \vec{\alpha} \cdot \vec{x_i} + \lambda \vec{\alpha} \cdot \vec{x_{ij}} = \beta_i + \lambda \, \beta_{ij}$$

$$K_L^{\pm} = \frac{1+t^2}{2F^2} \nu^2 \mu |\vec{x_{ij}}| \frac{\exp(\beta_j) - \exp(\beta_i)}{\beta_{ij}} \qquad (2\text{-}1)$$

When the hull is vertical-sided at the waterline, we have

$$\nu = \mu = \frac{y_j - y_i}{|\vec{x}_{ij}|} = \frac{y_j - y_i}{\sqrt{(x_i - x_j)^2 + (y_j - y_i)^2}}$$

$$\Rightarrow K_i^{\pm} = \frac{\sqrt{1 + t^2}}{2} \frac{(y_j - y_i)^3}{(x_i - x_j)^2 + (y_i - y_j)^2} \cdot \frac{\exp(\beta_j^{\pm}) - \exp(\beta_i^{\pm})}{\gamma_{ij}} \tag{2-2}$$

When the hull is not vertical-sided at the waterline, we still have

$$\mu = \frac{y_j - y_i}{|\vec{x}_{ij}|} \tag{2-3}$$

Figure (2-2) shows how one can construct a triangle having $\vec{x}_{ij}$ as a side, in order to define the normal to the hull at the waterline, namely, $\vec{n}$.
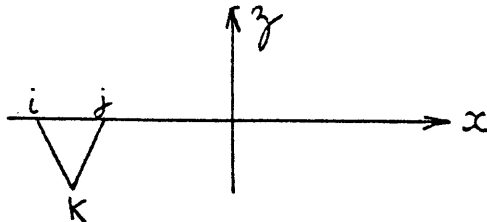
Figure 2-2

We can choose $\vec{n}$ as

$$\vec{n} = \frac{\vec{x_{jk}} \wedge \vec{x_{ij}}}{|\vec{x_{jk}}||\vec{x_{ij}}|}$$

making use of the fact that $z_i = z_j = 0$ we find

$$y = \vec{n} \cdot \vec{c} = \frac{z_k(y_i - y_j)}{\left((x_k - x_j)^2 + (y_k - y_j)^2 + z_k^2\right)^{1/2} \cdot \left((x_j - x_i)^2 + (y_j - y_i)^2\right)^{1/2}} \qquad (2\text{-}4)$$

Using (2-3) and (2-4) in (2-1) yields

$$K_L^{\pm} = \left(\frac{1 + t^2}{2}\right)^{1/2} (y_j - y_i)^3 \frac{\exp(\beta_j^{\pm}) - \exp(\beta_i^{\pm})}{\gamma_{ij}} \frac{z_k}{\left((x_k - x_j)^2 + (y_k - y_j)^2 + z_k^2\right)\left((x_j - x_i)^2 + (y_j - y_i)^2\right)}$$

$$(2\text{-}5)$$

APPENDIX III

EXPRESSIONS FOR R AND K(t)
USED IN CHAPTER III FOR PORT AND STARBOARD SYMMETRY

The formulas used in Chapter II were, we recall,

$$R = R^*/\rho U^2 L^2 = 4\pi^{-1}F^4 \int_0^\infty |K(t)|^2 (1+t^2)^{-3/2}\, dt \tag{1}$$

$$K(t) = \frac{1}{2}\left[\int_h E n_x\, da + F^2 \int_C E_0 n_x^2 C_y\, d\ell\right] \tag{2}$$

$$E(x, \eta, \gamma; t) = F^{-4}(1+t^2)\exp\left[F^{-2}(1+t^2)\gamma - iF^{-2}(1+t^2)^{1/2}x\right]\exp\left[-iF^{-2}t(1+t^2)^{1/2}y\right] \tag{3}$$

where h and C are defined as on the sketch below.
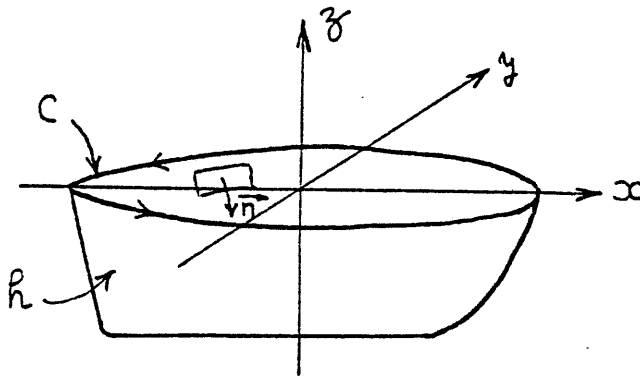
On the counter clockwise oriented waterline C,
define the local frame of reference $\vec{c}$, $\vec{m}$, $\vec{d}$.
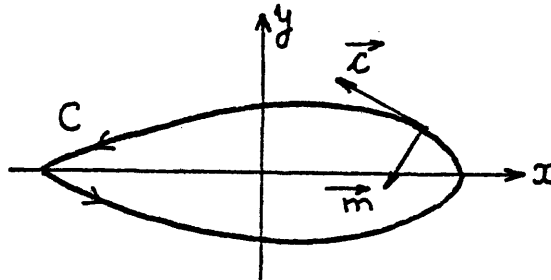
$\vec{c}(c_x, c_y)$

$\vec{m}(m_x, m_y)$ where $m_x = -c_y$

$\vec{d} = \vec{n} \times \vec{c}$.

Assume that the hull has port and starboard symmetry
and define C_+ and C_- as shown in the sketch below
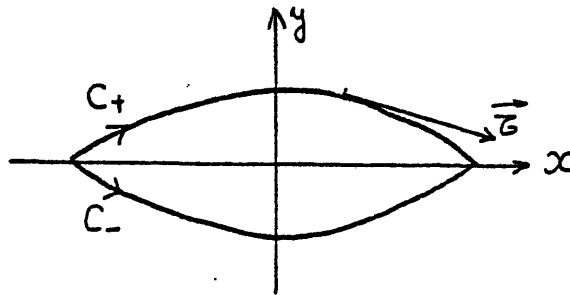
On c^+ we have $c_y = -c_y dl$ (4)

On c^- we have $dy = c_y dl$ (5)

where dl is the element of length along c^+ or c^-.

On c^+ we also have $C_y dl = -\zeta_y dl$ (6)

a. The line integral in equation (2) can be modified:

$$\oint_C E_o n_x^2 \, dy = \oint_{C^-} E_o^- n_x^2 \, C_y \, d\ell - \oint_{C^+} E_o^+ n_x^2 \left(-C_y \, d\ell\right)$$

$$\oint_C E n_x^2 \, d\ell = \oint_{C^+} \left(E_o^- + E_o^+\right) n_x^2 \, C_y \, d\ell \tag{7}$$

where $E_0^+ = E(x, y^+, 0)$ and $E_0^- = E(x, y^-, 0)$, using the convention that

$y^+ > 0$, $y^- < 0$ and $y^- = -y^+$.

$$E_o^- + E_o^+ \simeq 2F^{-4}\left(1 + t^2\right) \exp\left[-i F^{-2} x \left(1 + t^2\right)^{1/2}\right] \cos\left(F^{-2} t \left(1 + t^2\right)^{1/2} y\right) \tag{8}$$

using (6) and (8) in (7) we obtain:

$$\oint_C E n_x^2 \, dy = -2F^{-4}\left(1 + t^2\right) \oint_{C^+} \exp\left(-i F^{-2} \left(1 + t^2\right)^{1/2} x\right) \cos\left(F^{-2} t \left(1 + t^2\right)^{1/2} y\right) n_x^2 \, \zeta_y \, d\ell \tag{9}$$

b.   The surface integral in equation (2) is now modified:

$$\int_h E\, n_x\, da = \int_{h^+} E^+ n_x^+\, da^+ + \int_{h^-} E^- n_x^-\, da^-$$

(10)

where h^+ and h^- are the positive -y and negative -y half hulls repsectively, da^+ and da^- are the elementary surface areas on h^+ and h^- respectively and E^+ are defined as follows: $E^+=E(x,y^+,z)$; $E^-=E(x,y^-,z)$ where y^+ and y^- are defined as before.

$$n_x^+ = -n_x^-$$

$$\int_h E\, n_x\, da = \int_{h^+} \left(E^+ + E^-\right) n_x\, da$$

$$\int_h E\, n_x\, da = 2F^{-4}\left(1+t^2\right)\int_{h^+} \exp\left[F^{-2}\left(1+t^2\right)\mathfrak{z} - i\, F^{-2}\left(1+t^2\right)^{1/2} x\right] \cos\left(F^{-2}t\left(1+t^2\right)^{1/2} y\right) n_x\, da$$

(11)

define

$$\mathfrak{Z} = \exp\left[F^{-2}\left(1+t^2\right)\mathfrak{z} - i\, F^{-2}\left(1+t^2\right)^{1/2} x\right] \cos\left(F^{-2}t\left(1+t^2\right)^{1/2} y\right)$$

(12)

and

$$\mathcal{K}(t) = F^4 \left(1+t^2\right)^{-1} K(t) \tag{13}$$

Equations (1) and (3) now become:

$$R = R^* / \rho U^2 L^2 = 4\pi^{-1} F^{-4} \int_0^\infty \left|\mathcal{K}(t)\right|^2 \left(1+t^2\right)^{1/2} dt \tag{14}$$

$$\mathcal{K}(t) = \int_{h^+} \mathfrak{Z} n_x \, da - F^2 \int_{C^+} \mathfrak{Z} n_x^2 \, \mathfrak{S}_y \, d\ell \tag{15}$$

APPENDIX IV

EXPRESSIONS FOR R AND K(t) USED IN CHAPTER III
FOR PORT AND STARBOARD SYMMETRY TOGETHER WITH
FORE AND AFT SYMMETRY

$$R = R^* / \rho U^2 L^2 = 4\pi^{-1} F^{-4} \int_0^\infty |K(t)|^2 (1+t^2)^{1/2} dt \tag{1}$$

$$K(t) = \int_{R^+} \zeta n_x \, da - F^2 \oint_{C^+} \zeta n_x^2 \, \zeta_y \, d\ell \tag{2}$$

$$\zeta = \exp\left[F^{-2}(1+t^2)\zeta - i F^{-2}(1+t^2)^{1/2} x \right] \cos\left(F^{-2} t (1+t^2)^{1/2} y \right) \tag{3}$$

a.   The surface integral in equation (2) is modified as follows:

$$\int_{R^+} \zeta n_x \, da = \int_{h_+^-} \zeta^- n_x^- \, da + \int_{h_+^+} \zeta^+ n_x^+ \, da \tag{4}$$

where h_+^- and h_+^+ are defined on the sketch below
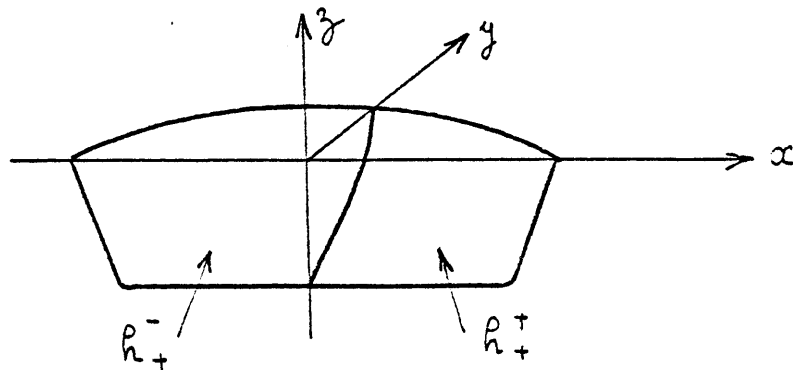
n_x^- and n_x^+ are the x component of the unit inward vectors on h_+^- and h_+^+ respectively and ζ^- and ζ^+ are defined as

$$\xi^- = \xi\left(x_i^-, y_i, z_i; t\right) \quad ; \quad \xi^+ = \xi\left(x_i^+, y_i, z_i; t\right) \qquad \text{where } x^- = -x^+.$$

since $n_x^- = -n_x^+$ (4) becomes

$$\int_{h_+^+} \xi n_x \, da = \int_{h_+^+} \left(\xi^+ - \xi^-\right) n_x^+ \, da \tag{5}$$

$$\xi^+ - \xi^- = 2i \exp\left[F^{-2}\left(1+t^2\right)z\right] \cos\left(F^{-2}t\left(1+t^2\right)^{1/2} y\right) \sin\left(F^{-2}\left(1+t^2\right)^{1/2} x^-\right) \tag{6}$$

Use (6) in (5) and obtain:

$$\int_{h_+^+} \xi n_x \, da = 2i \int_{h_+^+} \exp\left(F^{-2}\left(1+t^2\right)z\right) \cos\left(F^{-2}t\left(1+t^2\right)^{1/2} y\right) \sin\left(F^{-2}\left(1+t^2\right)^{1/2} x\right) n_x \, da \tag{7}$$

b.   We now modify the line integral in equation (2)

$$\oint_{C^+} \xi n_x^2 \, \sigma_y \, d\ell = \int_{C_+^-} \xi_0^- n_x^2 \, \sigma_y^- \, d\ell + \int_{C_+^+} \xi_0^\top n_x^2 \, \sigma_y^+ \, d\ell$$

where C_+^- and C_+^+ are the intersection of the plane z=0 with h_+^- and h_+^+ respectively.

Using the fact that $_y{}^+ = -{}_y{}^-$, obtain

$$\oint_{C^+} \zeta n_x^2 \, \sigma_y \, d\ell = \oint_{C_+^+} \left(\zeta_0^+ - \zeta_0^- \right) n_x^2 \, \sigma_y^+ \, d\ell$$

that is:

$$\oint_{C^+} \zeta n_x^2 \, \sigma_y \, d\ell = 2i \oint_{C_+^+} \cos\left(F^{-2} t (1+t^2)^{1/2} y \right) \sin\left(F^{-2}(1+t^2)^{1/2} x \right) n_x^2 \, \sigma_y \, d\ell \tag{8}$$

If we define $K(t) = +\dfrac{1}{2i} \mathbb{K}(t)$ we obtain:

$$R = R^* / \rho U^2 L^2 = 16 \pi^{-1} F^{-4} \int_0^\infty \left| K(t) \right|^2 (1+t^2)^{1/2} \, dt \tag{9}$$

$$K(t) = \int_{h_+^+} E n_x \, da - F^2 \int_{C_+^+} E n_x^2 \, \sigma_y \, d\ell \tag{10}$$

$$E = \exp\left(F^{-2}(1+t^2) z \right) \cos\left(F^{-2} t(1+t^2)^{1/2} y \right) \sin\left(F^{-2}(1+t^2)^{1/2} x \right) \tag{11}$$

APPENDIX V

DERIVATION OF EQUATIONS (3-8), (3-9) AND (3-10)

$$R = R^*/\rho U^2 L^2 = 16\pi^{-1} F^{-4} \int_0^\infty |K(t)|^2 (1+t^2)^{1/2} \, dt \tag{1}$$

$$K(t) = \int_{h^\ddagger_+}^{\rho^\ddagger_+} E \, n_x \, da - F^2 \int_{C^\ddagger_+} E \, n_x^2 \, \sigma_y \, d\ell \tag{2}$$

$$E = \exp\left(F^{-2}(1+t^2) z\right) \cos\left(F^{-2} t (1+t^2)^{1/2} y\right) \sin\left(F^{-2}(1+t^2)^{1/2} x\right) \tag{3}$$

$$y = b\left(1 - z^2/d^2\right)\left(1 - (1+\gamma) x^2 + \gamma x^4\right) = y(x, z) \tag{4}$$

$$\left.\frac{\partial y}{\partial x}\right|_{z=0} \equiv \dot{y} \tag{5}$$

$$n_x \, da = \dot{y}\left(1 - z^2/d^2\right) dx \, dz \tag{6}$$

$$\sigma_y = \dot{y}\left(1 + \dot{y}^2\right)^{-1/2} \tag{7}$$

$$d\ell = \left(1 + \dot{y}^2\right)^{1/2} dx \tag{8}$$

$$n_x^2 \left(\mathfrak{z} = 0 \right) = \dot{y}^2 \left(1 + \dot{y}^2 \right)^{-1} \tag{9}$$

Use (3), (6), (7), (8) and (9) in (2), we obtain:

$$K(t) = \int_0^1 dx \int_{-d}^0 d\mathfrak{z} \, E \, \dot{y} \left(1 - \mathfrak{z}^2/d^2 \right) - F^2 \int_0^1 E \, \dot{y}^2 \left(1 + \dot{y}^2 \right)^{-1} \dot{y} \, dx$$

$$K(t) = \int_0^1 dx \, \dot{y} \sin\left(F^{-2} \left(1 + t^2 \right)^{1/2} x \right) \left\{ \int_{-d}^0 \left(1 - \mathfrak{z}^2/d^2 \right) \exp\left(F^{-2} \left(1 + t^2 \right) \mathfrak{z} \right) \cos\left(F^{-2} t \left(1 + t^2 \right)^{1/2} y \right) d\mathfrak{z} \right.$$

$$\left. - F^2 \, \dot{y}^2 \left(1 + \dot{y}^2 \right)^{-1} \cos\left(F^{-2} t \left(1 + t^2 \right)^{1/2} y_0 \right) \right\} \tag{10}$$

or

$$K(t) = -2b \int_0^1 x \left(1 + \gamma - 2\gamma x^2 \right) \sin\left(F^{-2} \left(1 + t^2 \right)^{1/2} x \right) I \, dx \tag{11}$$

where:

$$I = \int_0^1 \exp\left(-F^{-2} \left(1 + t^2 \right) d\mathfrak{z} \right) \left(1 - \mathfrak{z}^2 \right) \cos\left(F^{-2} t \left(1 + t^2 \right)^{1/2} b \left(1 - (1 + \gamma) x^2 + \gamma x^4 \right) \left(1 - \mathfrak{z}^2 \right) \right) d\mathfrak{z}$$

$$- F^2 \, \frac{4 b^2 x^2 \left(1 + \gamma - 2\gamma x^2 \right)^2}{1 + 4 b^2 x^2 \left(1 + \gamma - 2\gamma x^2 \right)^2} \cos\left(F^{-2} t \left(1 + t^2 \right)^{1/2} b \left(1 - (1 + \gamma) x^2 + \gamma x^4 \right) \right) \tag{12}$$

Use (11) and (12) in (1), and obtain:

$$R = R^* / \rho U^2 L^2 = 64 b^2 \pi^{-1} \int_0^\infty |K(t)|^2 (1+t^2)^{1/2} \, dt \tag{13}$$

where

$$K(t) = \int_0^1 x(1+\gamma - 2\gamma x^2) \sin\left(F^{-2}(1+t^2)^{1/2} x\right) I \, dx \tag{14}$$

and

$$I = d F^{-2} \int_0^1 \exp\left(-d F^{-2}(1+t^2)\zeta\right) \cos\left(F^{-2} t (1+t^2)^{1/2} b \left(1-(1+\gamma)x^2 + \gamma x^4\right)(1-\zeta^2)\right)(1-\zeta^2) d\zeta$$

$$- \frac{4 b^2 x^2 (1+\gamma - 2\gamma x^2)^2}{1+4 b^2 x^2 (1+\gamma - 2\gamma x^2)^2} \cos\left(F^{-2} t (1+t^2)^{1/2} b \left(1-(1+\gamma)x^2 + \gamma x^4\right)\right) \tag{15}$$

APPENDIX VI

EVALUATION OF I_a AND I_n

$$I_0^a = \int_0^\alpha \exp(-\delta\zeta)\cos(\beta\delta)(1-\zeta^2)\,d\zeta$$

$$I_0^a = \cos(\beta\delta)\left[\delta^{-1}\left(1+(\alpha^2-1)\exp(-\delta\alpha)\right)+2\delta^{-3}(1+\delta\alpha)\exp(-\delta\alpha)-2\delta^{-3}\right] \quad (1)$$

$$I_0^m = \int_0^\alpha \exp(-\delta\zeta)\left[\cos(\beta\delta)-\cos(\beta\delta-\beta\delta\zeta^2)\right](1-\zeta^2)\,d\zeta$$

$$I_0^n = \int_0^\alpha \exp(-\delta\zeta)\left[\cos(\beta\delta)(1-\cos\beta\delta\zeta^2)-\sin(\beta\delta)\sin(\beta\delta\zeta^2)\right](1-\zeta^2)\,d\zeta \quad (2)$$

$$I_1^a = \int_{1-\alpha}^1 \exp(-\delta\zeta)(1-\zeta^2)\cos(2\beta\delta(1-\zeta))\,d\zeta$$

Using the new variable x such that $\zeta = 1 - \dfrac{x}{2\beta\delta}$, we find

$$I_1^a = 2^{-1}(\beta\delta)^{-2}\exp(-\delta)\int_0^{2\alpha\beta\delta} x\,\exp(x/2\beta)\cos x\,dx -$$

$$- 8^{-1}(\beta\delta)^{-3}\exp(-\delta)\int_0^{2\alpha\beta\delta} x^2\,\exp(x/2\beta)\cos x\,dx$$

making use of

$$\int x \, \exp(ax) \cos(bx) \, dx =$$

$$\left(a^2+b^2\right)^{-1} \exp(ax)\left[\left(ax - \left(a^2-b^2\right)/\left(a^2+b^2\right)\right)\cos(bx) + \left(bx - 2ab/\left(a^2+b^2\right)\right)\sin(bx)\right] \tag{3}$$

([12],p.198,2.667,6)

$$\int x^2 \exp(ax) \cos(bx) \, dx =$$

$$\left(a^2+b^2\right)^{-1} \exp(ax)\left\{\left[ax^2 - 2\left(a^2-b^2\right)\left(a^2+b^2\right)^{-1}x + 2a\left(a^2-3b^2\right)\left(a^2+b^2\right)^{-2}\right]\cos(bx) + \right.$$

$$\left. + \left[bx^2 - 4ab\left(a^2+b^2\right)^{-1}x + 2b\left(3a^2-b^2\right)\left(a^2+b^2\right)^{-2}\right]\sin(bx)\right\} \tag{4}$$

([12],p.198,2.667,8).

finally yields

$$I_1^\alpha = \delta^{-3}\left(1+4\beta^2\right)^{-3}\exp(-\delta)\left[\exp(\alpha\delta)\left(A\cos(2\alpha\beta\delta) + 2\beta B \sin(2\alpha\beta\delta)\right) + \mathbb{C}\right] \tag{5}$$

$$A = 16\delta\left[\alpha\delta(2-\alpha) + 2(1-\alpha)\right]\beta^4 + 8\left[\alpha\delta^2(2-\alpha) + 3\right]\beta^2 +$$

$$+ 2\left(\delta+1\right)\left(\alpha\delta-1\right) - \alpha^2\delta^2 \tag{6}$$

$$B = 16\alpha\ \delta^2(2-\alpha)\beta^4 + 8\left[\alpha\delta^2(2-\alpha)+2\delta(\alpha-1)+1\right]\beta^2 +$$

$$+ \alpha\delta^2(2-\alpha) + 4\delta(\alpha-1) - 6 \ . \tag{7}$$

$$\mathbb{C} = -32\ \delta\beta^4 - 24\ \beta^2 + 2(\delta+1) \tag{8}$$

$$I_1^n = \int_{1-\alpha}^{1} \exp(-\delta\zeta)\left\{\cos\left(2\beta\delta(1-\zeta)\right) - \cos\left(\beta\delta(1-\zeta^2)\right)\right\}(1-\zeta^2)\,d\zeta$$

$$I_1^n = \int_0^\alpha \exp\left(-\delta(1-\zeta)\right)\left\{\left[1-\cos(\beta\delta\zeta^2)\right]\cos(2\beta\delta\zeta) - \sin(2\beta\delta\zeta)\sin\left(\beta\delta\zeta^2\right)\right\}\zeta(2-\zeta)\,d\zeta \tag{9}$$

$$I_m^a = \int_\alpha^{1-\alpha} \exp(-\delta\zeta)\cos\left(\beta\delta(c-\zeta)\right)(1-\zeta^2)\,d\zeta$$

Using the new variable $x=\beta\delta(C-\zeta)$ leads to:

$$I_m^a = (1-c^2)(\beta\delta)^{-1}\exp(-c\delta)\int_{\beta\delta(c-1+\alpha)}^{\beta\delta(c-\alpha)} \exp(x/\beta)\cos x\,dx + 2c(\beta\delta)^{-2}\exp(-c\delta)\ \ast$$

$$\ast \int_{\beta\delta(c-1+\alpha)}^{\beta\delta(c-\alpha)} x\exp(x/\beta)\cos(x)\,dx - (\beta\delta)^{-3}\exp(-c\delta)\int_{\beta\delta(c-1+\alpha)}^{\beta\delta(c-\alpha)} x^2\exp(x/\beta)\cos x\,dx$$

making use of (3), (4) and

$$\int \exp(ax)\cos(bx)\,dx = \exp(ax)\left(a\cos(bx)+b\sin(bx)\right)(a^2+b^2)^{-1} \tag{10}$$

finally leads to

$$I_m^a = \delta^{-3}\left(4\beta^2\right)^{-3}\exp(-c\delta)\left[\exp(\delta u)\left(D\cos\left(\beta\delta u\right)+\beta E\sin\left(\beta\delta u\right)\right) - \right.$$
$$\left. - \exp(\delta v)\left(F\cos\left(\beta\delta v\right)+\beta G\sin\left(\beta\delta v\right)\right)\right] \tag{11}$$

where

$$u = c - \alpha \tag{12}$$

$$v = c - 1 + \alpha \tag{13}$$

$$D = \delta\left(2\alpha + \delta(1-\alpha^2)\right)\beta^4 + 2\left(\delta^2(1-\alpha^2)+3\right)\beta^2 +$$
$$+ \delta^2(1-\alpha^2) - 2\delta\alpha - 2 \tag{14}$$

$$E = \delta^2\left(1-\alpha^2\right)\beta^4 + 2\left(\delta^2(1-\alpha^2) - 2\delta\alpha + 1\right)\beta^2 +$$
$$+ \delta^2(1-\alpha^2) - 4\delta\alpha - 6 \tag{15}$$

$$F = \delta\left(2(1-\alpha) + \delta\alpha(2-\alpha)\right)\beta^4 + 2\left(\delta^2\alpha(2-\alpha)+3\right)\beta^2 +$$
$$+ \delta^2\alpha(2-\alpha) + 2\delta(\alpha-1) - 2 \tag{16}$$

$$G = \delta^2\alpha(2-\alpha)\beta^4 + 2\left(\delta^2\alpha(2-\alpha) + 2\delta(\alpha-1)+1\right)\beta^2 +$$
$$+ \delta^2\alpha(2-\alpha) + 4\delta(\alpha-1) - 6 \tag{17}$$

$$I_m^n = \int_\alpha^{1-\alpha}(1-z^2)\exp(-\delta z)\left\{\cos\left(\beta\delta(c-z)\right) - \cos\left(\beta\delta(1-z^2)\right)\right\}dz$$

Use $z = \zeta - \alpha$ and obtain

$$I_m^n = \int_0^\alpha \alpha^{-1}(1-2\alpha)\exp(-\delta\alpha)\exp\left(-\delta\alpha^{-1}(1-2\alpha)\zeta\right)\left\{\cos\left[\beta\delta\left(c-\alpha-\alpha^{-1}(1-2\alpha)\zeta\right)\right]-\right.$$

$$\left. -\cos\left[\beta\delta\left(1-\alpha^2-2(1-2\alpha)\zeta-(1-2\alpha)^2\alpha^{-2}\zeta^2\right)\right]\right\}\left[1-\alpha^2-2(1-2\alpha)\zeta-\right.$$

$$\left. -(1-2\alpha)^2\alpha^{-2}\zeta^2\right]d\zeta \tag{18}$$

It is now possible to obtain $I_a = I_0{}^a + I_m{}^a + I_1{}^a$ and
$I_n = I_0{}^n + I_m{}^n + I_1{}^n$.

$$\delta^3 I_a = \exp(-\delta\alpha)\left[H\cos(\beta\delta)+(1+\beta^2)^{-3}\left(D\cos(\beta\delta u)+\beta E\sin(\beta\delta u)\right)\right]+$$

$$+\exp(\delta(\alpha-1))\left[\left(A\cos(2\alpha\beta\delta)+2\beta B\sin(2\alpha\beta\delta)\right)(1+4\beta^2)^{-3}-\right.$$

$$\left. -\left(F\cos(\beta\delta v)+\beta G\sin(\beta\delta v)\right)(1+\beta^2)^{-3}+(1+4\beta^2)^{-3}\exp(-\delta)C+J\cos(\beta\delta)\right. \tag{19}$$

where A, B, C, D, E, F, G are defined by equations (6)
through (8) and (14) through (17). H and J are defined
as follows:

$$H = \left[2(1+\delta\alpha)+\delta^2(\alpha^2-1)\right] \tag{20}$$

$$J = \delta^2-2 \tag{21}$$

(I_n) on the other hand can be expressed as

$$I_n = \int_0^\alpha \left(-U \zeta^2_{+} + 2 V \zeta + W \right) d\zeta \tag{22}$$

where U, V and W are defined by

$$U = \exp(-\delta\zeta) \left[\cos(\beta\delta)\left(1 - \cos(\beta\delta\zeta^2)\right) - \sin(\beta\delta)\sin(\beta\delta\zeta^2) \right] +$$

$$+ \exp(\delta(\zeta-1)) \left[\cos(2\beta\delta\zeta)\left(1 - \cos(\beta\delta\zeta^2)\right) - \sin(2\beta\delta\zeta)\sin(\beta\delta\zeta^2) \right] +$$

$$+ (1-2\alpha)^3 \alpha^{-3} \exp\left(-\delta(\alpha+\alpha^{-1}(1-2\alpha)\zeta)\right) \left[\cos\left(\beta\delta(c - \alpha - (1-2\alpha)\alpha^{-1}\zeta)\right) -\right.$$

$$\left. - \cos\left(\beta\delta\left(1-\alpha^2 - 2(1-2\alpha)\zeta - (1-2\alpha)^2\alpha^{-2}\zeta^2\right)\right) \right]$$

$$\tag{23}$$

$$V = \exp(\delta(\zeta-1)) \left[\cos(2\beta\delta\zeta)\left(1 - \cos(\beta\delta\zeta^2)\right) - \sin(2\beta\delta\zeta)\sin(\beta\delta\zeta^2) \right] -$$

$$- (1-2\alpha)^2 \alpha^{-1} \exp\left(-\delta(\alpha+(1-2\alpha)\alpha^{-1}\zeta)\right) \left[\cos\left(\beta\delta(c - \alpha - (1-2\alpha)\alpha^{-1}\zeta)\right) -\right.$$

$$\left. - \cos\left(\beta\delta\left(1-\alpha^2 - 2(1-2\alpha)\zeta - \alpha^{-2}(1-2\alpha)^2\zeta^2\right)\right) \right]$$

$$\tag{24}$$

$$W = \exp(-\delta \zeta)\left[\cos(\beta \delta)(1 - \cos(\beta \delta \zeta^2)) - \sin(\beta \delta)\sin(\beta \delta \zeta^2)\right] +$$

$$+ (1 - \alpha^2)(1 - 2\alpha)\alpha^{-1}\exp(-\delta(\alpha + (1-2\alpha)\alpha^{-1}\zeta))\left[\cos(\beta \delta(c - \alpha - (1-2\alpha)\alpha^{-1}\zeta)) - \right.$$

$$\left. - \cos(\beta \delta(1 - \alpha^2 - 2(1-2\alpha)\zeta - (1-2\alpha)^2\alpha^{-2}\zeta^2))\right]$$

$$(25)$$

APPENDIX VII

DERIVATION OF THE EXPRESSIONS FOR R, K AND I FOR THE PARABOLIC STRUT

$$R = 16\pi^{-1} F^{-4} \int_0^\infty |\bar{K}(t)|^2 (1+t^2)^{1/2} dt \tag{1}$$

$$y = b(1-x^2)$$

$$\dot{y} = -2bx$$

$$\sigma_y = \dot{y}(1+\dot{y}^2)^{-1/2}$$

$$d\ell = (1+\dot{y}^2)^{1/2} dx$$

$$n_x^2 = \dot{y}^2(1+\dot{y}^2)^{-1}$$

$$n_x \, da = \dot{y} \, dx \, dy$$

$$\bar{K}(t) = \int_{h_+^+} E \, n_x \, da - F^2 \int_{C_+^+} E \, n_x^{\dot{y}} \, \sigma_y \, d\ell$$

$$E = \exp\left(F^{-2}(1+t^2)y\right) \cos\left(F^{-2}t(1+t^2)^{1/2}y\right) \sin\left(F^{-2}(1+t^2)^{1/2}x\right)$$

Use the above equations to find

$$\bar{K}(t) = -2b \int_0^1 I x \cos\left(F^{-2}t(1+t^2)^{1/2} b(1-x^2)\right) \sin\left(F^{-2}(1+t^2)^{1/2}x\right) dx \tag{2}$$

where $\quad \bar{I} = \int_{-d}^{0} \exp\left(F^{-2}(1+t^2)\, \mathfrak{z}\right) d\mathfrak{z} - 4F^2 b^2 x^2 / (1+4b^2 x^2)$

or $\quad \bar{I} = d \int_{0}^{1} \exp\left(-F^{-2}(1+t^2)\, \mathfrak{z} d\right) d\mathfrak{z} - 4F^2 b^2 x^2 / (1+4b^2 x^2)$ $\qquad$ (3)

We can rewrite (1) as

$$R = 64\, b^2\, \pi^{-1} \int_{0}^{\infty} |K(t)|^2 \left(1+t^2\right)^{1/2} dt \qquad (4)$$

where

$$K(t) = \int_{0}^{1} \bar{I}\, x\, \cos\left(F^{-2} t (1+t^2)^{1/2} b (1-x^2)\right) \sin\left(F^{-2}(1+t^2)^{1/2} x\right) dx \qquad (5)$$

and

$$\text{(6)}$$

$$I = F^{-2} d \int_{0}^{1} \exp\left(-dF^{-2}(1+t^2)\mathfrak{z}\right) d\mathfrak{z} - 4b^2 x^2 / (1+4b^2 x^2)$$

The integral in equation (6) is straight forward and (6) becomes

$$I = (1+t^2)^{-1}\left[1 - \exp\left(-dF^{-2}(1+t^2)\right)\right] - 4b^2 x^2 / (1+4b^2 x^2) \qquad (7)$$

APPENDIX VIII

DERIVATION OF K(t) FOR THE
PARABOLIC ELLIPTIC HULL

The wave resistance is given by $\quad R = 4\pi^{-1} F^{-4} \int_0^\infty |K(t)|^2 (1+t^2)^{1/2} dt$

where $\quad K(t) = \int_{R^+} \zeta n_x \, da - F^2 \oint_{C^+} \zeta_o n_x^2 \, \zeta_y \, d\ell \qquad$ (1)

and $\quad \zeta = \exp\left[F^{-2}(1+t^2)\, \zeta - i x F^{-2}(1+t^2)^{1/2}\right] \cos\left(F^{-2} t (1+t^2)^{1/2}\, y\right) \qquad$ (2)

In the fore part, the hull is defined by

$$\alpha = x \qquad\qquad\qquad (3)$$

$$y = b a^{-1} x (1 - x/2a) \sin \varphi \qquad (4)$$

$$\zeta = -d \cos \varphi \qquad\qquad (5)$$

$$y = y(\alpha, \varphi) \;\; ; \;\; \zeta = \zeta(\varphi) \;\; ; \;\; \vec{x} = \vec{x}(\alpha, \varphi)$$

The vector normal to the hull is defined by

$$\vec{n} = \left(\vec{x}_\alpha \wedge \vec{x}_\varphi\right) / |\vec{x}_\alpha \wedge \vec{x}_\varphi|$$

The element of area da is given by

$$da = |\vec{x}_\alpha \wedge \vec{x}_\varphi| \, d\alpha \, d\varphi$$

So we get $\qquad n_x\, da = (\vec{x}_x \wedge \vec{x}_\varphi)_x\, dx\, d\varphi$ $\qquad$ (6)

Since $\vec{x}_x = (1, y_x, 0)$ $\qquad$ and $\vec{x}_\varphi = (0, y_\varphi, y')$, (6) becomes

$$n_x\, da = y_x\, y'\, dx\, d\varphi$$

or, using (3), (4) and (5):

$$n_x\, da = b\, d\, a^{-1}(1 - x/a)\sin^2\varphi \qquad (7)$$

If we define $\quad y' = \left.\dfrac{\partial y}{\partial x}\right|_{\varphi = 0}$, the tangent vector to
the waterline, $\quad$ is given by

$$\vec{c} = (1, y', 0) * (1 + y'^2)^{-1/2} \qquad (8)$$

The element of arc dl is given by

$$d\ell = (1 + y'^2)^{1/2}\, dx \qquad (9)$$

The normal vector at the waterline is defined by

$$\vec{n}_o = (-y', 1, 0) * (1 + y'^2)^{1/2}$$

So at the waterline we have

$$n_x^2 = y'^2 (1 + y'^2)^{-1} \tag{10}$$

Define $\quad \delta = dF^{-2}(1 + t^2) \tag{11}$

and $\quad \beta_1 = b a^{-1} d^{-1} x (1 - x/2a) t (1 + t^2)^{-1/2} \tag{12}$

Use (7) to (12) together with (2) in (1) to obtain

$$K(t) = b a^{-1} \int_0^a \exp\left(-i F^{-2}(1+t^2)^{1/2} x\right)(1 - x/a) I_1 \, dx \tag{13}$$

$$I_1 = d \int_0^{\pi/2} \exp\left(-\delta \cos\varphi\right) \cos\left(\beta_1 \delta \sin\varphi\right) \sin^2\varphi \, d\varphi \; -$$

$$- F^2 \cos\left(\beta_1 \delta\right) \frac{b^2 (1 - x/a)^2}{a^2 + b^2(1 - x/a)^2} \tag{14}$$

In the after part, the hull is defined by

$$x = a + (1 - a)\sin\theta \tag{15}$$

$$y = (b/2)\cos\theta \sin\varphi \tag{16}$$

$$\gamma = -d \cdot \cos\varphi \tag{17}$$

$$x = x(\theta) \; ; \quad y = y(\theta, \varphi) \; ; \quad \gamma = \gamma(\varphi).$$

The vector normal to the hull is defined by

$$\vec{n} = \left(\vec{x}_\theta \wedge \vec{x}_\varphi\right) \Big/ \left|\vec{x}_\theta \wedge \vec{x}_\varphi\right|$$

and the element of surface area by

$$da = \left|\vec{x}_\theta \wedge \vec{x}_\varphi\right| d\theta\, d\varphi$$

$$\Rightarrow n_x\, da = \left(\vec{x}_\theta \wedge \vec{x}_\varphi\right)_x d\theta\, d\varphi$$

Since $\vec{x}_\theta = (x', y_\theta, 0)$ and $\vec{x}_\varphi = (0, y_\varphi, z')$, we obtain

$$n_x\, da = y_\theta\, z'\, d\theta\, d\varphi$$

$$n_x\, da = -\left(bd/2\right) \sin\theta \sin^2\varphi\, d\theta\, d\varphi \tag{18}$$

Using again the convention $y' = \dfrac{\partial y}{\partial \theta}\Big|_{\varphi = 0}$, we have

$$\vec{\tau} = (x', y', 0) \big/ (x'^2 + y'^2)^{1/2} \tag{19}$$

$$d\ell = (x'^2 + y'^2)^{1/2} d\theta \tag{20}$$

$$\tau_y\, d\ell = y'\, d\theta \tag{21}$$

$$n_x^2 = y'^2 \left(x'^2 + y'^2 \right)^{-1} \tag{22}$$

Defining $$\beta_2 = \left(b/2d \right) t \left(1 + t^2 \right)^{-1/2} \cos\theta \tag{23}$$

Use (18) to (23) together with (2) in (1) to obtain

$$K(t) = -\left(b/2 \right) \exp\left(-i\, F^{-2} \left(1 + t^2 \right)^{1/2} a \right) \int_0^{\pi/2} \exp\left(-i\, F^{-2} \left(1 + t^2 \right)^{1/2} (1-a) \sin\theta \right) \sin\theta\ I_2\, d\theta \tag{24}$$

$$I_2 = d \int_0^{\pi/2} \exp\left(-\delta \cos\varphi \right) \cos\left(\beta_2\, \delta \sin\varphi \right) \sin^2\varphi\, d\varphi -$$

$$- F^2 \cos\left(\beta_2\, \delta \right) \frac{b^2 \sin^2\theta}{4 (1-a)^2 \cos^2\theta + b^2 \sin^2\theta} \tag{25}$$